Candidate gene identification from the wheat QTL-2DL for resistance against Fusarium head blight based on metabolo-genomics approach

Udaykumar Kage

Department of Plant Science

McGill University, Montreal, Canada

August 2016

A thesis submitted to the McGill University in partial fulfillment of the requirements of the degree of Doctor of Philosophy

Dedicated to my beloved parents

TABLE OF CONTENTS

LIST OF TABLES

LIST OF FIGURES

DC = anthranilate N-hydroxycinnamoyl/benzoyltransferase [*Dianthus caryophyllus* - Z84383], TC2 = 2-debenzoyl-7,13-diacetylbaccatin III-2-O-benzoyl transferase [*Taxus cuspidate*= AAG38049.1], TC1 = 10-deacetylbaccatin III-10-O-acetyl transferase [*Taxus cuspidate* - AAF27621.1], TC3 =taxadienol acetyl transferase [*Taxus cuspidate* - AAF34254.1], TC = 3'-N-debenzoyltaxol N-benzoyltransferase [*Taxus Canadensis* - AAM75818.1], CR =deacetylvindoline 4-O-acetyltransferase [*Catharanthus roseus* - AAC99311.1], PS =salutaridinol 7-O-acetyltransferase [*Papaver somniferum* - AAK73661.1], FA - alcohol acyltransferase [*Fragaria ananassa* - AAG13130.1], CC =acetyl-CoA:benzylalcoholacetyltranferase [*Clarkia concinna* - AAF04784.1], CB = acetyl CoA: benzylalcohol acetyltransferase [*Clarkia breweri* - AAC18062.1], SS =malonylCoA:anthocyanin 5-O-glucoside-6'''-O-malonyltransferase [*Salvia splendens* - AAL50566.1], PF =malonylCoA:anthocyanin 5-O-glucoside-6'''-O-malonyltransferase [*Perilla frutescens* - AAL50565.1], GT = Anthocyanin 5-aromatic acyltransferase [*Gentiana triflora* - BAA74428.1]. Numbers in red represents branch support values.

Figure 3.8: Purification of bacterial expressed TaACT. L is Protein marker, S1, S2 & S3, S4 are sequential eluted fractions of recombinant TaACT protein, S5 is a crude TaACT extract. Where, S2 and S3 show purified TaACT protein. The protein size is comparable to the reported barley HvACT protein size (~48 kDa).

Figure 3.9: Expression of *TaACT* gene in wheat rachis at 72 hpi, **a)** Expression of *TaACT* based on semi-qPCR; **b)** Expression of *TaACT* in pathogen inoculated treatments based on RT-qPCR. *TaActin* was used as internal standard. RM = Resistant mock, RP = Resistant pathogen, SM = Susceptible mock, SP = Susceptible pathogen treatments. Significant difference in expression levels of NIL-R as compared to NIL-S using Students *t*-test: $^{*}P<0.05$.

Figure 3.10: Effect of *TaACT* silencing in NIL-R on resistance to spread of *F. graminearum*. **a)** Relative transcript expression of *TaACT*; **b)** Relative metabolite abundances of coumaroylagmatine and coumaroylputrescine in silenced (NIL-R+BSMV$_{TaACT}$), non-silenced (NIL-R+BSMV$_0$) NIL-R; **c)** Biomass (as relative gene copy number based on RT-qPCR) of *F. graminearum* in wheat rachis of silenced (NIL-R+BSMV$_{TaACT}$), non-silenced (NIL-R+BSMV$_0$) NIL-R and NIL-S.

Figure 3.11: Effect of *TaACT* over-expressing *Arabidopsis* plants on resistance to *F. graminearum.* **a-1)** Relative metabolite abundances of coumaroylagmatine and coumaroylputrescine in NIL-R (TaACT_NIL-R) and NIL-S (TaACT_NIL-S) *TaACT* expressing *Arabidopsis* plants; **a-2)** Symptoms observed in *Arabidopsis* plants expressing *TaACT* gene from NIL-R (TaACT_ NIL-R) and NIL-S (TaACT_ NIL-S); **b)** *F. graminearum* disease development. Disease development was quantified based on number of plants with dead inflorescence; **c)** Biomass (relative gene copy number based on RT-qPCR) of *F. graminearum in* NIL-R (TaACT_NIL-R) and NIL-S (TaACT_NIL-S) *TaACT* expressing *Arabidopsis* plants.

Figure 3.12: Silencing of the phytoene desaturase (PDS) gene. Photograph indicates the phenotypes of resistant wheat plants infected with *BSMV:00* and *BSMV:TaPDS*

Figure 4.1: Physical map of the QTL-2DL on the long arm of wheat chromosome 2D. Location of the flanking markers (red color) reported in different studies are shown on left side and location of candidate genes (green color) identified within the QTL-2DL are shown on the right side.

Figure 4.2: *In-silico* analysis of *TaWRKY70*. (a) Schematic diagram depicting the *TaWRKY70* gene structure containing exon, intron and coding regions; (b) Conserved domain predicted based on NCBI Conserved Domain Database Search, it shows presence of conserved WRKY domain; (c) Figure showing the characteristic features of Group III WRKY transcription factors, showing the DNA binding domain containing 69 amino acids underlined. It has WRKYGQK and C2HC, WRKY and zinc finger conserved motifs, respectively.

Figure 4.3: Phylogenetic relationships of *TaWRKY70* (in red box) with other plant *WRKY* sequences obtained from NCBI database for wheat (*TaWRKY1A, TaWRKY19A, TaWRKY74a, TaWRKY53a, TaWRKY71, TaWRKY74b*, and *TaWRKY19b*), rice (*OsWRKY45* and *OsWRKY32*), arabidospsis (*AtWRKY18, AtWRKY6, AtWRKY70* and *AtWRKY4*), barley (*HvWRKY32*), *Aegilops tauschii* (*WRKY70*), *Triticum urartu* (*WRKY70*). Maximum likelihood tree representing relationships among WRKY proteins from different plant species. Numbers in red color represents branch length.

Figure 4.4: a) Comparison of DNA sequence variation between NIL-R, NIL-S and Chinese spring *TaWRKY70.* There is a SNP at exon-intron junction. **b)** Comparison of protein sequence variation between NIL-R, NIL-S and Chinese spring *TaWRKY70.* The box shows the predicted nuclear localization signal.

Figure 4.5: Relative transcriptional changes of *TaWRKY70* and its downstream genes induced by *Fg* and mock (water) inoculation based on qRT-PCR. Here target gene expression is normalized to reference gene *TaActin.* (a) Relative transcriptional changes of *TaWRKY70* at 48 and 72 hpi; (b) Gene expression of *TaDGK* and *TaGLI1* and *TaACT* (which did not show any expression in mock treated samples) at 72 hpi. RP = Resistant pathogen, RM = Resistant mock, SP = Susceptible pathogen and SM = Susceptible mock. Significant differences in expression levels of RP as compared to SP using Students *t*-test: **P*<0.05; ***P*<0.01.

Figure 4.6: In-silico DNA-protein interaction using GeneMANIA server. Here dark colored rounds indicate target genes, DGK8 (*TaDGK*), HCT (*TaACT*), WRKY70 (*TaWRKY70*) and NHO1 (*TaGLI1*).

Figure 4.7: Transcriptional regulation of RRI metabolite biosynthetic genes by *TaWRKY70*: (A) constructs used in the transient expression assay and (B) relative luciferase (LUC) reporter activity by *TaWRKY70*. The relative reporter gene expression levels were expressed as LUC/GUS ratios. Values are averages of three replicates. Significant differences in expression levels in promoters compared with vector (DNA without w-box) based on Student's *t*-test: ***P*<0.01.

Figure 4.8: Nuclear localization of TaWRKY70 protein. (a) Nuclear localization signal (NLS) predicted. Red colored amino acid region in bold font and underlined is a NLS; (b) Nuclear localization analysis. Constructs consisting of either TaWRKY70-GFP fusion or GFP alone were used to transiently transform into potato protoplasts. Free GFP and TaWRKY70-GFP fusion proteins were transiently expressed in potato protoplast and observed with a fluorescence microscope. Here, the extreme left panel (GFP fluorescence), the middle panel (bright field) and the right panel (merged view of two images). Transient expression assays were conducted at least three times.

Figure 4.9: Effect of *TaWRKY70* silencing in FHB resistant near-isogenic line (NIL-R), inoculated with *F. graminearum* or mock-solution. (A) Confirmation of knocking down of *TaWRKY70* by assaying relative transcript expression of *TaWRKY70* normalized to reference gene *TaActin* in silenced plant (BSMV:*TaWRKY70*) compared to non-silenced (BSMV:00) at 3 dpi after *Fg* inoculation; (B) Fungal biomass in BSMV-infected plants at 6 dpi with *Fg*. Relative copy number of *tri6* fungal housekeeping gene (=fungal biomass) was quantified in *TaWRKY70* knocked down (BSMV:*TaWRKY70*) plants and compared with control (BSMV:00). Here relative target gene copy number is normalized to reference gene *TaActin*; and (C) Relative transcript levels of *TaDGK*, *TaACT* and *TaGLI1* assayed individually in *TaWRKY70* knocked down (BSMV:*TaWRKY70*) plants compared to non-silenced (BSMV:00) at 3 dpi after *Fg* inoculation. Here target gene expression is normalized to reference gene *TaActin*; (D) Relative metabolite abundances of RRI metabolites in silenced (BSMV:*TaWRKY70*) and non-silenced (BSMV:00) NIL-Rat 3 dpi after *Fg* inoculation. PA-1 – PA(17:0/20:4(5Z,8Z,11Z,14Z)), PA-2 – PA(15:0/20:3(8Z,11Z,14Z)), PA-3 – PA(19:1(9Z)/22:2(13Z,16Z)), Cou-Ag – p-coumaroylagmatine and Cou-put – p-coumaroylputrescine. Significant differences in expression levels as compared in silenced (BSMV:*TaWRKY70*) with non-silenced (BSMV:00) using Students *t*-test: **P*<0.05; ***P*<0.01.

Figure 4.10: A proposed model showing *TaWRKY70* regulating downstream genes involved in the biosynthesis of hydroxycinnamic acid amides (HCAAs) and phosphotidic acid and derivatives (PAs) to resist the pathogen through cell wall fortification, intensified signaling and reduced cell death. After pathogen perception, *TaWRKY70* gets activated by unknown pathways (ex: MAP kinase) and this intern regulates the transcript expression of downstream genes involved in biosynthesis of resistance related induced (RRI) metabolites.

Figure 4.11: a) Primers designed for knocking down *TaGLI1* gene. Virus-induced gene silencing (VIGS) fragments were designed to specifically knock-down the *TaGLI1* gene. The knock-down fragment is boxed; b) Representation of typical BSMV based VIGS vectors and c) The *TaWRKY70* cDNA fragment was cloned to pSL038-1 vector (Test, in the top) downstream of the γb gene. pSL038-1 vector carrying either *phytoene desaturase* (*PDS*) gene (BSMV:*TaPDS,* in

the middle) or without any plant gene (BSMV:00, in the down) served as positive control and negative controls, respectively.

Figure 5.1: *F. graminearum* fungal biomass estimated based on the relative gene copy number of *Tri6* gene in spikelets of near-isogenic lines (NILs), at 6 dpi. Significant differences in NIL-R compared with NIL-S using student *t*-test: $^{**}P<0.01$.

Figure 5.2: Scatter plot of canonical discriminant analysis of significant ($P<0.05$) metabolites from resistant and susceptible NILs following *F. graminearum* or mock inoculation. Where, RM is resistant mock treated, RP is resistant pathogen treated, SM is susceptible mock treated, and SP is susceptible pathogen treated samples. Can1 and Can2 explained 21.7% and 20.6% of variance.

Figure 5.3: Dendrogram based on hierarchical cluster analysis (HCA) of principal components with significant ($P<0.05$) metabolites. The treatments are: RM, resistant mock treated; RP, resistant pathogen treated; SM, susceptible mock treated; and SP, susceptible pathogen treated samples.

Figure 5.4: The chemical groups of resistant related (RR) metabolites detected in NILs upon pathogen inoculation. a) Total RR metabolites accumulated upon *F. graminearum* inoculations in NILs, (b) RRI metabolites accumulated in NILs upon *F. graminearum* inoculations, (c) RRC metabolites accumulated in NILs upon *F. graminearum* inoculations**.**

Figure 5.5: Relative transcript expression of resistance genes. The relative transcript expression was measured in the mock and pathogen treated resistant and susceptible NILs compared with mock-inoculated susceptible NIL at 72 hpi. RM is resistant mock treated, RP is resistant pathogen treated, SM is susceptible mock treated, and SP is susceptible pathogen treated samples. Significant differences in expression levels as compared in RP compared with SP using the student *t*-test: $^{**}P<0.01$.

Figure 5.6: A proposed model showing the role of QTL-2DL in spikelet resistance through regulation of genes and accumulation of metabolites involved in cell wall enforcement to resist the pathogen.

LIST OF APPENDICES

LIST OF ABBREVIATIONS

AME	Accurate mass error
AUDPC	Area under disease progress curve
BAC	Bacterial artificial chromosomes
BLAST	Basic local alignment search tool
BSMV	Barley stripe mosaic virus
CER5	Eceriferum 5
CDA	Canonical discriminant analysis
cDNA	Complimentary deoxyribonucleic acid
D3G	DON-3-O-glucoside
DNA	Deoxyribonucleic acid
DON	Deoxynivalenol
dpi	Days post inoculation
FAO	Food and agriculture organization
FHB	Fusarium head blight
GC-MS	Gas chromatography mass spectrometry
GFP	Green fluorescent protein
GPAT	Glyceraldehyde 3-Phosphate Acyltransferase
GS	Growth stages
HCAAs	Hydroxycinnamic acid amides
HCA	Hierarchical cluster analysis
hpi	Hours post inoculation
IWGSC	International wheat genome sequencing consortium
kDa	Kilo Dalton
LC-MS	Liquid chromatography mass spectrometry
LC-HRMS	Liquid chromatography high resolution mass spectrometry
LUC	Luciferase
m/z ratio	Mass to charge ratio
MS	Mass spectrometry
NIL	Near-isogenic line

NIV	Nivalenol
NLS	Nuclear localization signal
PA	Phosphatidic acid
PAGE	Polyacrylamide gel electrophoresis
PAL	Phenylalanine ammonia lyase
PCR	Polymerase chain reaction
PDS	Phytoene desaturase
PR	Pathogenesis related
PSD	Proportion of spikelets diseased
QTL	Quantitative trait loci
RCBD	Randomized complete block design
RM	Mock inoculated resistant genotype
RNA	Ribonucleic Acid
RP	Pathogen inoculated resistant genotype
RR	Resistance related
RRC	Resistance related constitutive metabolite
RRI	Resistance related induced metabolite
SM	Mock inoculated susceptible genotype
SNP	Single nucleotide polymorphism
SP	Pathogen inoculated susceptible genotype
SSR	Simple Sequence Repeat
TaACT	*Triticum aestivum* agmatine coumaroyltransferase
TaGLI1	*Triticum aestivum* glycerol kinase-1
TaDGK	*Triticum aestivum* diacylglycerol kinase
Tri6	Trichodiene synthase-6
TaWRKY-TF	*Triticum aestivum* WRKY transcription factor
VIGS	Virud-induced gene silencing
ZON	Zearalenone

Abstract

Wheat (*Triticum aestivum* L.) is the most important cereal food crop cultivated around the world. Fusarium head blight (FHB) caused by *Fusarium graminearum* is one of the most destructive diseases of wheat. Apart from causing huge yield losses, FHB is also known to contaminate grains with mycotoxins that are harmful to human and animal health. Several quantitative trait loci (QTL) have been identified for FHB resistance in wheat, but the mechanisms of resistance and candidate genes underlying them are still unknown. Therefore, in the present study an integrated metabolomics and genomics approach was used to identify the candidate genes and mechanisms of resistance in near-isogenic lines (NILs) of QTL-2DL. The high fold-change in abundance, resistance related (RR) metabolites, identified in rachis samples of NIL-R following pathogen inoculation were, *p*-coumaroylagmatine, *p*-coumaroylputrescine, and phosphatidic acids. The candidate gene, *p*-coumaroylagmatine transferase (*TaACT*) is associated with the biosynthesis of *p*-coumaroylagmatine and *p*-coumaroylputrescine. The diacylglycerol kinase (*TaDGK*) and glycerol kinase (*TaGLI1*) are involved in the production of phosphatidic acids. The dissection of QTL based on flanking marker sequencing led to the identification of the transcription factor *TaWRKY70* within the QTL-2DL region. *In-silico* and manual analysis of promoter sequences of *TaACT, TaDGK* and *TaGLI1* showed the presence of WRKY binding sites, and luciferase assay proved their physical interaction *in-vivo*. Further, functional validation of *TaWRKY70* based on virus-induced gene silencing (VIGS) in NIL-R not only confirmed an increase in fungal biomass, but also a decrease in the expression of the downstream resistance genes *TaACT, TaDGK* and *TaGLI1*. This was associated with a decrease in abundance of RR metabolites biosynthesized by them, confirming the plausible FHB resistance mechanisms in rachis governed by this QTL. Similarly, in spikelet samples of NIL-R, we found high abundances of phenylpropanoids, glycerophospholipids and fatty acids. These are known to be involved in cutin and suberin biosynthesis. The genes involved in their biosynthetic pathways (*TaGPAT3, TaCER5* and *TaPAL*) were also found in the QTL-2DL region. Transcript abundance of genes in spikelets based on qRT-PCR showed higher expression in the NIL-R compared to NIL-S, confirming the potential role of QTL-2DL in spikelet resistance. However, these genes also have to be functionally validated for further use in breeding. Among the several FHB resistance QTL identified in wheat, this is the first study to identify functional genes from the QTL and their resistance functions.

RÉSUMÉ

Le blé (*Triticum aestivum* L.) est la plus importante culture céréalière du monde. La fusariose (Fusarium head blight ou FHB) causée par *Fusarium graminearum* est l'une des maladies les plus destructrices du blé. Outre les énormes pertes de rendement qu'elle engendre, la fusariose est également connue pour contaminer les grains avec des mycotoxines nocives pour la santé des humains et des animaux. Plusieurs QTL ont été identifiés pour la résistance à la fusariose chez le blé, mais les mécanismes de résistance et gènes sous-jacents restaient jusqu'alors inconnus. Par conséquent, la présente étude démontre une approche intégrée de métabolomique et de génomique ayant pour but d'identifier les gènes et les mécanismes de résistance de la fusariose dans les lignes quasi-isogéniques (NILS) de QTL-2DL. Les métabolites liées à la résistance (RR), soit les p-coumaroylagmatine, p-coumaroylputrescine, et acides phosphatidiques, ont montré des changements d'abondance de forte amplitude dans des échantillons de rachis de NIL-R suivant l'inoculation du pathogène. Un gène candidat, codant pour la p-coumaroylagmatine transférase (*TaACT*) est associé à la biosynthèse de la p-coumaroylagmatine et le p-coumaroylputrescine. La kinase du diacylglycérol (*TaDGK*) et celle du glycérol (*TaGLI1*) sont impliquées dans la production d'acides phosphatidiques. La dissection par séquençage des QTL sur la base adjacente du marqueur a conduit à l'identification de *TaWRKY70*, un facteur de transcription dans la région QTL-2DL. Des analyses *in-silico* et manuelle des séquences de promoteur de *TaACT, TaDGK* et *TaGLI1* ont montré la présence de sites de liaison WRKY. Leur interaction physique *in vivo* a aussi été demontrée lors d'un test de luciférase. En outre, la validation fonctionnelle de *TaWRKY70* par une technique de silençage de gène induit par virus (VIGS) dans NIL-R, a non seulement confirmé une augmentation de la biomasse fongique, mais aussi une diminution de l'expression des gènes de résistance en aval: *TaACT*, et *TaDGK TaGLI1*; ceci a aussi été associé à une diminution des métabolites RR biosynthétisés par ces derniers, ce qui confirme que des mécanismes de résistance à la fusariose sont régies par ce QTL. De même, dans les épillets de NIL-R, nous avons mesuré un taux élevé de phénylpropanoïdes, de glycérophospholipides et d'acides gras. Ceux-ci sont connus pour leur implication dans la biosynthèse de la cutine et de la subérine. Les gènes responsables de leur biosynthèse (*TaGPAT3, TaCER5* et *TaPAL*) ont également été identifiés dans la région de QTL-2DL. L'abondance des transcrits de gènes mesuré par qRT-PCR a montré une expression plus élevée dans NIL-R par rapport à NIL-S, ce qui confirme le rôle potentiel de QTL-2DL dans la

résistance de l'épillet. Cependant, la fonction de ces gènes doit être validée au cours d'études fonctionnelles avant d'être utilisés lors de croisements. Parmi les nombreux QTL de résistance de la fusariose identifiés dans le blé, cette étude est la première à identifier les gènes fonctionnels du QTL et révéler leur fonction.

Acknowledgement

I would like to convey my special appreciation and gratitude to my supervisor Dr Ajjamada C. Kushalappa; he has been a tremendous support and mentor for me. I would like to thank him for his continuous supervision, support and motivation for my Ph.D thesis research. His advice on both, research as well as on my career has been priceless and allowed me to grow as an independent research scientist. I am grateful to him for his guidance, which helped me throughout my Ph.D thesis research and writing of this thesis, I could not imagine having a better advisor.

I am deeply grateful to my advisory committee members, Dr. Valerie Gravel and Dr. Reza Salavati, for their constructive criticism, insightful comments, suggestions and encouragement, but also for the tough questions which helped to widen my research and thinking skills from various perspectives. It's my fortune to gratefully convey my acknowledgement to Dr. Raj Duggavathi for his insightful advice, discussion and suggestion, and also for allowing me to use lab space for qRT-PCR, microscopy and microtome to take tissue sections for histochemical studies. I am grateful to our collaborator Dr. Curt McCartney, for providing research material and help. I would like to express my gratitude to Dr. Denis Faubert and his team members Mrs. Boulos Marguerite and Dr. Sylvian from IRCM, Montreal not only for the analysis of metabolites but also teaching me how to use LC-MS. I am also thankful to Mr. Serge Dernovici, technician, Institute of Parasitology, for teaching me to use confocal microscopy for my histochemical studies. Many thanks go in particular to the Department chair and past graduate co-ordinator of Dept. of Plant Science, Dr. Martina Stromvik and current graduate coordinator Dr. Jean-Benoit Charron for their constant support and recommendations for faculty scholarships. I am also grateful to the plant science staff, Guy Rimmer, Ian Ritchie, Carolyn Bowes and Lynn Bachand, for their much needed and assistance in green house experiments and administrative tasks.

My sincere acknowledgement goes to my colleagues in Monsanto Holdings Pvt Ltd, Bangalore, India especially Dr. Girish Patil, Mis. Shailaja, Mr. Prakash, Mr. Ravishankar, Mr. Pravin and Mr. Shivanand for their unconditional help, support and encouragement to pursue my higher education. Heartfelt gratitude to my friend and lab mate Shailesh Karre for his unconditional help and support in making me cope with basics of metabolomics and genomics. I

also record my special thanks to my other lab members Shivappa Hukkeri, Dhananjay Dhokane, Liyao Ji, Kobir Sarkar, Nancy Soni and Sripad Joshi. Further, past and present post-docs in our lab, Dr. Arun Kumar, Dr. Yogendra Kalenahalli, Dr. Kareem Mosa, Dr. Alinne Ambrosio and Dr. Yuan Liang to whom I also owe my heartfelt acknowledgment, for their help during my experiments, long discussions on the research topics and their valuable suggestions and comments on my research progress helped me enormously in reaching the end of my Ph.D journey. My special thanks to Boris Mayer and Alexander Martel for their help in translating the abstract from English to French. I extend my individual gratitude to all my friends and colleagues in the Plant Science Dept. for their help and support.

I am greatly beholden of words and owe deep sense of honor to my beloved parents and all family members for their boundless love, needed inspirations and for their unshakable confidence in me. I feel lucky and very proud to have intimate wife like Dr. Deepa Madalageri who has always actively participated in my problems and disappointments and to rebuild my confidence at appropriate stages. Without which, I would not have attained this milestone in my life.

With immense pleasure I record my sincere thanks to the Indian Council of Agricultural Research, New Delhi for awarding me the "ICAR-International fellowship" for three years of my Ph.D. I thank Mr. Bhagwat Singh for timely processing of the fellowship. I am indebted to the Government of Karnataka, India for giving me "National Overseas Scholarship for Minorities" scholarship. I would like to extend my gratitude to Sir Ratan Tata trust for providing me travel grant to travel to Montreal, Canada for the Ph.D. My appreciation to the McGill University for awarding the Schulich graduate fellowship, graduate research excellence awards in the department of plant science. I wish to mention my gratefulness to the Innovagrains Network, Quebec, Canada for awarding me the Ph.D excellence research award for the year 2014. Plant science department and student travel grant coordinators of Plant and Animal Genomics conference and Canadian society of plant biologists (Plant Biotech-2016 conference) also owe my gratitude for providing various travel awards to attend national and international conferences. This project was funded by the Ministère de l'Agriculture, des Pêcherieset de l'Alimentation du Québec (MAPAQ), Québec, Canada, I am also grateful to this funding agency for believing in us and providing the funds to do research in the novel area, metabolo-genomics.

Preface and contribution of the authors

Preface

This thesis work is presented in a manuscript-based format. Here I have used a novel integrated technique, metabolo-genomics to identify candidate genes and to decipher the resistance mechanisms of a major Fusarium head blight (FHB) resistance QTL-2DL in wheat. I also present here a functional characterization of candidate genes based on the virus-induced gene silencing (VIGS) in wheat and a complementation study in *Arabidopsis*. The following elements of this study are considered original scholarship and distinct contributions to knowledge:

- High fold-changes in abundance of candidate metabolites in resistant NIL, compared to susceptible NIL, which are associated with resistance, were identified. These can be further used as biomarkers following validation.
- The flanking markers were sequenced and the QTL-2DL region was physically mapped to chromosome 2D. This will help with direct exploration of other resistance genes in this QTL from source cultivars.
- Functional genes (*TaACT, TaDGK* and *TaGLI1*) leading to biosynthesis of high fold-change resistance related (RR) metabolites were identified and physically mapped within the QTL region.
- We also identified a transcription factor, *TaWRKY70* within the QTL-2DL region. This regulates downstream resistance genes (*TaACT, TaDGK* and *TaGLI1*), to impart FHB resistance in wheat.
- These candidate genes have been sequenced and sequences have been deposited in the NCBI database. This information will be of interest to the research community to identify candidate gene sequence polymorphisms based on allele mining using different cultivars and genotypes. These results could be used to develop novel functional markers for the development of resistant cultivars of wheat or the non-functional genes can be potentially replaced based on genome editing tools. Further, orthologues gene search in related crops like barley would help in advancing FHB resistance programs.
- We identified *TaGPAT3, TaCER5* and *TaPAL* as candidate genes for spikelet resistance. Additionally, gene prediction and synteny based approaches helped in identifying other

putative candidate genes from the QTL-2DL, this could further serve in resistance breeding, following functional validation.

- Metabolomics (forward functional genomics) and VIGS (reverse functional genomics) can be used to discover and functionally validate plant biotic stress related genes, respectively.

Contribution of authors

This thesis involves three studies (Chapter III to V) presented as three manuscripts according to the McGill guidelines for thesis preparation. The research work presented here was completely designed by me under the guidance of my supervisor Dr. Ajjamada C. Kushalappa. I conducted all the greenhouse experiments, laboratory experiments and bioinformatics analysis. I analyzed the data, wrote manuscripts and the thesis under the supervision of Dr. Ajjamada C. Kushalappa. He significantly contributed in providing guidance and funds to conduct the research, also thoroughly edited the manuscripts and thesis and has given priceless suggestions throughout. His contributions are the same for all the manuscripts.

The first manuscript (Chapter III) was co-authored by Mr. Shailesh Karre, Dr. Ajjamada C. Kushalappa and Dr. Curt McCartney. Mr. Shailesh Karre helped in greenhouse experiments and complementation study in *Arabidopsis* and Dr. Curt McCartney developed and provided the wheat lines and their background information used in this study. The second manuscript (Chapter IV) was co-authored by Dr. Kalenahalli N. Yogendra, in addition to Dr. Ajjamada C. Kushalappa. He (Dr. Kalenahalli N. Yogendra) helped in greenhouse experiments and luciferase assay. The third manuscript (Chapter V) was co-authored by Mr. Shivappa Hukkeri and Dr. Ajjamada C. Kushalappa, the former helped in statistical analysis.

Chapter I: Introduction

Wheat (*Triticum aestivum L.*) is an important cereal food crop that belongs to the family Graminae (Poaceae). It is also known as bread wheat which is allohexaploid (AABBDD; 2n=6x=42). It is originally derived from ancient hybridization between the A (*Triticum urartu*) and B (*Aegilops speltoides*) genome donors, resulting in the extant tetraploid emmer wheat (*T. turgidum*; AABB). This species subsequently hybridized with the D genome (*Aegilops tauschii*) donor to form modern hexaploid bread wheat (AABBDD) (Marcussen et al., 2014). Wheat contributes 20% of total calories consumed worldwide (CIMMYT, 2015). It is the second largest cereal crop produced globally, with a total production of 733 million tonnes (mt) and Canada ranks sixth in position with a total production of 27.6 mt (FAO, 2016). Crop plants in a natural environment are confronted with several devastating diseases, leading to severe economic losses.

Fusarium head blight (FHB), also known as wheat scab, is one of the major destructive diseases of wheat. FHB received much attention because of severe disease outbreaks (Bai and Shaner, 1994; McMullen et al., 1997). Several species of Fusarium cause FHB, but the major ones are *Fusarium graminearum* Schwabe (telomorph: *Gibberella zeae*), *Fusarium culmorum*, *Fusarium avenaceum* (telomorph: *Gibberella avenaceum*) (Parry et al., 1995). *F. graminearum* is the most common pathogen in North America. The coincidence of anthesis and early grain-filling stage with warm and wet weather is conducive for FHB infection (Bai et al., 2001). A typical symptom of FHB is bleaching of spikelets. As the fungus move to rachis, the spikelets above and below the initial point of infection in the spike may also be bleached (Matny, 2015). Infected grains will have poor gluten strength (McMullen et al., 1997) and the crop is contaminated with toxic fungal secondary metabolites known as mycotoxins, such as deoxynivalenol (DON), nivalenol (NIV) and zearalenone (ZON). These toxins affect milling and baking qualities (Dexter et al., 1996) and also are very harmful to human and animal health, causing cancers, immunosuppression, fertilization problems and abortion (Matny, 2015). The Canadian Food Inspection Agency (CFIA) rejects grains with >1 ppm of DON for human consumption (McMullen et al., 1997). This disease cause yield losses up to 61 % (Matny, 2015), posing a high risk for the wheat crop. In the meantime, wheat production is required to increase by 70 % from today's levels by the year 2050 to meet the demand (CIMMYT, 2015).

Four main strategies are commonly used to manage FHB: a) Agronomic practices, b) Chemical application, c) Biological approaches and d) Development of resistant varieties. Several agronomic approaches (like clean cultivation, deep ploughing and crop rotation), chemicals and biological agents can manage disease to some extent, but cannot effectively prevent disease epidemics (Buerstmayr et al., 2002). Chemical application can reduce the severity of FHB by 50 to 60 %, however, this approach is not economically and environmentally sustainable. Further, it has potential health risks due to fungicidal residues in food and feed products and their effectiveness is variable, depending on environmental conditions (Stack, 2000; Xue et al., 2008). Therefore, development and cultivation of FHB resistant varieties is considered to be the most important strategy in integrated FHB disease management and to reduce toxin contamination of grains (Buerstmayr et al., 2002).

The inheritance of FHB resistance is polygenic in nature (Bai and Shaner, 1994), and thus is highly influenced by environmental conditions. This makes the selection of resistant genotypes very difficult in the field (Buerstmayr et al., 2002). Three different types of FHB resistance in wheat have been recognized and used in breeding: type I - resistance to initial infection, type II - resistance to disease spread within a spike through rachis and type III - resistance to mycotoxin accumulation in grains (Mesterhazy, 1995). Type II is the most stable type of resistance in wheat because it is evaluated as disease severity or the area under disease progress curve (AUDPC) over 15-20 days post inoculation, following inoculation of a single middle pair of spikelets of a spike with a known spore concentration, thus reducing much of the field variability. Type I resistance is evaluated based on spray inoculation, which is associated with several problems like uneven distribution and variable inoculum quantity reaching spikelets and interaction with environmental conditions. The experimental error has been reduced by individually inoculating several spikelets in a spike with known inoculum level under green house conditions (Kumar et al., 2015).

With the use of modern molecular biology tools, more than 100 QTLs have been identified for resistance to FHB in different wheat mapping populations (Buerstmayr et al., 2009). For type I resistance two major QTL have been mapped: 5A (*Fhb5*) and 4B (*Fhb4*), whereas for the type II resistance three major QTL have been mapped: 2D (QTL-2DL), 3B (*Fhb1*) and 6B (*Fhb2*), and these were stable across environments (Buerstmayr et al., 2009).

These QTL contain several genes, each with major and minor effects on phenotype. Still, efforts made to identify genes and their functions failed to result in fruitful outcomes. Thus, identification and elucidation of functions of the genes present in these QTL regions are crucial for their potential transfer into elite cultivars.

The QTL-2DL is one of the major resistance QTL against FHB with both type I and type II resistance, identified from the Wuhan-1 x Nyubai cross (Somers et al., 2003; McCartney et al., 2007). The source of resistance comes from Wuhan-1 and this QTL has been consistently associated with resistance to disease spread within spike in different genetic backgrounds such as Wuhan-1 (Somers et al., 2003), Wangshubai (Jia et al., 2005; Mardi et al., 2006), and CJ-9306 (Jiang et al., 2007a). QTL-2DL showed a 32 % decrease in disease spread after single floret inoculation (Somers et al., 2003); 9.9 - 28.4 % of phenotypic variation was due to QTL-2DL (Jiang et al., 2007b) and reduced DON content in scabby grains by about 45 % (Jiang et al., 2007a). It was also proved that QTL-2DL exhibits spikelet resistance (type I) based on spray inoculation in field condition (McCartney et al., 2007). Therefore, exploring this QTL for candidate genes and its mechanistic role in FHB resistance will help improve FHB resistance breeding programs. Unfortunately, using an introgressed QTL to develop FHB resistance poses problems associated with linkage drag. Hence, it is crucial to identify candidate genes controlling disease resistance in these major QTL and to decipher the resistance mechanisms. Genes with validated resistance functions can be securely used in breeding programs.

The QTL *Fhb1* conferring type II resistance was fine-mapped using different mapping populations to identify the candidate genes involved in resistance (Cuthbert et al., 2006; Liu et al., 2006). Positional cloning of QTL *Fhb1* revealed seven novel genes within a 261 kb region of bacterial artificial chromosome (BAC) clones. Transgenic wheat lines were developed for four of the putative genes, but none was effective against FHB (Liu et al., 2008). Several studies of lines containing QTL *Fhb1* (Gunnaiah et al., 2012; Jia et al., 2009; Kugler et al., 2013; Nussbaumer et al., 2015; Schweiger et al., 2013; Walter et al., 2015; Warth et al., 2015; Xiao et al., 2013; Zhuang et al., 2013), QTL *Fhb5* (Jia et al., 2009; Kugler et al., 2013; Nussbaumer et al., 2015; Schweiger et al., 2013; Warth et al., 2015) and QTL-2DL (Hamzehzarghani et al., 2008; Long et al., 2015) did not lead to the discovery and functional characterization of effective causal genes responsible for FHB resistance. Instead, functional analysis of mapped QTL using alternative

disciplines like metabolomics combined with genomic resources is considered to be a promising tool to decipher the underlying genes (Kushalappa and Gunnaiah, 2013). Such an approach has divulged the molecular network of glucosinolate metabolism and a few novel genes involved in flavonoid biosynthesis in *Arabidopsis* (Chen et al., 2012). It is possible that the metabolomics approach can also identify candidate resistance gene(s) within QTL-2DL against FHB. A forward genetics approach (e.g., metabolomics, proteomics and transcriptomics) to identify candidate genes for resistance, and a reverse genetics approach (e.g., VIGS) to confirm the phenotypic effect of a gene is the best way to decipher the mechanisms of resistance in plants against biotic stress (Kushalappa and Gunnaiah, 2013).

Metabolomics is a new branch of functional genomics and has been chiefly used in biomedical fields (Duez et al., 1996; Gopaul et al., 2000). However, metabolite profiling technologies are now being used in plant systems (Bollina et al., 2010; Roessner et al., 2001; Tohge and Fernie, 2010). Non-targeted metabolite profiling of barley and wheat genotypes with varying levels of resistance to FHB led to the identification of several resistance related (RR) metabolites and their roles in resistance against FHB in barley (Bollina et al., 2010; Bollina et al., 2011; Chamarthi et al., 2014; Kumaraswamy et al., 2011a; Kumaraswamy et al., 2011b) and wheat (Gunnaiah and Kushalappa, 2014; Gunnaiah et al., 2012; Hamzehzarghani et al., 2005; Hamzehzarghani et al., 2008). Metabolomics in resistant and susceptible cultivars of barley (Kumar et al., 2016) and potato (Pushpa et al., 2013; Yogendra et al., 2014; Yogendra et al., 2015; Yogendra and Kushalappa, 2016) led to the identification of several RR metabolites and their biosynthetic and regulatory genes for FHB and late blight diseases respectively. Thus, it is possible to decipher the mechanisms of resistance in QTL-2DL based on metabolite profiling of near-isogenic lines (NILs), which have the same genetic background (susceptible) except for the alleles at the QTL region. The use of NILs reduces background genetic effects and thus helps in better explaining the resistance mechanism by QTL locus in contrasting lines with alternate alleles for resistance (Gunnaiah et al., 2012).

Association of RR metabolite with gene is not enough to claim the role of that gene in FHB resistance; functional validation is required. For functional validation of the candidate genes identified against FHB resistance, tools such as mutagenesis, RNAi, VIGS and complementation studies can be used. However, VIGS is an easy and rapid knockdown

technique to study gene function in plant development, biotic and abiotic stress resistance (Cakir et al., 2010; Ramegowda et al., 2014; Senthil-Kumar et al., 2008). It has been successfully utilized in several crops including tomato, wheat, barley and potato. Once the candidate gene functionality is validated, that gene can be used in breeding programs through cisgenic or marker assisted selection (MAS) for crop improvement. In this context, the present study used an integrated metabolo-genomics approach to decode genetic determinants underlying major FHB resistance QTL, QTL-2DL.

General hypothesis

Wheat NILs, with resistance and susceptible alleles for FHB resistance at QTL-2DL on chromosome 2D, differ in metabolic profiles, gene expression, and gene sequence. The functional gene(s) in the resistant NIL biosynthesizes specific metabolite(s) or in significantly high abundance, while the mutated/non-functional gene(s) in the susceptible NIL are unable to synthesize these metabolite(s) or even if it can, the abundance would be significantly low.

General objectives

I. To identify candidate gene(s) localized in the QTL-2DL region imparting type-II FHB resistance (rachis resistance), based on metabolome profiles of NILs carrying resistant and susceptible alleles of QTL-2DL.

II. To validate the candidate gene resistance functions based on VIGS.

III. To identify candidate gene(s) localized in the QTL-2DL region for type-I FHB resistance (spikelet resistance), based on metabolic profiles of NILs carrying resistant and susceptible alleles of QTL-2DL.

Chapter II: Review of Literature

2.1 Fusarium head blight of wheat at a glance

2.1.1 Fusarium head blight epidemiology and impact on wheat production

Fusarium head blight (FHB) is a devastating disease of wheat and barley. About 17 Fusarium species are known to cause FHB (Parry et al., 1995). Globally, *Fusarium graminearum Schwabe* [teleomorph: *Gibberella zeae* Schw. (Petch)] is the most predominant species (Xu and Nicholson, 2009). Different species of Fusarium can cause similar disease severity symptoms, thus indicating possible host resistance similar to *F. graminearum* (Mesterhazy et al., 2005). Fusarium being saprophytic during the initial stages, it can survive on crop residues between the host crop cycles. Apart from wheat, the fungus has other hosts such as oat, corn, barley and soybean. Thus, the crop residues from a previous season can act as a major source of inoculum. Initial inoculum for FHB during natural infection can be sexual ascospores and asexual macroconidia, chlamydospores, and hyphal fragments (Bai and Shaner, 2004). Wind and rain splash are considered to be common modes of disease spread (Dill-Macky et al., 2003). Ascospores and macroconidia are considered as the principal sources of inoculum because the wind takes the spores to the site of infection (Bai and Shaner, 1994). Upon reaching wheat spikelets, ascospores and/or macroconidia germinate and start colonizing in the wheat spike tissues to initiate infection (Bai and Shaner, 2004). During favourable conditions, Fusarium can enter wheat florets through anthers or natural openings such as stomata and crevices, openings between the lemma and pelea (Kang and Buchenauer, 2000). The optimum temperature for pathogen growth and development is 25°C and the incidence of infection increases with increase in temperature from 20 to 30°C (Bushnell et al., 2003). The first visible symptom appears as brown colored patches on the spikelets within 2-4 days (Bushnell et al., 2003).

FHB causes drastic reduction in grain yield and quality, especially in humid and semi-humid wheat growing areas (Bai and Shaner, 1994; Matny, 2015). When warm wet weather coincides with anthesis and the early grain filling stage, conditions are optimal for the pathogen to cause disease (Bushnell et al., 2003). FHB infection affects wheat in two ways: a) direct damage to grains; b) contamination of grains with mycotoxins (De Wolf et al., 2003). FHB has

direct effects on kernel size, number and accumulation of mycotoxins such as DON and ZON in seeds. Mycotoxins are very harmful to human and animal health. In humans, DON causes burning sensations in the mouth and stomach, headache, reduction in red blood cell count, bleeding and even death in severe cases (Rotter, 1996). These mycotoxins are known to have adverse effects on the nervous system, liver, kidneys, circulatory system, endocrine system and digestive tract (Champeil et al., 2004). In animals, they have drastic effect on feed intake and feed denial; also causes vomiting and weight loss (De Wolf et al., 2003). They also cause cancers, immunosuppression, fertilization problems, and abortion in animals and humans (Matny, 2015). FHB also decreases the nutritive value (degradation of proteins, starch granules) and processing quality (baking quality, malting quality) of the grains (Gilbert and Tekauz, 2000; Buerstmayr et al., 2014). Thus, FHB significantly impacts marketing, exporting, processing and feed value of grains (McMullen et al., 1997).

Massive economic losses due to FHB epidemics have been reported worldwide. The USA and Canada frequently face adverse effects of FHB. There are reports of 288,000 metric tonnes losses in wheat yield in 1917 due to FHB in the USA (Atanasov, 1920). Again, during 1919 the USA faced much greater loss of 2.18 million metric tonnes (Dickson, 1942). Grain industries in Ontario and Quebec lost worth of US$ 200 million and Manitoba of US$300 million (Windels, 2000) during the 1990s due to FHB. During 1993, severe epidemics of FHB reduced wheat yields by 40-50% and barley yields by 20-37% in northeastern North Dakota and northwestern Minnesota (Buerstmayr et al., 2014). During 1998-2000, FHB inflicted an estimated US$ 2.7 billion loss due to reduced quality and quantity of the wheat produced in the northern Great Plains and central USA (Goswami and Kistler, 2004). More than 7 million hectares of wheat were affected by FHB and resulted in yield losses of more than 1 million tonnes in China (Bai and Shaner, 2004). Several wheat growing regions in China are regularly confronted with severe FHB epidemics, with yield losses of 20-40% (Buerstmayr et al., 2014). Calculations of losses due to mycotoxins costs in the United States vary, one report says it varies between 0.5 to 1.5 billion US$/year and another estimated 5 billion US$/year for the U.S. and Canada (Matny, 2015).

2.1.2 FHB management practices

Several strategies have been used to manage FHB including cultural practices, chemical approaches, biological agents, disease forecasting and breeding for resistant cultivars. Cultural practices include land preparation, crop rotation with non-cereal crops, clean cultivation and proper water management during anthesis, which can help in managing the disease (Champeil et al., 2004). Deep ploughing practices can reduce the primary inoculum by burying crop residues and early sowing or growing short duration cultivars results in disease escape in some areas (Champeil et al., 2004; Matny, 2015). FHB increases with reduced tillage and continuous maize cropping practices (Bateman et al., 2007; Buerstmayr et al., 2002).

Chemical approaches to FHB management are commonly followed by farmers. Foliar application or seed treatment with various fungicides minimizes disease severity and spread of seed-borne inocula (McMullen et al., 1997; Mesterhazy et al., 2005). Fungicides can partially control of FHB and mycotoxin contamination (Edwards, 2004; Mesterhazy et al., 2005; Parry et al., 1995; Stack, 2000). Effectiveness of fungicide control varies depending upon time of application, use of proper chemicals with specific active ingredients and environmental conditions (Champeil et al., 2004). It has also been reported that the prevailing species *F. graminearum* is inherently resistant to azole fungicides and some azoles influences increased DON accumulation (Brewer et al., 2015).

Biological control of FHB has emerged as a possibility, but has not been commercially practiced. Several studies have shown that different biocontrol agents including bacteria (*Bacillus* spp., *Kluyvera cryocrescens*, *Paenibacillus fluorescens*, and *Pseudomonas fluorescens*), yeasts (*Cryptococcus* spp, and *Sporobolomyces roseus*) and filamentous fungi (*Trichoderma harzianum* and *T. viren*, and *Clonostachys rosea)* can be quite effective for controlling FHB (Bacon and Hinton, 2007; Jochum et al., 2006; Xu and Nicholson, 2009). However, their viability, appropriateness of application with fungicides and conflicting results has hindered them from commercial application (Yuen et al., 2007).

Several forecasting systems have been developed to facilitate the judicial and economical use of fungicide applications to control FHB (Wegulo et al., 2013). Fusarium Head Blight Risk Assessment Tool (http://www.wheatscab.psu.edu/riskTool_2011.html) is an Internet-based FHB

forecasting system in USA. This uses different environmental parameters to calculate the risk of occurrence of FHB in 23 different states. The system outputs a risk category as low, moderate or high and farmers can then decide whether to apply a fungicide at early anthesis based on the risk predicted for their respective locations. In Canada, the DONcast® model is used by wheat farmers to predict DON accumulation. Based on these predictions farmers can make fungicide spray decisions more efficiently. FusaProg is an Internet-based decision support system which provides information about local and regional risks of FHB outbreaks; additionally it forecasts field-specific DON contamination of winter wheat in Switzerland (Musa et al., 2007). In Argentina, one of the forecasting systems has potential to forecast annual DON content in mature wheat grain using primary meteorological data (Martinez et al., 2012).

The best approach to managing FHB is to integrate multiple strategies (McMullen et al., 2008) including host resistance, fungicide application, crop rotation, residue management, and forecasting. A combination of two or more of these strategies can significantly reduce losses caused by FHB.

2.1.3 FHB management through breeding for disease resistance

Resistance in plants to biotic stress is genetically controlled and can be monogenic or polygenic in nature. Monogenic resistance is qualitative due to R-proteins or genes leading to hypersensitivity responses as in late blight of potato, and is considered as complete resistance. Polygenic resistance is quantitative with additive effects and is due to biochemicals or metabolites that suppress pathogen development. It is considered to be partial resistance or reduced susceptibility (Kushalappa and Gunnaiah, 2013; Kushalappa et al., 2016). No qualitative resistance or immunity has been observed in wheat against FHB. Resistance in wheat against FHB is quantitative, which is partial resistance.

In wheat, development and use of resistant strains seems to be the most economical and environmentally safe approach for managing FHB and preventing mycotoxin contamination (Arruda et al., 2016). However, breeding for resistance is complicated by association of resistant QTL with unacceptable traits, higher genotype × environment (G × E) interaction, and difficulties associated with phenotyping (Bai and Shaner, 2004; Buerstmayr et al., 2002; Rudd et al., 2001). FHB resistance, being a quantitative and low heritable trait, poses difficulty in efficient phenotyping (Bai and Shaner, 2004; Buerstmayr et al., 2002). However, molecular

markers are useful tools to use for selecting low heritable traits, so the use of molecular markers to assist in selection and mapping QTL for resistance to FHB is promising (Bai and Shaner, 2004; Buerstmayr et al., 2002). Breeders have used several source genotypes, such as Sumai 3, Ernie, Freedom, Truman, Wuhan-1, W14, Frontana, Wangshuibai, Ning 7840, and CJ 9306, in national and international breeding programs to improve FHB resistance. These resistance sources have been utilized in several breeding programs for developing different mapping populations, for mapping studies and identifying QTLs for resistance to FHB. However, only a few of the resistant sources have shown consistency in their performance across different environments and they have been used successfully in breeding for the development of resistance genotypes (Yu et al., 2008).

2.1.3.1 Types of Fusarium head blight resistance

FHB resistance mechanisms are classified as morphological or physiological (Gilsinger et al., 2005; Rudd et al., 2001). Plant characteristics such as closed floret affect pathogen inoculation, thus leading to disease avoidance, and higher plant height can reduce infection due to short duration of moisture on spikelets when the wind speed is high, thus mainly the environmental factors are the cause of the escape, and accordingly is considered as apparent resistance. Physiological resistance mechanisms include biochemical compounds that inhibit pathogen growth and development and are considered as true resistance (Gilsinger et al., 2005; Kushalappa and Gunnaiah, 2013; Rudd et al., 2001).

Breeders evaluate resistance based on five types of disease or toxin assessment, of which three types are most commonly used: type I is resistance to initial infection of spikelets. However, evaluation of disease resistance based on type I resistance is not consistent and leads to lots of experimental errors due to variations in inoculum availability, amount of inoculum, spore deposition and environment (Buerstmayr et al., 2009; Cuthbert et al., 2006; Kumar et al., 2015). Type II is resistance to pathogen spread among spikelets within a spike through rachis, which is considered to be stable due to the introduction of known amount of inoculum into the spikelet; and type III is resistance to mycotoxin accumulation in grains based on DON quantification, which vary with the chemotypes, as isolates varies in their ability to produce types and amounts of mycotoxins (Miller et al., 1985; Schroeder and Christensen, 1963). FHB resistance is

quantitative in nature, involving several genes with major and minor additive effects to the phenotype. As a result, resistance mechanisms against FHB are very complex and difficult to identify.

2.1.3.2 Molecular markers and QTL for FHB resistance

There are three types of molecular markers, hybridization based (RFLP), PCR based (RAPD, AFLP, SSR) and sequence-based markers (STS and SNPs) (Collard et al., 2005; Kage et al., 2015). PCR based markers have become more popular because of their advantages includes low amount of DNA required, no need of radioisotopes, high level of polymorphism, even distribution throughout the genome and the ability to screen multiple genes simultaneously (Jiang, 2013). Sequence-based markers like STS, a unique DNA fragment from a known sequence (Farooq and Azam, 2002) and the other newest marker is SNP (Jordan and Humphries, 1994), which can detect a single nucleotide change and is best suited for high throughput marker detection.

The marker systems discussed above have been used for QTL mapping of FHB resistance in different studies in different mapping populations. QTL mapping by the use of molecular markers is an effective method to study quantitative traits (Tanksley, 1993; Young, 1996). More than 100 QTL have been reported in different wheat populations and are mapped in about 50 wheat genotypes covering all 21 chromosomes (Buerstmayr et al., 2009; Liu et al., 2009). QTL residing on chromosomes 3A, 5AS, 7A, 1B, 3BS, 4B, 5B, 6BS and 2D have been validated in more than two populations (Liu et al., 2009). One major QTL is *Fhb1* residing on chromosome 3BS arm derived from Sumai-3 (Cuthbert et al., 2006). Apart from *Fhb1*, other major validated QTL include QTL-2DL, *Fhb2, Fhb4* and *Fhb5* (Buerstmayr et al., 2009; Liu et al., 2009).

QTL-2DL was first reported by Somers et al., (2003) and the resistance is mainly coming from Wuhal-1, a Chinese accession. This QTL was validated in different populations and confirmed its effectiveness towards reducing initial infection and disease spread (Balut et al., 2013; Jia et al., 2005; Mardi et al., 2006; McCartney et al., 2007). QTL-2DL was mapped in a uniform genetic background to increase the resolution by incorporating more SSR markers, leading to the identification of tightly linked flanking markers, WMC245, wmc144, GPW8003, gpw8004, cfd73, cfd233 and GWM608 (McCurtney, 2011). However, *XGWM539* is a peak

marker for the QTL-2DL (Somers et al., 2003) and has been confirmed in a different population (Balut et al., 2013; Jiang et al., 2007a). In addition, this QTL also exhibited spikelet resistance based on spray inoculation under field conditions (McCartney et al., 2007). These studies suggest that the region underlying QTL-2DL contains candidate alleles/genes for both type I and type II resistance. Functional characterization of QTL-2DL will help in elucidating type I and type II resistance mechanisms and candidate FHB resistance genes in wheat.

2.2 Functional genomics to identify candidate genes for FHB resistance

Developing linkage maps and identifying QTL and genome sequencing tools will not pinpoint the candidate gene for a specific trait. Therefore, functional characterization of genes in a genome is very important, however, this is a still challenging task in the post-genomic era. Gene functions can be identified by forward and reverse genetics approaches. Forward genetics goes from phenotype to gene level, while reverse genetics goes from gene to phenotype. Forward genetics is mainly based on transciptomics, metabolomics and proteomics approaches, to identify resistance related transcripts, metabolites and proteins. Mapping RR metabolites on a specific metabolic pathway can enable identification of the catalytic enzymes and the genes associated with these enzymes are discovered based on genomic databases and available literature. The metabolic approach has been demonstrated to be an effective strategy in revealing the resistance functions of genes (Kushalappa and Gunnaiah, 2013; Kushalappa et al., 2016). The resistance in plants against biotic stress is considered to be due to hierarchies of genes, which eventually biosynthesize resistance related metabolites that suppress pathogen progress or contain the pathogen to initial infection (Kushalappa and Gunnaiah, 2013; Kushalappa et al., 2016). A comprehensive metabolomics approach will enable us to identify the metabolites involved in resistance and helps in revealing the mechanisms of resistance associated with QTL-2DL.

2.2.1 Metabolomics and analytical platforms for metabolite profiling

The metabolome is the complete set of metabolites present in an individual under specific conditions. A comprehensive study of the metabolome is known as metabolomics (Shulaev et al., 2008). Recently, metabolomics has emerged as a potent technology for crop improvement. As metabolites are end products of gene regulation, metabolomics has the potential to identify gene functions which remained unannotated by genomics tools. Metabolomics is an excellent platform

for metabolic profiling of plant samples (Fiehn et al., 2000; Krishnan et al., 2005). Plants produces 100,000 – 200,000 metabolites, with different chemical properties; their detection, identification and quantification are very challenging, in spite of significant advances in metabolomics platforms (Oksman-Caldentey and Inzé, 2004).

No single analytical platform is able to identify all metabolites produced by plant system. A number of analytical methods to detect metabolites are available and have their own pros and cons. However, a combination of analytical methods increased the number of metabolites detected (Okazaki and Saito, 2014). Mass spectrometry (MS) is an often-used platform in metabolomics studies as it provides high sensitivity and mass-to-charge information. MS coupled with separation techniques such as chromatography a widely used platform and has the ability to detect a wide range of compounds (Okazaki and Saito, 2014). Liquid chromatography (LC) and gas chromatography (GC) are commonly used separation techniques in metabolomics and they have their own advantages and disadvantages. GC combined with mass spectroscopy (GC-MS) is a reliable tool for identifying volatile compounds (Fiehn et al., 2000; Hamzehzarghani et al., 2005; Lisec et al., 2006). GC-MS detects only volatile compounds, but most of the RR metabolites are non-volatile. Therefore, using hybrid liquid chromatography and high resolution mass spectrometry (LC-HRMS) is convenient and it has detected more than 3000 peaks and several RR metabolites in barley, wheat and potato (Bollina et al., 2010; Gunnaiah et al., 2012; Kumaraswamy et al., 2011a; Pushpa et al., 2013; Yogendra et al., 2014). This was possible because of the ability of LC-HRMS to separate thousands of metabolites from a complex mixture due to its high resolution power (De Vos et al., 2007; Gertsman et al., 2014; Moco et al., 2006; Rischer et al., 2006; Tolstikov et al., 2003). Nuclear magnetic resonance (NMR) is one of the best techniques used and it is non-destructive, non-biased, highly quantitative and it doesn't require prior separation and derivatization. However, it is appropriate for detecting highly bulk metabolite samples due to low sensitivity (Biais et al., 2010). Since it lacks sensitivity, low abundance metabolites, however may play important roles in plant resistance, cannot be detected, thus reducing its utilization over MS. Fourier transform-ion cyclotron resonance mass spectrometry (FT-ICR-MS) is a new platform and has very high sensitivity and resolution compared to other techniques (Okazaki and Saito, 2014). However, due to its low scan speed, it is not appropriate for the application of high/ultra-high performance liquid chromatography (HPLC/UHPLC) as the LC-HRMS with Orbitrap (LTQ-Orbitrap). The LC-HRMS platform is

highly in demand for metabolite identification because of extremely high levels of mass accuracy and resolution as well as the applicability to HPLC or UHPLC and high user-friendliness (Allwood and Goodacre, 2010).

2.2.2 Putative metabolite identification and databases

Metabolite identification/annotation is very challenging aspect of metabolomics and, increasing demands in the post-genomic era this technology has developed quickly. Metabolites are identified based on several basic criteria: i) Accurate mass match with metabolites in databases, such as PlantCyc, METLIN, KEGG, KNApSAcK, MetaCyc and LIPID MAPS, with accurate mass error of, AME<5ppm (Tohge and Fernie, 2010); ii) Fragmentation pattern match with available databases, literature and in-house fragmentation of pure compounds; iii) *In-silico* confirmation of fragmentation based on Masspec scissor in Chemsketch (ACD labs, Toronto) (Matsuda et al., 2009); iv) Based on the number of carbons in the molecular formula. v) NMR spectra (Okazaki and Saito, 2014). Some of the important metabolite databases available are: i) **PlantCyc,** a source of compounds from 350 plant species (http://pmn.plantcyc.org/cpd-search.shtml); ii) **METLIN,** which contains data on known plant metabolites and drug metabolites (Smith et al., 2005); iii) **KNApSAcK,** which contains plant metabolites (Afendi et al., 2012); iv) **KEGG,** a large collection of chemicals from plants and animals (Kanehisa and Goto, 2000); v) **MetaCyc,** the largest curated non redundant reference database of small molecules which are experimentally validated and reported in the scientific literature (Caspi et al., 2012); and vi) **LIPID MAPS,** a rich collection of information on different categories of lipid molecules such as fatty acyls, glycerolipids, glycerophospholipids, sphingolipids, sterol lipids, and prenol lipids (http://www.lipidmaps.org/). In addition, some of these databases also contain metabolic pathways and links to biosynthetic enzymes and genes.

2.2.3 Databases and bioinformatics tools to identify candidate genes

Identified and annotated metabolites are linked to their respective metabolic pathways to explore precursors and end products, which can give insight into unidentified metabolites that are detected and also can enable decipher resistance mechanisms. Bioinformatics tools such as Cytoscape (Smoot et al., 2011), MapMan (Usadel et al., 2009), and Metaboanalyst (Xia and Wishart, 2011) can be used to map the RR metabolites on metabolic pathways, and candidate *RR*

genes that biosynthesize RR metabolites can be identified from publicly available databases such as KEGG, MetaCyc and PlantCyc (Kushalappa and Gunnaiah, 2013) or based on literature.

2.2.4 Application of metabolomics

Metabolomics has been widely used in gene discovery and functional characterization, genotype evaluation for quality traits and for identifying biomarkers associated with disease phenotypes, evaluation of genetically modified crops, metabolomics QTL analysis and the study of plant-environment interaction (Bollina et al., 2010; Kumaraswamy et al., 2011a; Kushalappa and Gunnaiah, 2013; Okazaki and Saito, 2014; Schauer and Fernie, 2006). By comparing the metabolite composition between two individuals at a particular growth stage or time, differences in functionality can be assessed. Semi-comprehensive metabolite profiling of barley (Bollina et al., 2010; Bollina et al., 2011; Chamarthi et al., 2014; Gunnaiah et al., 2012; Kumaraswamy et al., 2011a; Kumaraswamy et al., 2011b) and wheat (Gunnaiah and Kushalappa, 2014; Gunnaiah et al., 2012; Hamzehzarghani et al., 2005; Hamzehzarghani et al., 2008) genotypes varying in levels of resistance to FHB have revealed several RR phenylpropanoid, flavonoid and fatty acids metabolites. The FHB resistance mechanism controlled by *Fhb1* has been reported to be due to cell wall reinforcement through deposition of hydroxycinnamic acid amides (HCAAs) and flavonoids (Gunnaiah et al., 2012).

Metabolo-genomics platform in tomato revealed candidate genes for the control of tomato fruit composition and development (Mounet et al., 2009). In rice, 24 candidate genes mainly involved in phenolics pathway were identified using metabolite profiling of rice populations (Gong et al., 2013). A genome-wide metabolite association study in tomato revealed 44 candidate loci for fruit metabolic traits (Sauvage et al., 2014). In potato, RR metabolites and their respective candidate resistance genes such as, CoA ligase (4-CL), tyrosine decarboxylase (TyDC), and tyramine hydroxycinnamoyltransferase (THT), were identified against late blight of potato based on metabolomics as a tool (Yogendra et al., 2014). Metabolomics genome-wide association mapping have been used for identification of candidate genes and causal variations in genomic regions involved in metabolic traits (Chen and Gao, 2014; Wen et al., 2014). Metabolic profiling of contrasting potato cultivars against late blight identified phenylpropanoids and their biosynthetic genes and their regulation by *StWRKY1* (Yogendra et al., 2015). Untargeted

metabolite profiling of wheat aneuploid lines was performed and identified putative candidate genes controlling trehalose biosynthesis (Francki et al., 2015). Anthocyanin biosynthetic genes were identified in potato using a metabolo-genomics approach (Cho et al., 2016). HvWIN1, a transcription factor, has been shown to enhance biosynthesis of ω-fatty acids, leading to the production of cutin monomers that enhance cuticle thickness to resist FHB in barley (Kumar et al., 2016).

2.2.5 Functional characterization of candidate genes

In many crops, genome sequencing has been completed; however, the gene functions are largely unknown. Functional genomics is one of the most important and challenging tasks for plant biologists in the post-genomics era. Gene function can be revealed by techniques like over-expression, knockout, or silencing. Techniques such as mutagenesis (chemical or irradiation), insertional mutagenesis, RNAi and VIGS are used to study gene function (Burch-Smith et al., 2004; Tadege et al., 2005). Insertion mutagenesis techniques are mainly used for functional analysis of single genes, since they do not allow the analysis of gene families (Parinov and Sundaresan, 2000). Methods such as stable transformation and VIGS can be utilized for silencing genes or gene families. However, stable transformation of grass species is a long process and not well established for crops like wheat. Therefore, VIGS in wheat is currently considered to be the important technique to study gene function in plant development, biotic and abiotic stress resistance (Burch-Smith et al., 2004; Cakir et al., 2010; Ramegowda et al., 2014; Robertson, 2004; Senthil-Kumar et al., 2008). VIGS has been used in wheat to identify candidate gene(s) functions against HMW-GS, leaf rust, powdery mildew and leaf blotch (Geng et al., 2013; Lee et al., 2015; Ma et al., 2012; Scofield et al., 2005).VIGS of *Mlo* genes has a positive impact on powdery mildew resistance in wheat (Várallyay et al., 2012) and a wheat ABC transporter contributing to both grain formation and mycotoxin tolerance has been functionally validated using VIGS (Walter et al., 2015). Using VIGS, *TaLHY*, a 1R MYB transcription responsible for ear heading and stripe rust resistance function was identified (Zhang et al., 2015).

As stable transformation in wheat is difficult and time consuming, a complementation study in *Arabidopsis* is also a valuable technique to reveal gene function. Transgenic *Arabidopsis thaliana* expressing a barley UDP-glucosyltransferase exhibited resistance to the mycotoxin

deoxynivalenol (Shin et al., 2012). Transgenic expression of polygalacturonase-inhibiting proteins in *Arabidopsis* and wheat increased resistance to the flower pathogen *F. graminearum* (Ferrari et al., 2012). Also, over-expression of *PvPGIP2* was effective against a wheat foliar pathogen, *B. sorokiniana,* due to increased polygalacturonase-inhibiting proteins (Janni et al., 2008). Heterologous expression of wheat VERNALIZATION 2 (*TaVRN2*) gene in *Arabidopsis* helped reveal its role in delayed flowering and freezing tolerance (Diallo et al., 2010). Roles of wheat and barley *DOG1*-(*Delay of germination*) like genes in seed dormancy were discovered by ectopic expression in *Arabidopsis* (Ashikawa et al., 2010). Functional validation of a role for *TaWRKY44* in multiple abiotic stress tolerance was shown by developing transgenic tobacco plants expressing *TaWRKY44* (Wang et al., 2015). Constitutive expression of the barley dehydrin gene aba2 in *Arabidopsis* enhanced salt tolerance by increasing seed germination (Calestani et al., 2015). Involvement of *TaAREB3* in drought and freezing tolerance was identified by creating stable transgenic *Arabidopsis* lines (Wang et al., 2016).

Connecting statement for Chapter III

Chapter III, entitled "Identification and characterization of a fusarium head blight resistance gene *TaACT* in wheat QTL-2DL" authored by Udaykumar Kage, Shailesh Karre, Ajjamada C. Kushalappa and Curt McCartney, has been accepted for publication in Plant Biotechnology.

Based on the critical literature review in the previous chapter, I observed that the development and cultivation of resistant cultivars for FHB resistance is an important aspect of FHB management in wheat. QTL-2DL is major QTL responsible for FHB resistance (mainly type II – resistance to the spread of the pathogen through rachis) in wheat, but the resistance mechanisms governed by this QTL are largely unknown. Resistance mechanisms to FHB are organ specific and biochemical mechanisms in rachis are not clearly understood (Golkari et al., 2007). Differences in structural and biochemical characteristics of rachis in resistant and susceptible lines play very important roles in containing pathogen progress (Lahlali et al., 2015; Miller et al., 2011). Metabolomics is considered to be a promising approach to decipher the mechanisms of resistance to pathogen stress (Kushalappa and Gunnaiah, 2013). Therefore, in the present study, metabolite profiling of NILs was performed to identify RR metabolites and their respective catalytic enzymes. This was integrated with different genomic resources to explore associated genes. Based on high fold-change induction of RR metabolites, we identified *TaACT*, *TaDGK* and *TaGLI1* as candidate genes. Physical mapping of *TaACT* (involved in the biosynthesis of coumaroylagmatine and coumaroylputrescine), *TaDGK* (directly involved in the biosynthesis of phosphatidic acid) and *TaGLI1* (indirectly involved in the biosynthesis of phosphatidic acid) within the QTL-2DL region and gene sequencing, revealed that there was no sequence difference in *TaDGK* between NILs. Therefore, *TaACT* was prioritized and the sequence analysis, gene expression and functional characterization of *TaACT* were conducted and reported in the following study.

Chapter III

Identification and characterization of a fusarium head blight resistance gene *TaACT* in wheat QTL-2DL

Udaykumar Kage[1], Shailesh Karre[1], Ajjamada C. Kushalappa[1] and Curt McCartney[2]

[1] Plant Science Department, McGill University, 2111 Lakeshore road, Sainte Anne De Bellevue, Quebec, Canada H9X 3V9; [2]Agriculture and Agri-Food Canada, Morden Research and Development Centre, 101 Route 100, Morden, MB, Canada R6M 1Y5

3.1 Abstract

Fusarium head blight (FHB) resistance in wheat is considered to be polygenic in nature. Cell wall fortification is one of the best resistance mechanisms in wheat against *Fusarium graminearum*, the cause of FHB. Metabolomics approach in our study led to the identification of a wide array of resistance-related (RR) metabolites, among which hydroxycinnamic acid amides (HCAAs), such as coumaroylagmatine and coumaroylputrescine were the highest fold-change RR metabolites in the rachis of a resistant near-isogenic line (NIL-R) upon *F. graminearum* infection. Placement of these metabolites in a secondary metabolic pathway led to the identification of a gene encoding agmatinecoumaroyl transferase, herein referred to as *TaACT*, as a candidate gene. Based on the wheat genome, the *TaACT* is located within a FHB quantitative trait locus on chromosome 2DL (FHB QTL-2DL) between the flanking markers WMC245 and GWM608. Phylogenetic analysis suggested that *TaACT* shares closest phylogenetic relationship with an *ACT* ortholog in barley. Sequence analysis of *TaACT* in resistant and susceptible NILs with contrasting levels of resistance to FHB led to the identification of several single nucleotide polymorphisms (SNPs) and two inversions that may be important for gene function. Further, a role for *TaACT* in FHB resistance was functionally validated by virus-induced gene silencing (VIGS) in wheat NIL-R and based on complementation studies in *Arabidopsis* with the *act*

mutant background. Disease severity, fungal biomass, and RR metabolite analysis confirmed *TaACT* as an important gene in wheat FHB QTL-2DL conferring resistance to *F. graminearum*.

3.2 Introduction

Fusarium head blight (FHB) is a worldwide wheat disease caused by *Fusarium graminearum* that significantly affects yield and grain quality (Bai and Shaner, 1994; Bai and Shaner, 2004; Dexter et al., 1996; Steiner et al., 2004). Many FHB QTL have been identified, but the genes and their functions are largely unknown. Thus, there is an urgent need to identify resistance genes underlying QTL and to decipher resistance mechanisms for their use in breeding programs. The FHB QTL present on chromosome 2DL is one of the major QTL conferring rachis resistance (type II resistance) by inhibiting the spread of pathogen from the initial point of infection, identified from a Wuhan-1 × Nyubai cross (Somers et al., 2003).

Despite significant efforts to identify and characterize the genes underlying FHB QTL, very few have led to new insights. Positional cloning of the QTL-Fhb1 region of chromosome 3B disclosed presence of seven novel genes in the 261 kb region. Transgenic wheat lines were developed for four genes but none of the transgenic lines carrying these genes exhibited rachis resistance (Liu *et al*., 2008). Transcriptomic studies involving NILs with QTL-3BS and QTL-5A have also identified many differentially expressed genes (Schweiger *et al*., 2013). RNA-Seq analysis of Wangshuibai and its FHB susceptible mutant with deletion of the QTL-Fhb1 region identified several differentially expressed genes but none affected rachis resistance (Xiao *et al*., 2013). Recently, gene expression profiling of NILs containing QTL-2DL revealed eight candidate genes, only one of which was localized on the chromosome 2DL (Long *et al*., 2015). Although several candidate genes were identified in most of the studies, none explained durable resistance mechanisms. Also, there were only a few attempts towards functional characterization of the genes. The application of new tools could help in understanding the genetic determinants underlying the FHB QTL. The functional characterization of mapped QTL using an alternative approach, such as metabolomics, is promising tool to decipher resistance mechanisms and identify gene underlying FHB resistance (Kushalappa and Gunnaiah, 2013). Such an approach led to the identification of several RR metabolites in barley (Bollina *et al*., 2010; Kumaraswamy *et al*., 2011) and wheat (Gunnaiah *et al*., 2012). In potato, RR metabolites and also their

biosynthetic resistance genes were identified by this strategy (Pushpa *et al*., 2013; Yogendra *et al*., 2015; Yogendra *et al*., 2014).

Hydroxycinnamic acid amides (HCAAs), a class of several complex secondary metabolites produced in the phenylpropanoid pathway, are induced in plants in response to pathogens (Gunnaiah *et al*., 2012; Muroi *et al*., 2009; Muroi *et al*., 2012;von Röpenack *et al*., 1998). HCAAs reduce pathogen advancement through their antimicrobial and cell wall reinforcement properties (Ishihara *et al*., 2008; Keller *et al*., 1996; Miyagawa *et al*., 1995; Schmidt *et al*., 1998). HCAAs such as coumaroylagmatine, coumaroylputrescine, feruloylagmatine and feruloylputrescine were identified as effective defense metabolites in *Arabidopsis thaliana* rosette leaves infected with *Alternaria brassicicola* (Muroi *et al*., 2009). HCAAs are biosynthesized by condensation of hydroxycinnamoyl-CoA thioesters produced from phenylalanine via the phenylpropanoid pathway with aromatic amines by amine specific hydroxycinnamoyl transferases (Edreva *et al*., 2007; Facchini *et al*., 2002).

We identified several fold-change differences in HCAA metabolites including coumaroylagmatine and coumaroylputrescine in FHB QTL-2DL NIL-R compared to the susceptible NIL (NIL-S). *TaACT* was identified as gene responsible for biosynthesizing these high-fold metabolites and is found within QTL-2DL region. Transcript expression, disease severity, and fungal biomass were also studied. Further, functional characterization of *TaACT* was performed using VIGS in NIL-R and a complementation study in an *Arabidopsis* mutant lacking the *AtACT* gene.

3.3 Material and Methods

3.3.1 Plant material and experimental layout

NILs carrying resistant and susceptible alleles of QTL-2DL were derived from a BW301 × HC374 cross (McCartney et al., 2007). BW301 is a FHB susceptible, hard red spring wheat line from western Canada and HC374 is a resistant line derived from Wuhan-1. The experiment was laid out in a randomized complete block design (RCBD) with two genotypes (resistant and susceptible NILs), two inoculations (pathogen and mock-solution) and five replications over time to include sufficient block effect. Initially, five seeds were planted per pot and later each pot was maintained at only three plants. Plants were grown in a greenhouse which was maintained at 23±2 °C with a 16 h light and 8 h of dark.

3.3.2 Pathogen production and inoculation

F. graminearum isolate GZ-3639 was grown on potato dextrose agar (PDA) plates incubated at 26 °C for 4days. For spore production, *F. graminearum* was further sub-cultured on Rye B agar media and kept inverted for another 3 days by exposing the plates to UV light. Macroconidia were harvested from 7 day old culture. Spore concentration was determined using a haemocytometer (American Scientific Products, USA), and the final concentration was adjusted to 1×10^5 macroconidia ml^{-1} (Chamarthi et al., 2014). At 50 % anthesis, three alternate spikelets of ten spikes per replicate were individually inoculated with 10 µl fungal spore suspension, containing 1×10^5 macroconidia ml^{-1} or mock-solution (water) using a syringe with an auto dispenser (GASTIGHT 1750DAD, Reno, USA). Inoculated plants were covered with water sprayed polythene bags to maintain high moisture content. At 48 hr post inoculation (hpi), the bags were removed.

3.3.3 Sample collection, metabolite extraction and metabolite analysis using liquid chromatography-high resolution mass spectrometry (LC-HRMS)

At 72 hpi, ten inoculated spikes per replicate were harvested. A spike region, with 3 inoculated and 3 uninoculated pairs of spikelets was harvested. Spikelets and rachis samples were separately collected, immediately frozen in liquid nitrogen and stored at -80 °C until further use. Out of ten, five rachis samples (remaining five were used for histochemical analysis) were ground in liquid nitrogen and the metabolites were extracted in 60 % ice cold aqueous methanol. The extract was sonicated for 15 min at 25 °C and centrifuged. The supernatant was filtered and then 5µl of the clear sample extract was used for metabolite analysis using LC-HRMS (at IRCM, Montreal, Canada), following previously established protocol (Bollina *et al*., 2010).

3.3.4 Data processing using MZmine software and statistical analysis

The output data Xcaliber RAW files from LC-HRMS were converted into mzXML format. Converted files were imported into the bioinformatics tool MZmine2 for peak de-convolution, peak detection, and spectral filtering (Katajamaa et al., 2006). The observed monoisotopic masses (negative ionization) and their respective abundances (relative intensity) were imported into MS-Excel. Relative peak intensities of monoisotopic masses of metabolites were subjected to Students *t*-test (SAS v 9.3), in pair-wise treatment combinations (RP vs RM, RM vs SM, SP

vs SM and RP vs SP, where RP = resistant NIL inoculated with the pathogen, RM= resistant NIL inoculated with a mock solution, SP = susceptible NIL inoculated with the pathogen, SM = susceptible NIL inoculated with mock-solution). Treatment significant metabolites (P<0.05) were retained for further analysis. Metabolites present in significantly higher abundance in resistant as susceptible NIL were termed as RR metabolites. These metabolites were grouped into RR constitutive (RRC=RM>SM) and RR induced (RRI = (RP>RM) > (SP>SM)) metabolites. The fold-change in abundance of metabolites in NIL-R was calculated relative to NIL-S (NIL-R/NIL-S) (Gunnaiah et al., 2012). Only selected high fold-change (>2) RRI metabolites were prioritized for further candidate gene identification.

3.3.5 Putative metabolite identification

RR metabolites were putatively identified based on three criteria: i) Accurate mass match with metabolites reported in several databases, such as PlantCyc, METLIN, KNApSAcK, LIPIDMAPS, NIST and KEGG with an accurate mass error, AME ≤ 5 ppm (Kushalappa and Gunnaiah, 2013; Tohge and Fernie, 2010); ii) Fragmentation pattern mass match with databases and literature (Matsuda et al., 2009); iii) *In-silico* confirmation of fragmentation based on Masspec scissor in ChemSketch (ACD labs, Toronto) (Matsuda et al., 2009).

3.3.6 Disease severity and quantification of fungal biomass

To evaluate rachis resistance in wheat genotypes, two NIL-R and NIL-S were planted in an RCBD with three biological replications at three day intervals. At the 50 % anthesis stage, a single pair of spikelets in the middle of the spike (5 spikes / replicate) was point inoculated with 10 µl spore suspension (1×10^5 macroconidia ml^{-1}). The number of diseased spikelets was recorded at 3 day intervals until 15 days post inoculation (dpi). Spikelets with both dark brown discoloration and bleaching symptoms were considered as diseased. From these data, the PSD (proportion of spikelets diseased = number of spikelets diseased / total number of spikelets in spike) and the area under the disease progress curve (AUDPC) were calculated (Hamzehzarghani et al., 2008). PSD was analyzed for significance based on the ANOVA using SAS program (SAS v 9.3).

To quantify the fungal biomass a separate experiment was conducted with two treatments (NIL-R and NIL-S) and three biological replications over time. At the 50 % anthesis (GS=65),

three alternate pairs of spikelets, in the middle of the spike, with five spikes per replicate, was point inoculated with 10 µl of spore suspension (1×10^5 macroconidia ml^{-1}). Fungal biomass was quantified in rachis samples collected at 6 dpi as the relative gene copy number of the fungal housekeeping gene, trichothecene biosynthetic cluster (*Tri6*). Genomic DNA was isolated from rachis samples using a DNeasy Plant Mini Kit (Qiagen, Canada) and DNA quality was assessed by gel electrophoresis on 1% agarose gel and quantified by nano-drop (Thermo-Scientific, USA). Equal quantities of DNA (20 ng) were used for relative fungal biomass quantification in the NILs under study. Quantitative PCR (qPCR) was performed using *Tri6* primers. The abundance of *Tri6* gene was normalized with *TaActin* and the results obtained from qPCR experiment were used to estimate the fungal biomass (Kumar et al., 2015).

3.3.7 Physical localization of QTL-2DL and identification of *TaACT* gene

The presence of the SSR markers WMC245, GPW8003, GWM539 and GWM608 was used to define the interval for QTL-2DL. Sequence of WMC245 was retrieved from available GrainGenes database and markers GPW8003, GWM539 and GWM608 were sequenced in our lab. We directly sequenced the PCR products and subjected to a BLASTN (Altschul et al., 1990) search on the International wheat genome sequencing consortium (IWGSC) database for physical localization of the QTL (We considered only the best 2DL BLAST hits). High fold-change RRI metabolites were mapped in metabolic pathways to identify the catalytic enzymes and their coding genes. Sequences of these genes were searched by BLASTN against the IWGSC database to confirm their co-localization within the predicted QTL-2DL region. Contigs identified as best hits were retrieved from the database and gene prediction was done using the SoftBery – FGENESH program (Solovyev et al., 2006) to study gene structure. The identified gene was amplified using specific primers designed using the NCBI Primer-BLAST tool (Ye et al., 2012).

3.3.8 Cloning, sequencing and sequence analysis of *TaACT* gene

Genomic DNA was isolated from NILs using a DNeasy Plant Mini Kit (Qiagen, Canada) and used for the amplification of full length *TaACT* gene using gene specific primers. PCR was performed as follows: Initial denaturation at 95 °C for 5 min, followed by 35 cycles of 94 °C for 30 s, 55°C for 1 min, 72 °C for 2 min, followed by a final extension at 72 °C for 10 min. The

PCR product was separated by electrophoresis through a 1 % agarose gel. A band size corresponding to ~1350 bp was purified from the gel, cloned into the pGEM-T Easy vector (Promega, Canada), and Sanger sequenced (Genome Quebec, McGill University). The sequence of *TaACT* (Accession No. KT962210) was deposited in the NCBI database. The sequences from both the NILs were aligned to identify variations using MultAlin (Corpet, 1988). MOTIF Search tool (http://www.genome.jp/tools/motif/) was used to see the presence of conserved domains in translated amino acid sequences. The Phylogey.fr (http://www.phylogeny.fr/) program was used to perform a multiple sequence alignment and to construct the phylogenetic tree.

3.3.9 RNA isolation and candidate gene expression based on semi-qPCR and qPCR

Total RNA was isolated from five biological replicates using an RNeasy plant mini kit (Qiagen, Canada). Purified total RNA (1-2 µg) was used to reverse transcribe RNA into cDNA using the AffinityScript cDNA synthesis kit (Agilent Technologies, USA). The level of *TaACT* expression was determined using gene specific primers by semi-qPCR at an increasing number of cycles (25, 30, 35, 40 and 45) in three biological replicates. The following PCR conditions were used: initial denaturation at 95 °C for 5 min followed by 36 cycles: 1 min of denaturation at 95 °C, 40 s of annealing at 53 °C, and followed by a final extension of 1 min at 72 °C. qPCR was performed using Qi SYBR Green supermix (BioRad, Canada) in a CFX384^{TM} Real-Time PCR system (BioRad, Canada) in five biological replicates. The gene transcript level was normalized to the *TaActin* transcript levels. PCR results were analyzed using comparative $2^{-\Delta\Delta C}{}_{T}$ method (Livak and Schmittgen, 2001).

3.3.10 Histochemical localization of HCAA's

The five rachis samples in the region of inoculated spikelets, out of ten collected at 72 hpi in the metabolomics study, were stored at -20 °C for further use. Rachis samples were collected at 72 hpi and stored at -20 °C for further use. The cross sections of five rachis samples per treatment at the point of inoculation and with one internode above were used to take sections. Samples were preparation for cryosectioning by embedding tissues in cryomoulds containing Shandon CRYOMATRIX (Richard-Allan Scientific, Kalamazoo, USA). Cryosectioning (15 µm) was carried out using a cryotome (Leica, CM1850, Canada) machine at -20 °C and sections were collected on slides coated with 5% 3-aminopropyltriethoxy-silane (APES) solution. Sections

were washed with distilled water and stained with Neu's reagent (1% 2-amino ethyl diphenylborinate (Sigma Aldrich, Canada) prepared in absolute methanol) for 5 min and mounted in 15% glycerol. Stained samples were observed under a confocal microscope (Nikon, Eclipse E800, USA) for HCAA chemifluorescence with excitation at 405 nm fitted with emission filter HQ442/45.

3.3.11 Expression and purification of recombinant TaACT protein in *E. coli*

The coding region of the *TaACT* gene was amplified from cDNA using primers containing *EcoRI* and *BglII* restriction sites. The PCR product was digested with *EcoRI* and *BglII*, the fragment was ligated into the trees-His B vector (Invitrogen, USA). Recombinant vector and empty vector without cloned gene were transformed into *E. coli* BL21 cells and grown in Luria Bertani medium at 28 °C to an optical density of 0.6 at 600 nm (A_{600}). The induction of expression was carried out at 18 °C for 15 h by the addition of isopropyl-1-thio-D-galactopyranoside (IPTG) to a final concentration of 1 mM. After 15 h, a 1 ml sample from both recombinant and empty suspension was collected, centrifuged at 10, 000 ×*g*, processed further, and the expression was confirmed on 12 % sodium dodecyl sulfate-polyacrylamide gel (SDS-PAGE). Remaining cells were immediately pelleted by centrifugation at 4 °C. The pellet was resuspended in 1X LEW buffer (50 mM NaH_2PO_4, 300 mM NaCl, pH 8.0) and cells were lysed by adding lysozyme (1 $mgml^{-1}$), incubating at 4 °C for 1 h, followed by sonication. The supernatant was collected after centrifugation at 12,000 ×*g* for 20 min at 4 °C and purification was achieved using nickel-nitrilotriacetic acid (Ni-NTA) column (Affimetrix, Canada). Purified protein was detected by Coomassie Brilliant Blue Staining after electrophoresis in 12 % SDS-PAGE. The average protein size of TaACT was predicted using ExPAsy-Compute pI/Mw tool (http://web.expasy.org/compute_pi/).

3.3.12 Virus-induced gene silencing of *TaACT*

The PCR product amplified from cDNA using VIGS primers (Table 3.2) was used to construct the silencing vector. VIGS primers were designed using the NCBI Primer-BLAST tool (Ye et al., 2012). A 271-bp fragment of the *TaACT* gene with efficient siRNA generation and no off-target genes in the modified viral genome using siRNA Scan tool (http://bioinfo2.noble.org/RNAiScan.htm) and a BLAST search of fragment against GenBank

database was chosen. The PCR product was cloned into the pGEM-T Easy Vector (Promega Corp., WI, USA), confirmed by sequencing, and excised using *NotI* (New England Biolabs, MA, USA), thereby, generating *NotI* ends. These fragments were subsequently cloned in the *NotI* site of pSL038-1, a plasmid encoding a modified BSMV γ genome segment with a cloning site downstream of the γb gene (Cakir and Scofield, 2008). Clones containing the fragments in the γ vector were sequenced to confirm their identity and subsequently used for gene silencing.

The procedures for *in-vitro* transcription of α, β and γ RNAs of the BSMV genome were as described before (Scofield et al., 2005). *In-vitro* synthesized BSMV RNAs were three times rub-inoculated on both flag leaf and spikes at growth stage 50-55 (Zadoks*et al*., 1974) with a solution containing 1:1:1 µl (α, β and γ RNAs) + 22.5 µl of abrasive buffer (1% sodium pyrophosphate, 1% bentonite, 1% celite in 0.1 M glycine, 0.06 M dipotassium phosphate). Ten spikes per replicate were infected with each of BSMV + *TaACT* insert and BSMV:0, respectively, with five biological replicates. Construct BSMV:0 and BSMV + PDS (phytoene desaturase) served as negative and positive controls, respectively. An experiment involving VIGS of PDS resulted in photo-bleaching symptoms in the wheat spikes 12 days after the viral inoculation (Fig. 3.12). At 13 days after the viral infection, five spikes each in the negative control and test treatment were inoculated with 10 µl *F. graminearum* spore suspension (1×10^5 macroconidia ml^{-1}) and covered with a plastic cover to maintain high humidity. After 48 hpi with *F. graminearum*, plastic covers were removed and samples were collected at 72 hpi for metabolite analysis and qPCR to measure the transcript abundance of *TaACT*. Similarly, total DNA isolated from 6 dpi samples was used in the fungal biomass study. Fungal biomass was quantified in NIL-R+$BSMV_0$ (Non-silenced), NIL-R+$BSMV_{TaACT}$ (silenced) and NIL-S.

3.3.13 *TaACT* functional complementation study in *Arabidopsis*

The *TaACT* alleles from NIL-R and NIL-S were over-expressed in an *Arabidopsis act* mutant (At5g61160) background (obtained from TAIR - The Arabidopsis Information Resource) for functional validation and also to determine the effect of SNPs associated with resistance. The coding sequence was amplified from cDNA and cloned into a ZeBaTA-based expression vector (Chen et al., 2009). Constructs were introduced into *Agrobacterium tumefaciens* strain GV3101 by the freeze-thaw method (Weigel and Glazebrook, 2005). *Agrobacterium* (GV3101) carrying the recombinant constructs was cultured in 5 ml liquid LB with 50 mg L^{-1} hygromycin. One ml

of this feeder culture was used to inoculate 500 ml of liquid LB containing 50 mg L^{-1} hygromycin and grown at 28°C for 16 - 24 hr (OD = 1.5). *Agrobacterium* was separated from the LB medium by centrifugation at 4000 rpm for 10 min at room temperature, and cell pellets gently were re-suspended in 5 % sucrose solution. To this mixture 0.02 % Tween-20 was added and mixed well. *Arabidopsis ACT* gene T-DNA insertion mutant plants (At5g61160) deficient in coumaroylagmatine and coumaroylputrescien were grown. At the flowering stage, plants were transformed by the floral dip method. Transformed plants were covered with plastic cover for 24 hr to maintain high humidity. After maturity, seeds were collected and used to screen primary transformants on selection plates (half strength of Murashige and Skoog medium + 50 mg L^{-1} hygromycin + 100 mg L^{-1} carbenicillin) after sequentially sterilizing them with 70 % ethanol and 50 % bleach. Homozygous T1 lines for four transgenic events were identified by examining the segregation for hygromycin resistance. Progenies derived from transgenic events were 100% hygromycin resistant and homozygous T2 lines derived from these were used for further testing. Samples were collected from 6 week old plants for targeted metabolite analysis with three biological replicates.

A set of 25 T2 plants each with *TaACT* of NIL-R and NIL-S were inoculated with *F. graminearum* at the flowering stage to determine the effect on *F. graminearum* infection in 4 independent experiments. Inoculation of *Arabidopsis* plants was performed by placing 10 µl droplets of spore suspension (1×10^5 macroconidia ml^{-1}) on the open flowers of 6 week old plants. Inoculated plants were covered with a plastic bag for 3 days to maintain high humidity and symptom development was monitored. The inoculated flowers were diseased in four dpi and by six dpi the disease spread to uninoculated flowers within the inflorescence. At 6 dpi, plants were categorized according to the symptoms into two classes: i) number of dead inoculated flowers (Fig. 3.11 a-2 - right); ii) number of surviving inoculated flowers (Fig. 3.11 a-2 - left) (Ferrari *et al*., 2012). Data were analyzed using a Student *t*-test. At the same time, samples were collected and fungal biomass was quantified using the same method as in wheat with *protodermal factor 2 (AtPDF2)* used as the *Arabidopsis* reference gene at 6 dpi with 3 biological replicates.

3.4 Results

3.4.1 Disease severity in NILs

The disease severity of NILs was assessed. Dark brown discoloration due to fungal infection was observed at 3 dpi in inoculated spikelets of a NIL-S, whereas it was observed only at 6 dpi in NIL-R. Uninoculated spikelets above and below the inoculated spikelets in NIL-S were diseased and bleached at nine dpi. At 15 dpi, almost all of the spikelets were diseased in NIL-S, whereas only a few were diseased in NIL-R (Fig. 3.1). The PSD (Fig. 3.2a) and AUDPC (Fig. 3.2b) at 15 dpi were significantly *(P<0.05)* lower in the NIL-R (0.17 and 1.48, respectively) than in NIL-S (0.36 and 2.33, respectively).

The fungal biomass in rachis samples, estimated by measuring the relative transcript levels of the *F. graminearum* housekeeping gene *Tri6*, was significantly *(P<0.05)* lower in NIL-R than in NIL-S (Fig. 3.2c), confirming the discrimination of resistance based on disease severity. This indicated that the NIL-R was significantly more resistant than the NIL-S.

3.4.2 Metabolite profiling in NILs

Metabolite profiling of wheat rachis inoculated with *F. graminearum* at 72 hpi identified a wide range of metabolites. Among these, the abundance of two HCAAs, coumaroylagmatine and coumaroylputrescine, were 28- and 9.5-fold higher in NIL-R than in NIL-S, respectively (Table 3.1). No other HCAAs were detected.

3.4.3 Histochemical localization of HCAAs

The induction of coumaroylagmatine and coumaroylputrescine in NIL-R was confirmed by specific staining and fluorescence of cross sections of infected rachis. Strong chemifluorescence (405 nm, the typical spectrum of HCAA) was observed in pathogen-infected NIL-R cells compared to NIL-S and also compared to mock treated NIL-R and NIL-S (Fig. 3.3). This high chemifloroscence was considered to be mainly due to HCAAs as we did not find other high-fold phenolics or flavones, which also can be stained with Neu's reagent.

3.4.4 Identification of candidate gene *TaACT* in the QTL-2DL

The two HCAA candidate metabolites were mapped on metabolic pathways to identify their biosynthetic enzymes. Agmatinecoumaroyl transferase (ACT) is a rate-limiting enzyme involved in the biosynthesis of these metabolites (Burhenne et al., 2003; Muroi et al., 2009; Muroi et al., 2012). BLAST analysis positioned the closest gene match for this enzyme, *TaACT*, within the

QTL interval on 2DL.The *TaACT* full length gene, including a 546 bp promoter region, was sequenced in genomic DNA from resistant and susceptible NILs. An analysis of TaACT using both genomic DNA and cDNA suggested TaACT to be 1326 bp in length and was devoid of introns. Sequence comparison of *TaACT* from NIL-R and the *T. aestivum* cv. Chinese Spring showed that the gene sequence is highly conserved. Comparison of the DNA sequences between NIL-R and NIL-S revealed 2 inversions (2 bp) and 67 SNPs (Fig. 3.4 & 3.5). Conserved domain analysis of the encoded protein using the MOTIF Search tool (http://www.genome.jp/tools/motif/) revealed the presence of a transferase domain. The predicted protein consisted of two consensus motifs (Fig. 3.6a): (i) an HLVSD motif that starts at His-153, and is identical to the HXXXD motif commonly found in the transferase family, which is responsible for CoA-dependent acyl transfer (St-Pierre et al., 1998) and (ii) an DFGGGQP motif that starts at residue Asp-387, is a motif of unknown function (Burhenne et al., 2003). This protein also has an N-terminal 15 amino acid sequence MKITVLSSRAVKPDY that is found in most other reported ACTs (Burhenne et al., 2003). TaACT protein sequence variation between NILs is showed in Fig. 3.6b. BLASTP search of *TaACT* in UniProt database indicated 83% identity with barley ACT (*HvACT*) protein. Phylogentic analysis further demonstrated close relatedness of these orthologs (Fig. 3.7). Plant acyltransferases form five evolutionary groups (Burhenne et al., 2003) and *HvACT* falls in the fifth group. This group includes plant acyltransferases that are involved in transferring acyl groups to the acceptors. For confirmation of predicted protein size (~48 kDa), the *TaACT* was heterologously expressed in *E. coli* (BL21) cells. The protein extract from a cell supernatant was analyzed on the SDS-PAGE. A protein band with molecular weight approximately 48 kDa was observed (Fig. 3.8), comparable to the reported *HvACT* (Burhenne et al., 2003). Our results confirmed the presence of *ACT* gene within the QTL region on 2DL, thus, suggesting a possible link of this gene to the induction of high levels of coumaroylagmatine and coumaroylputrescine observed following pathogen inoculation.

3.4.5 Expression of gene *TaACT* based on semi-quantitative PCR and qPCR

The expression of *TaACT* was examined using semi-qPCR and RT-qPCR. Although semi-qPCR did not reveal any expression in mock treated samples of NIL-R and NIL-S; at 72 hpi, high expression was observed in NIL-R, relative to NIL-S upon pathogen inoculation (Fig. 3.9a). This suggested that *TaACT* was induced in wheat rachis only after pathogen inoculation. This was

further confirmed by semi-qPCR using increased template (cDNA) quantity from 20 to 100 ng (data not shown), and also by qPCR, which indicated the expression to be 3.2-fold higher in NIL-R relative to NIL-S *(P<0.05)* (Fig. 3.9b).

3.4.6 Functional characterization of *TaACT* using VIGS

At 72 hpi of *F. graminearum*, silenced plants (NIL-R+BSMV$_{TaACT}$) showed significant *(P<0.05)* (74.29%) reduction in *TaACT* transcript abundance compared to non-silenced plants (NIL-R+BSMV$_0$) confirming the silencing of target gene in wheat rachis (Fig. 3.10a). Metabolite analysis revealed that the abundance of coumaroylagmatine and coumaroylputrescine was significantly reduced in NIL-R+BSMV$_{TaACT}$ compared to NIL-R+BSMV$_0$ by 6.4 and 3.2-fold, respectively (Fig. 3.10b). The fungal biomass in NIL-R+BSMV$_{TaACT}$ was significantly higher than in NIL-R+BSMV$_0$ (1.86-fold, *P<0.05*) (Fig. 3.10c), whereas the fungal biomass in NIL-R+BSMV$_{TaACT}$ was 1.47-fold lower than in NIL-S, indicating possible involvement of other genes associated with the QTL-2DL.

3.4.7 Functional characterization of *TaACT* based on complementation study in *Arabidopsis*

Metabolite profiling of transgenic *Arabidopsis* plants revealed significantly (*P<0.05*) higher abundance of coumaroylagmatine (4.1-fold) and coumaroylputrescine (2.5-fold) in plants over-expressing *TaACT* in NIL-R (*TaACT*_NIL-R) compared to NIL-S (*TaACT*_NIL-S) (Fig. 3.11a-1). Further, the inflorescence of transgenic *Arabidopsis* plants were inoculated with *F. graminearum* and the disease progress was monitored. At 6 dpi, plants were grouped into diseased and not diseased (Fig. 3.11a-2). The percentage of dead inflorescences was significantly (*P<0.01*) reduced in NIL-R *TaACT* over-expressing plants compared to NIL-S *TaACT* (Fig. 3.11b). At the same time, fungal biomass was also significantly reduced. Fungal biomass in *TaACT*_NIL-S was 3.8-fold higher than in *TaACT*_NIL-R over-expressing plants (Fig. 3.11c). Though the *TaACT* gene from NIL-R can be used to replace non-functional genes in commercial wheat cultivars, based on genome editing, the use of specific nucleotide replacement requires further studies to validate the functions of these SNPs.

3.5 Discussion

The present study reports an integrated approach of metabolomics, gene sequencing, gene expression, histochemical studies and heterologous protein expression to identify and validate the existence of a candidate gene *TaACT* in the FHB QTL-2DL region. Furthermore, for the first time in wheat, our study reports the functional characterization of *TaACT* through VIGS and a complementation study in *Arabidopsis*. Taken together, our results revealed the location of the candidate gene *TaACT* in FHB QTL-2DL and its resistance functions against FHB. Its role in resistance and its application in breeding are discussed.

3.5.1 FHB resistance in NIL-R is due to high-fold induction of HCAAs

Resistance in plants is controlled by hierarchies of resistance (*R*) genes, including regulatory genes and the regulated genes that biosynthesize RR metabolites and proteins, which directly suppress the pathogen through their antimicrobial and cell wall reinforcement properties (Kushalappa et al., 2016). Resistance in wheat to the spread of *F. graminearum* through rachis is mainly due to the production of phytoalexins that are antifungal, and/or to the deposition of phenylpropanoids to reinforce the cell wall, thus, preventing further progress of pathogens (Gunnaiah et al., 2012). Coumaroylagmatine and coumaroylputrescine were induced in high-fold change in resistant NILs. The reinforcement of cell walls by these compounds was confirmed by histochemical localization of HCAAs. Deposition of feruloyl-3'-methoxytyramine, feruloyltyramine, and *p*-coumaroyltyramine have been reported on onion cells at infection sites following inoculation with *Botrytis allii* (Ishihara et al., 2008). HCAAs including coumaroylagmatine and coumaroylputrescine were proved to be antifungal and highly induced in *Arabidopsis thaliana* rosette leaves infected with *Alternaria brassicicola* (Muroi et al., 2009) and in transgenic torentia expressing *AtACT* to resist *Botrytis cinerea* and arthropod herbivores (Muroi et al., 2012). Accumulation of coumaroylagmatine and its antifungal effect was reported in barley leaves infected with *Erysiphe graminis* f. sp. *hordei* (von Röpenack et al., 1998). HCAAs such as, *p*-coumaroylserotonin and feruloylserotonin were detected in rice leaves infected with *Bipolaris oryzae* (McLusky et al., 1999). Several HCAAs, including feruloylputrescine, *p*-coumaroyltyramine, N-feruloyltyramine, 4-coumaroyl-3-hydroxyagmatine, feruloylagmatine, coumaroylagmatine, terrestriamide, and feruloylserotonin, were induced in potato leaves against *Phytophthora infestans* (Keller et al., 1996; Pushpa et al., 2013; Yogendra et al., 2014). In our study, cell wall reinforcement in NIL-R was associated with lower disease

severity and fungal biomass relative to NIL-S. Accordingly, our results suggest that coumaroylagmatine and coumaroylputrescine are at least partly responsible for resistance in QTL-2DL against the spread of *F. graminearum* through rachis.

3.5.2 *TaACT* induced high levels of coumaroylagmatine and coumaroylputrescine

Coumaroylagmatine and coumaroylputrescine were placed within metabolic pathways to identify their respective biosynthesizing enzymes and genes. This led to the identification of the *ACT* gene, which is known to catalyze the last step of biosynthesis of these two HCAAs (Burhenne et al., 2003; Muroi et al., 2009; Muroi et al., 2012). We temporarily located the FHB QTL-2DL on wheat chromosome 2DL and the gene encoding *TaACT* within the QTL-2DL region. This gene was sequenced and confirmed by comparing with the sequences and conserved protein domains of the previously characterized *HvACT* gene (Burhenne et al., 2003). A close phylogenetic relationship with *HvACT* confirmed that *TaACT* is a group five acyltransferase, which is involved in transferring acyl groups to the acceptors. The recombinant protein was expressed in *E.coli* and the protein size is comparable to the protein size of barley *HvACT*. In barley and wheat, the co-existence of hydroxycinnamoyl agmatines and putrescines has been demonstrated, and they are induced by the same biological stimuli (Fester et al., 1999; Ogura et al., 2001). This confirms that the *TaACT* in wheat QTL-2DL is responsible for the production of coumaroylagmatine and coumaroylputrescine. In addition, based on semi-qPCR and RT-qPCR studies, it was confirmed that *TaACT* was expressed only after pathogen invasion. Similarly, in *Arabidopsis*, the *AtACT* gene was highly expressed after pathogen inoculation (Muroi et al., 2009).

3.5.3 Functional validation of *TaACT*

To further assess the effect of *TaACT* on resistance to spread of *F. graminearum* through rachis, it was silenced in NIL-R. The abundance of *TaACT* and its respective metabolites coumaroylagmatine and coumaroylputrescine were significantly reduced after silencing. Fungal biomass was increased in silenced NIL-R relative to non-silenced. In the same way, transient gene silencing of MYB10 decreased flavonoid/phenylpropanoid metabolism in strawberry (Medina-Puche et al., 2014). Silencing of a hydroxycinnamoyl-CoA:hydroxycinnamoyl transferase gene in *N. benthamiana* stems inhibited the accumulation of a lignin polymer,

dimethoxylated syringyl, affecting cell wall reinforcement (Hoffmann et al., 2004). Similarly, virus-induced silencing of *StWRKY1* significantly reduced the abundance of N-feruloyltyramine, N-feruloyloctopamine, feruloylputrescine, and feruloylagmatine types of HCAAs, compromising late blight resistance by reducing reinforcement of secondary cell walls in potato (Yogendra et al., 2015). Knock-down of *FcWRKY70* in kumquat down-regulated *ADC* (arginine decarboxylase) abundance and decreased putrescine levels were accompanied by compromised dehydration tolerance (Gong et al., 2015).

TaACT gene function was also proved based on a complementation study in *act* mutant *Arabidopsis* lines, which lacked the ability to biosynthesize coumaroylagmatine and coumaroylputrescine. Mutant *Arabidopsis* plants over-expressing *TaACT* from NIL-R had higher abundances of coumaroylagmatine and coumaroylputrescine metabolites compared to plants over-expressing *TaACT* from NIL-S. In addition, the former also resulted in decreased disease severity and amount of fungal biomass, thus confirming that this difference is mainly due to polymorphic sequences at *TaACT.* Model plants have been used to prove the functions of several genes. Transgenic *A. thaliana* expressing a barley UDP-glucosyltransferase exhibited resistance to the mycotoxin deoxynivalenol (Shin et al., 2012). Transgenic expression of polygalacturonase-inhibiting proteins in *Arabidopsis* and wheat increased the resistance to flower pathogen *F. graminearum* (Ferrari et al., 2012). Also, over-expression of *PvPGIP2* was shown to be effective against a wheat foliar pathogen, *B. sorokiniana,* due to increased polygalacturonase-inhibiting proteins (Janni et al., 2008). Taken together, these results provide compelling evidence that *TaACT* is one of the candidate genes responsible for FHB resistance in wheat QTL-2DL, through deposition of HCAAs to reinforce secondary cell walls, thus preventing further spread of fungus throughout rachis.

In conclusion, the *TaACT* gene identified here is an excellent candidate to increase FHB resistance in a controlled greenhouse environment, and certainly it should increase the effectiveness of the resistance under field conditions, especially when combined with other resistance genes; therefore, it can be used in FHB resistance breeding. The polymorphism, based on allele mining, can be searched in commercial cultivars. If non-functional, they can be replaced with either partial (only polymorphic) or full functional gene identified here based on genome editing (Shan et al., 2013). Alternatively, genic markers can be developed for use in

marker assisted breeding (Kage et al., 2015). Pyramiding of additional genes could enable the development of resistant cultivars that may reduce fungicide application.

Table 3.1: Fold change in abundance of resistance related (RR) metabolites detected in wheat rachis following *F. graminearum* inoculation

Observed Mass	AME (ppm)	Name	Molecular formula	Retention time (min)	Fold change in NIL-R relative to NIL-S	Category
276.1592	2.3	Coumaroylagmatine	C14H20N402	12.2	28.7	HCAAs
234.1373	2.2	Coumaroylputrescine	C13H18N202	10.1	9.5	HCAAs

Table 3.2: List of primers used in the experiments

Experiments	Gene/Primer Name	Forward primer (5´- 3´)	Reverse primer (5´- 3´)
Fungal biomass	*Tri6*	TCTTTGTGAGCGGACGGGACTTTA	TGTTGGTTTGTGCTTGGACTCAT
Gene Sequencing	*TaACT*	CACAGACATACAGTGATAGTA CAAGG	CGATGCAAATCTACTCGAGG
Promoter sequencing	*TaACT promoter*	CCAGATCCAATCGCGGTCCGAGGA	GGCGACAAGTGCAAGGTTA
RT-qPCR	*TaACTq*	ACCACGCGATCCGCCGCGAG	CGGCGTGGCGTTCGTCGTCGTT
Protein expression	*TaACT protein*	GACAGATCTATGAAGGTCACCGTGCTCTC	GGTGAATTCCTACTCGAGGTTGTAGCAGC
VIGS fragment	*TaACT VIGS*	GAGGTGGACAGCTGGCTG	GGCACTGCAGATACATTTCAAAAC
VIGS Expression	*TaACT VIGS EXP*	ACCACGCGATCCGCCGCGAG	CGGCGTGGCGTTCGTCGTCGTT
Over expression	*TaACT cDNA*	ATGAAGGTCACCGTGCTCTC	CTACTCGAGGTTGTAGCAG
Reference genes	*TaActin*	ACCTTCAGTTGCCCAGCAAT	CAGAGTCGAGCACAATACCAGTTG
	AtPDF2	TCATTCCGATAGTCGACCAAG	TTGATTTGCGAAATACCGAAC
SSR Markers	*WMC245*	GCTCAGATCATCCACCAACTTC	AGATGCTCTGGGAGAGTCCTTA
	GWM539	CTGCTCTAAGATTCATGCAACC	GAGGCTTGTGCCCTCTGTAG
	GWM608	ACATTGTGTGTGCGGCC	GATCCCTCTCCGCTAGAAGC

Figure 3.1: *F. graminearum* infected spikes of wheat NILs with resistant and susceptible alleles of QTL-2DL, at 15 dpi. The arrows indicate the spikelet inoculated.

Figure 3.2: Disease severity and fungal biomass in NILs, based on visual observations and RT-qPCR following point inoculation of *F. graminearum*; **a)** Proportion of spikelets diseased (PSD); **b)** Area under disease progress curve (AUDPC), calculated based on observations taken every 3 dpi until 15 dpi; **c)** Fungal biomass (relative gene copy number based on RT-qPCR) in resistant NIL and susceptible NIL at 7dpi upon *F. graminearum* inoculation. Significant difference in expression levels of NIL-R as compared to NIL-S using Students *t*-test: $^{*}P<0.05$.

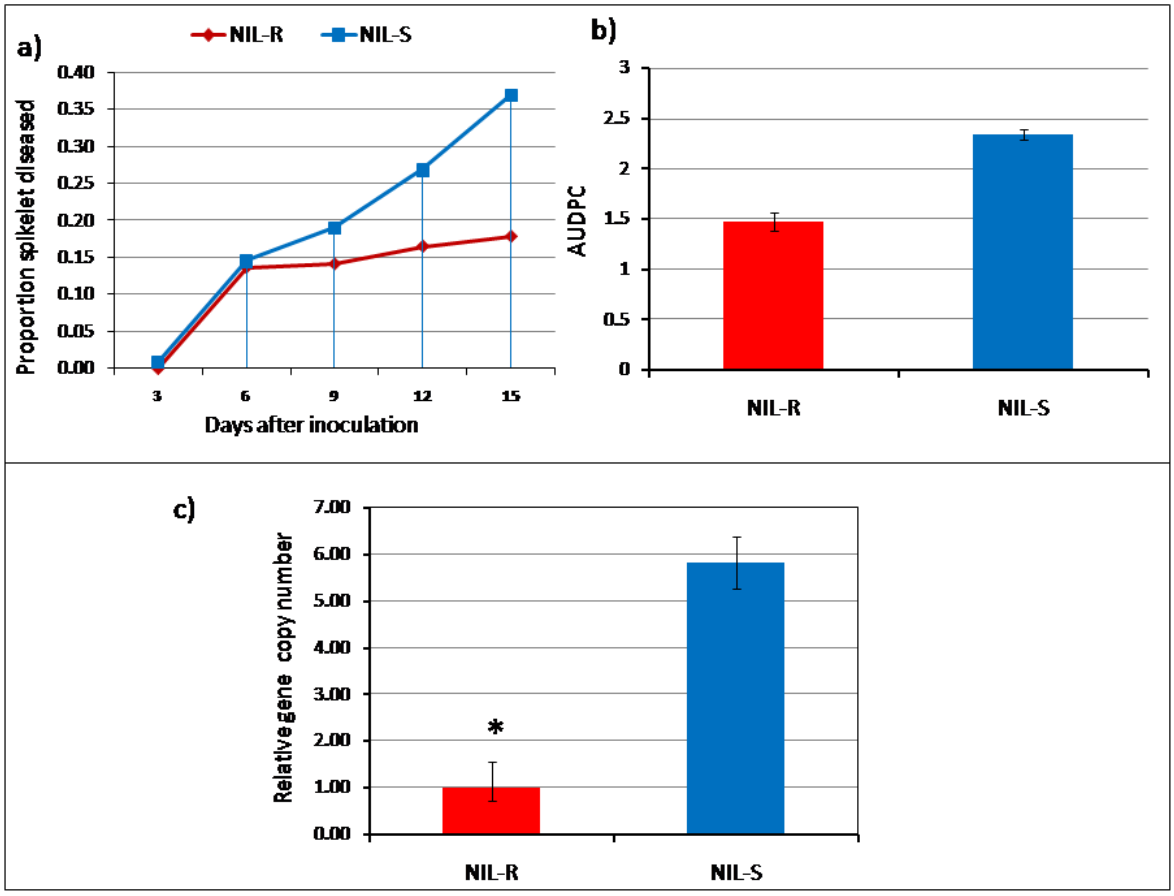

Figure 3.3: a) Histochemical localization of HCAAs in rachis cross sections using laser scanning confocal microscopy; **b)** Histochemical localization of HCAAs in expanded vascular bundles. RP is NIL-R with *F. graminearum* (pathogen) inoculation, RM is NIL-R with mock inoculation, SP is NIL-S with *F. graminearum* inoculation, SM is NIL-S with mock inoculation. The acronyms are: mx is metaxylem, px is protoxylem, ph is phloem and vb is vascular bundle.

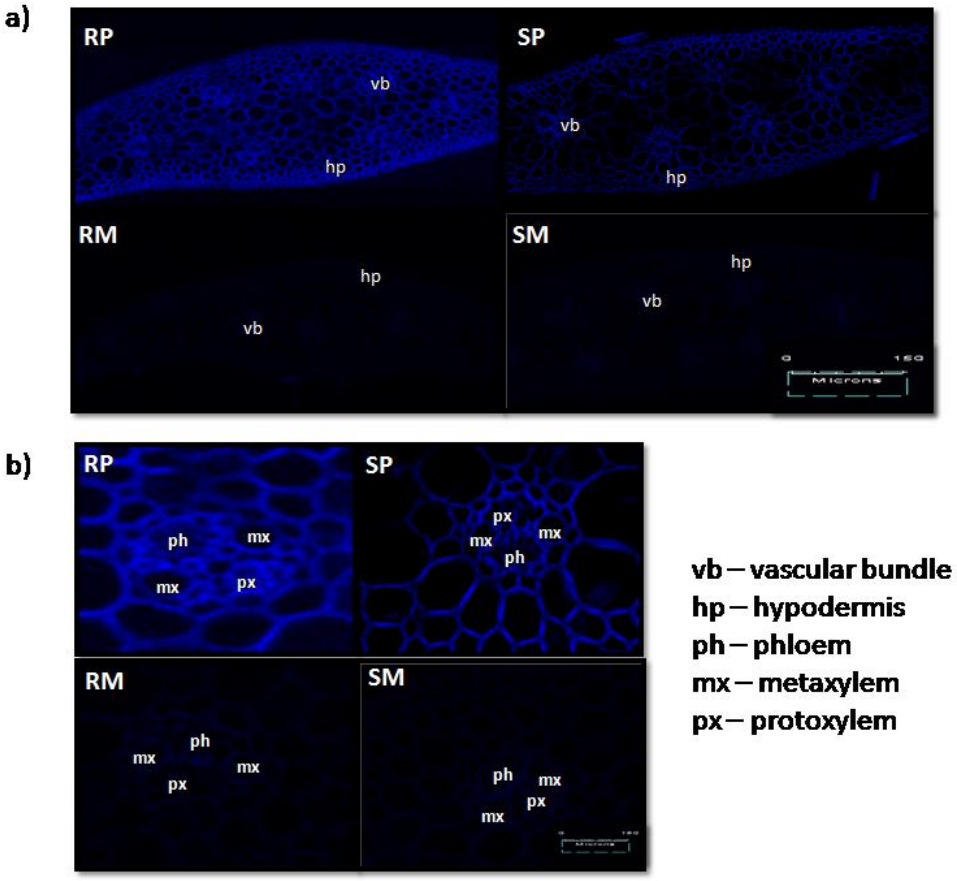

Figure 3.4: Comparison of DNA sequence variation between NIL-R, NIL-S and Chinese spring *TaACT*. Green underlined indicates 5´ and 3´ regions.

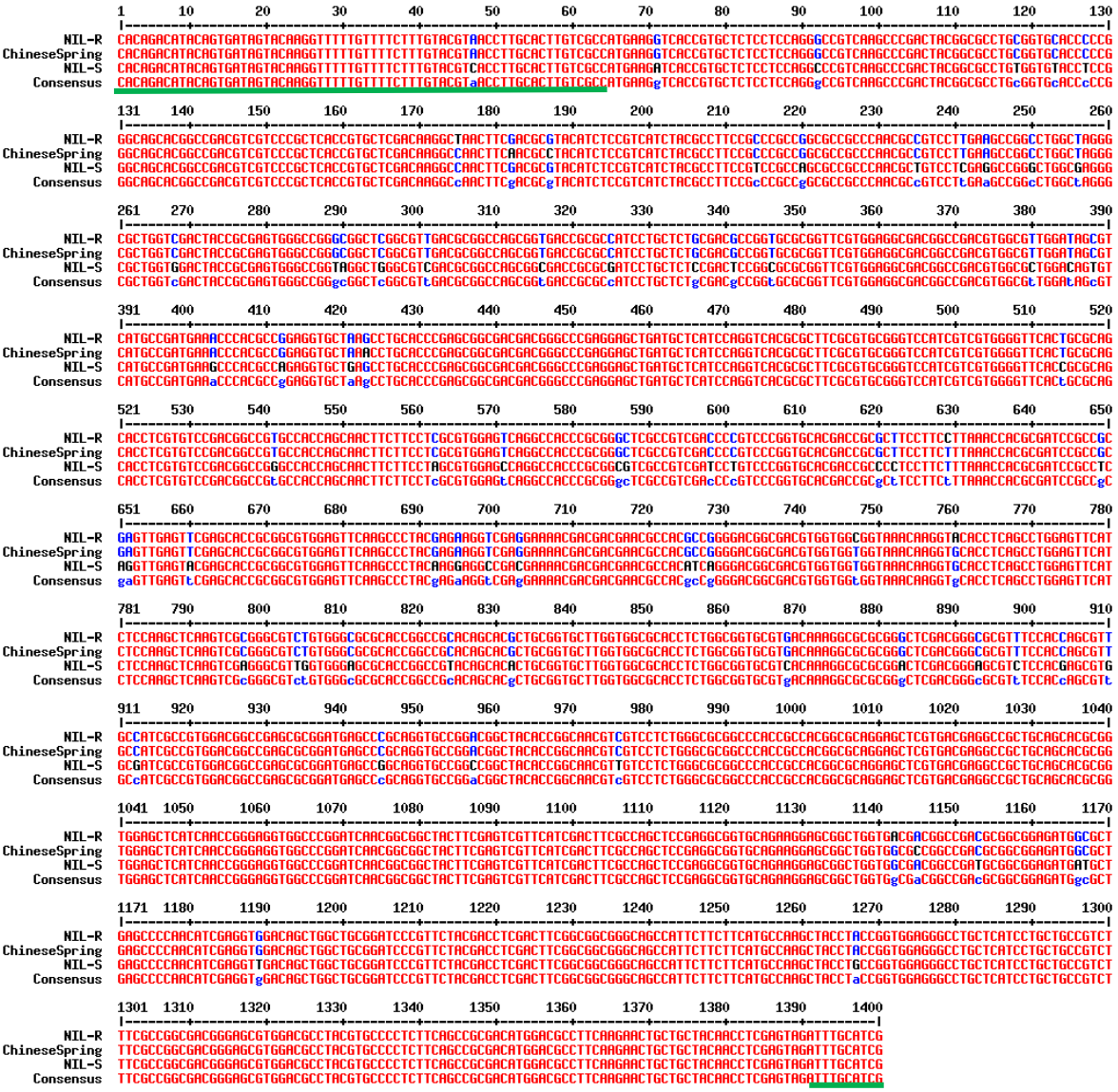

Figure 3.5: Comparison of promoter DNA sequence variation between NIL-R, NIL-S and Chinese spring *TaACT*.

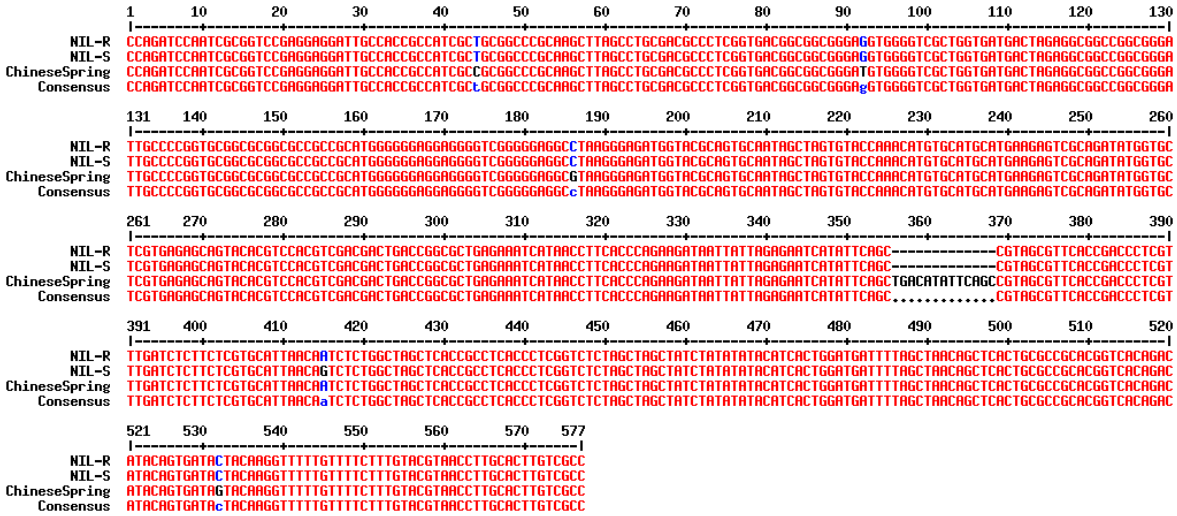

Figure 3.6: a) Amino acid sequence of TaACT. The two amino acid motifs conserved in the super family are underlined below the sequences.

MKITVLSSRAVKPDYGACGAPPGSTADVVPLTVLDKANFDAYISVIYA
FRPPAPPNAVLEAGLARALVDYREWAGRLGVDAASGDRAILLCDAGA
RFVEATADVALDSVMPMKPTPEVLSLHPSGDDGPEELMLIQVTRFAC
GSIVVGFTAQHLVSDGRATSNFFLAWSQATRGLAVDPVPVHDRASFL
KPRDPPRVEFEHRGVEFKPYEKVEENDDERHAGDGDVVAVNKVHLSL
EFISKLKSRASVGAHRPHSTLRCLVAHLWRCVTKARGLDGRVSTSVAI
AVDGRARMSPQVPDGYTGNVVLWARPTATAQELVTRPLQHAVELIN
REVARINGGYFESFIDFASSEAVQKERLVTTADAAEMALSPNIEVDSW
LRIPFYDLDFGGGQPFFFMPSYLPVEGLLILLPSFAGDGSVDAYVPLFSR
DMDAFKNCCYNLE

b) TaACT protein sequence variation between NILs.

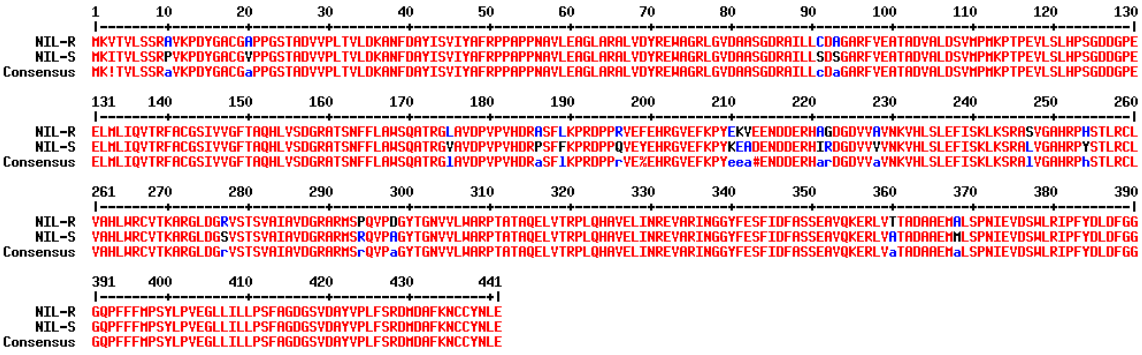

Figure 3.7: Maximum likelihood method of evolutionary analysis of *TaACT*. Protein sequences used for phylogenetic analysis are: HV =agmatinecoumaroyltransferase [*Hordeum vulgare* - AAO73071.1], TaACT= Wheat Agmatinecoumaroyltransferase (*Triticum aestivum* - KT962210), OS = Putative anthranilate N-benzoyltransferase [*Oryza sativa Japonica Group* - AAM74310.1], NT =hydroxycinnamoyl transferase [*Nicotiana tabacum* - AJ507825], AT =hydroxycinnamoyl-CoA shikimate/quinatehydroxycinnamoyl transferase [*Arabidopsis thaliana* - NM_124270], IB = N-hydroxycinnamoyl/benzoyltransferase [*Ipomoea batatas* - AB035183], DC = anthranilate N-hydroxycinnamoyl/benzoyltransferase [*Dianthus caryophyllus* - Z84383], TC2 = 2-debenzoyl-7,13-diacetylbaccatin III-2-O-benzoyl transferase [*Taxus cuspidate*= AAG38049.1], TC1 = 10-deacetylbaccatin III-10-O-acetyl transferase [*Taxus cuspidate* - AAF27621.1], TC3 =taxadienol acetyl transferase [*Taxus cuspidate* - AAF34254.1], TC = 3'-N-debenzoyltaxol N-benzoyltransferase [*Taxus Canadensis* - AAM75818.1], CR =deacetylvindoline 4-O-acetyltransferase [*Catharanthus roseus* - AAC99311.1], PS =salutaridinol 7-O-acetyltransferase [*Papaver somniferum* - AAK73661.1], FA - alcohol acyltransferase [*Fragaria ananassa* - AAG13130.1], CC =acetyl-CoA:benzylalcoholacetyltranferase [*Clarkia concinna* - AAF04784.1], CB = acetyl CoA: benzylalcohol acetyltransferase [*Clarkia breweri* - AAC18062.1], SS =malonylCoA:anthocyanin 5-O-glucoside-6'''-O-malonyltransferase [*Salvia splendens* - AAL50566.1], PF =malonylCoA:anthocyanin 5-O-glucoside-6'''-O-malonyltransferase [*Perilla frutescens* - AAL50565.1], GT = Anthocyanin 5-aromatic acyltransferase [*Gentiana triflora* - BAA74428.1]. Numbers in red represents branch support values.

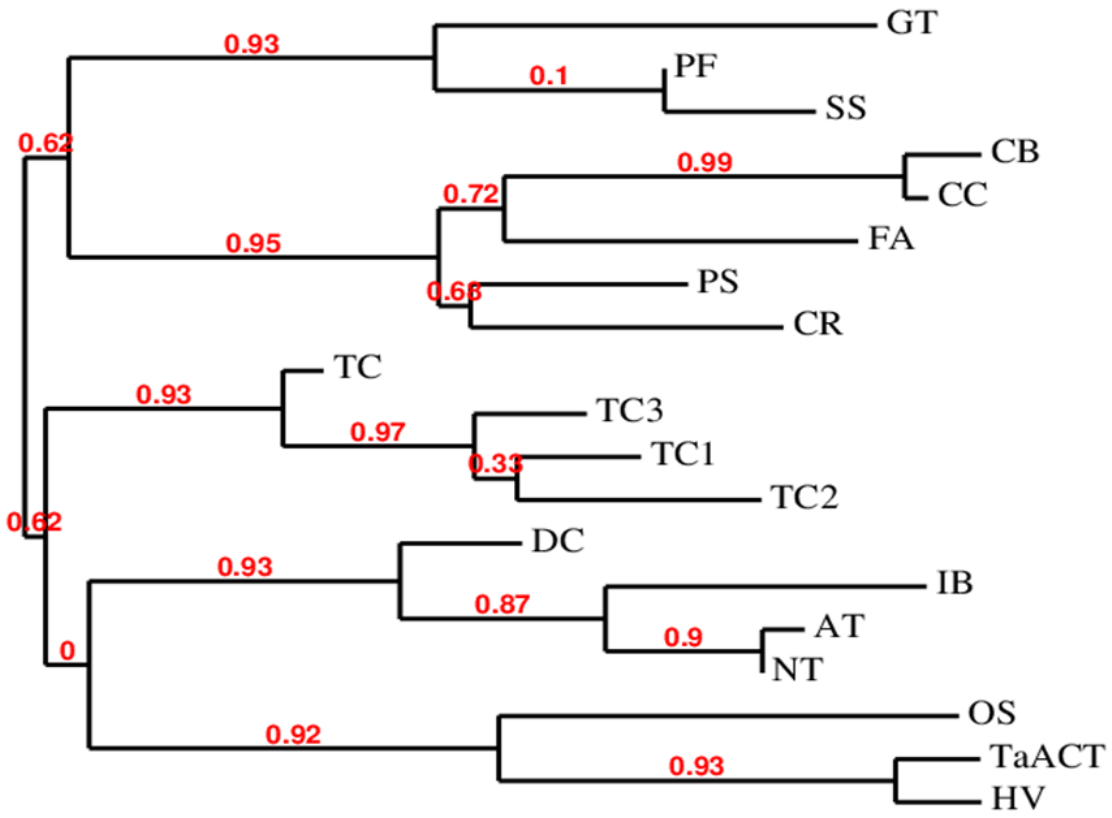

Figure 3.8: Purification of bacterial expressed TaACT. L is Protein marker, S1, S2 & S3, S4 are sequential eluted fractions of recombinant TaACT protein, S5 is a crude TaACT extract. Where, S2 and S3 show purified TaACT protein. The protein size is comparable to the reported barley HvACT protein size (~48 kDa).

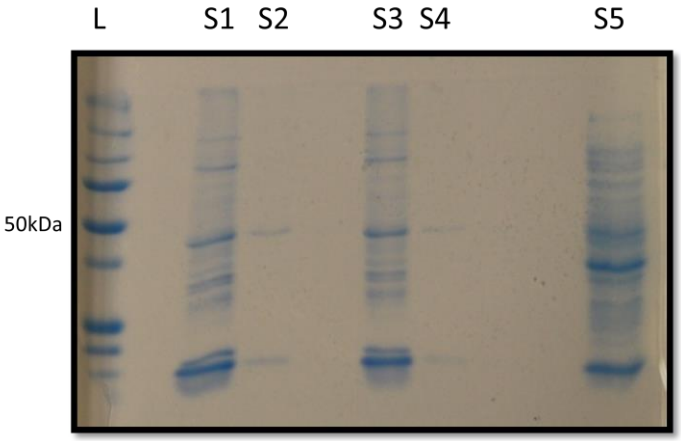

Figure 3.9: Expression of *TaACT* gene in wheat rachis at 72 hpi, **a)** Expression of *TaACT* based on semi-qPCR; **b)** Expression of *TaACT* in pathogen inoculated treatments based on RT-qPCR. *TaActin* was used as internal standard. RM = Resistant mock, RP = Resistant pathogen, SM = Susceptible mock, SP = Susceptible pathogen treatments. Significant difference in expression levels of NIL-R as compared to NIL-S using Students *t*-test: $^{*}P<0.05$.

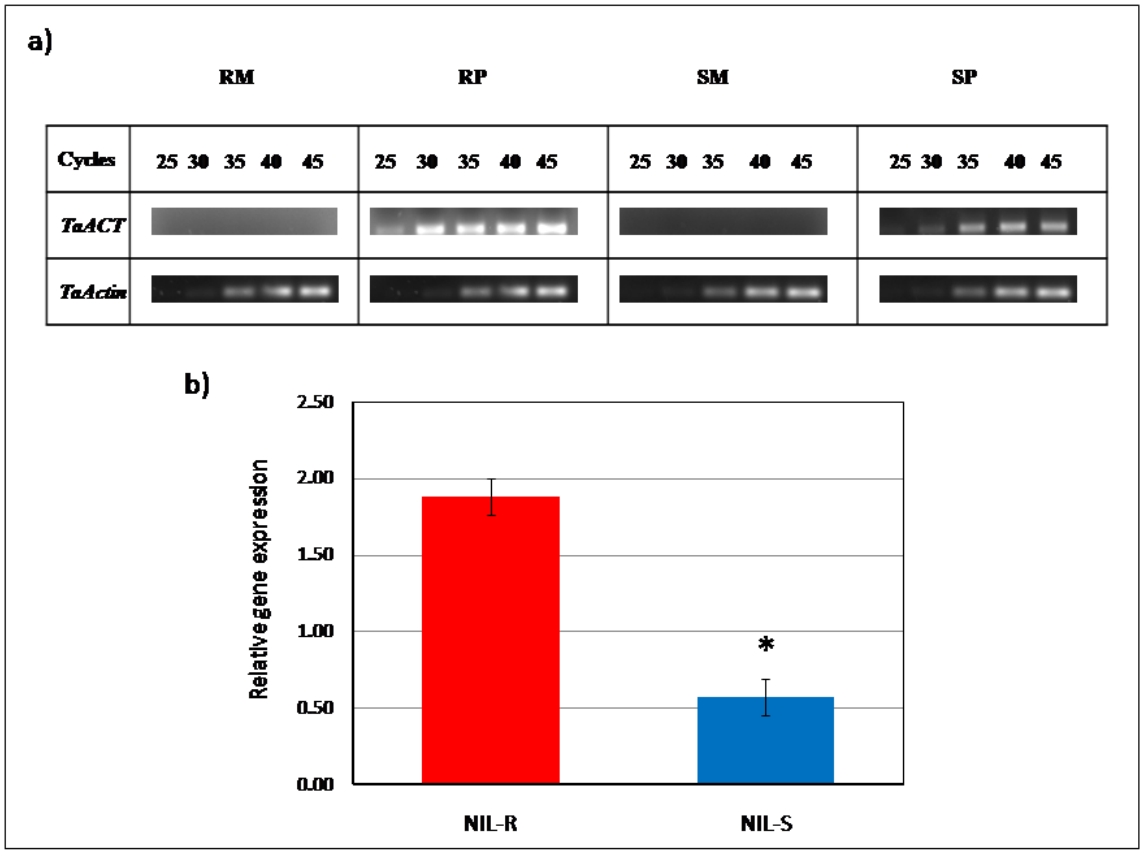

Figure 3.10: Effect of *TaACT* silencing in NIL-R on resistance to spread of *F. graminearum*. **a)** Relative transcript expression of *TaACT*; **b)** Relative metabolite abundances of coumaroylagmatine and coumaroylputrescine in silenced (NIL-R+BSMV$_{TaACT}$), non-silenced (NIL-R+BSMV$_0$) NIL-R; **c)** Biomass (as relative gene copy number based on RT-qPCR) of *F. graminearum* in wheat rachis of silenced (NIL-R+BSMV$_{TaACT}$), non-silenced (NIL-R+BSMV$_0$) NIL-R and NIL-S.

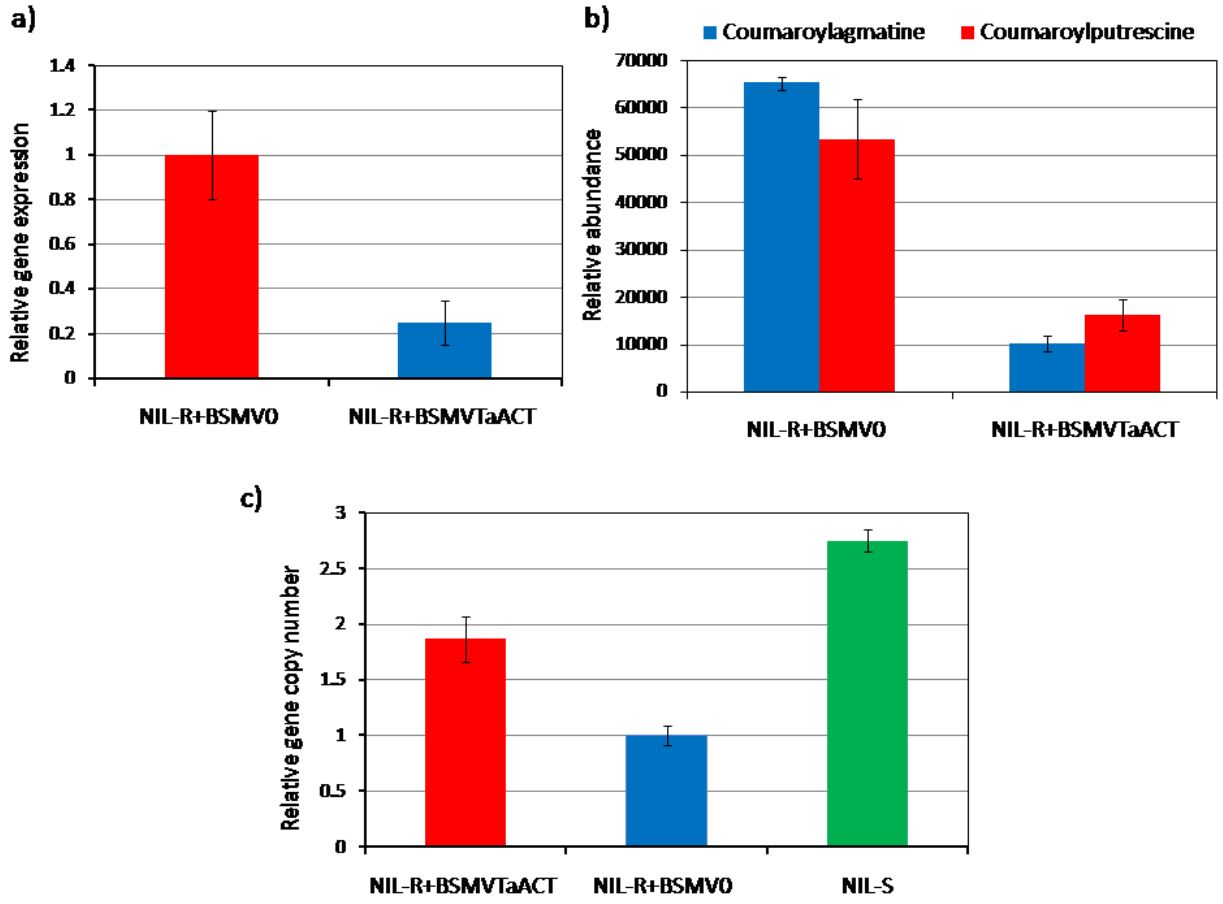

Figure 3.11: Effect of *TaACT* over-expressing *Arabidopsis* plants on resistance to *F. graminearum.* **a-1)** Relative metabolite abundances of coumaroylagmatine and coumaroylputrescine in NIL-R (TaACT_NIL-R) and NIL-S (TaACT_NIL-S) *TaACT* expressing *Arabidopsis* plants; **a-2)** Symptoms observed in *Arabidopsis* plants expressing *TaACT* gene from NIL-R (TaACT_ NIL-R) and NIL-S (TaACT_ NIL-S); **b)** *F. graminearum* disease development. Disease development was quantified based on number of plants with dead inflorescence; **c)** Biomass (relative gene copy number based on RT-qPCR) of *F. graminearum in* NIL-R (TaACT_NIL-R) and NIL-S (TaACT_NIL-S) *TaACT* expressing *Arabidopsis* plants.

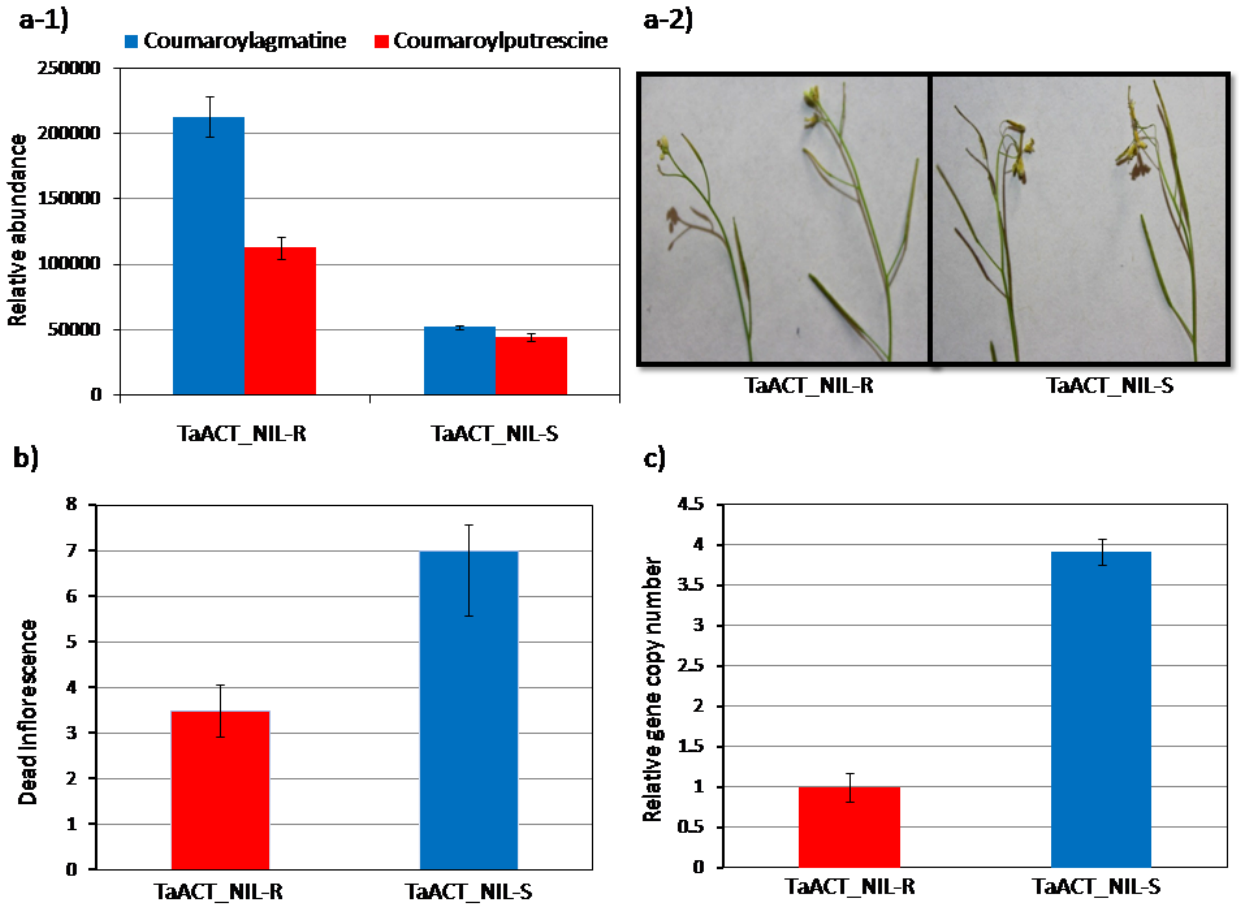

Figure 3.12: Silencing of the phytoene desaturase (PDS) gene. Photograph indicates the phenotypes of resistant wheat plants infected with *BSMV:00* and *BSMV:TaPDS*

BSMV:00 BSMV:*TaPDS*

Connecting statement for Chapter IV

Chapter IV, entitled "*TaWRKY70* transcription factor in wheat QTL-2DL regulates downstream genes to biosynthesize metabolites to contain *Fusarium graminearum* spread within spike", authored by Udaykumar Kage, Yogendra N. Kalenahalli and Ajjamada C. Kushalappa, will be submitted to the peer reviewed scientific journal for publication.

Based on a metabolo-genomics approach *TaACT* was identified as a candidate gene responsible for FHB resistance in wheat. Virus-induced gene silencing (VIGS) in wheat and a complementation study in *Arabidopsis* were used to validate the function of the *TaACT*. The fungal biomass in *TaACT* silenced plants (NIL-R+BSMV$_{TaACT}$) was significantly higher than in non-silenced (NIL-R+BSMV$_0$) plants, whereas the fungal biomass in silenced NIL-R was lower than in the non-silenced NIL-S, indicating that the remainder of resistance may be due to genes other than *TaACT*, associated with the NIL-R, in the QTL-2DL. Consequently, the fold-change increase in other metabolites and corresponding gene expressions were explored to discover other resistance genes. *TaDGK* was associated with high fold-change in its biosynthetic metabolites, but the sequencing in NILs revealed no variation at the DNA level. Therefore, it prompted us to suspect the involvement of a transcription factor (TF) in regulating the expression of *TaDGK* after pathogen invasion. Consequently, we found a *WRKY* like TF while searching for more genes in the QTL-2DL region. Hence, this study was planned to prove the involvement *TaWRKY70* TF in FHB resistance and its further regulation of downstream genes.

Chapter IV

TaWRKY70 transcription factor in wheat QTL-2DL regulates downstream genes to biosynthesize metabolites to contain *Fusarium graminearum* spread within spike

Udaykumar Kage, Yogendra N. Kalenahalli and Ajjamada C. Kushalappa

Plant Science Department, McGill University, Sainte-Anne-de-Bellevue,
Quebec, Canada H9X 3V9

4.1 Abstract

Fusarium head blight (FHB) caused by *Fusarium graminearum* is one of the most destructive diseases of wheat (*Triticum aestivum* L.). Several quantitative trait loci (QTL) have been identified against FHB, but the mechanisms of resistance and candidate genes underlying them are unknown. Therefore, in the present study a semi-comprehensive metabolomics was used to identify candidate genes and decipher mechanisms of resistance in wheat near-isogenic lines (NILs) of QTL-2DL. Metabolites with high fold-change in the abundances included hydroxycinnamic acid amides *(HCAAs)*: such as coumaroylagmatine, coumaroylputrescine and *Glycerophospholoipids*: phosphatidic acids (PAs), which were identified as resistance related induced (RRI) metabolites in rachis of resistant NIL (NIL-R) inoculated with *F. graminearum.* A WRKY like transcription factor (TF) was identified within the QTL-2DL region, along with three resistance genes that biosynthesized RRI metabolites. Sequencing and *in-silico* analysis of *WRKY* confirmed it to be wheat *TaWRKY70*. Quantitative real time-PCR (qPCR) studies showed higher expression of *TaWRKY70* in NIL-R compared to susceptible NIL (NIL-S) after *F. graminearum* inoculation. Furthermore, the functional validation of *TaWRKY70* based on virus-induced gene silencing (VIGS) in NIL-R, not only confirmed an increased fungal biomass, but also decreased expression of the downstream resistance genes *TaACT*, *TaDGK* and *TaGLI1*,

along with decreased abundances of RRI metabolites biosynthesized by them. Among more than 200 FHB resistance QTL identified in wheat, this is the first study that identified a TF and its downstream target genes, and as well deciphered FHB resistance functions.

4.2 Introduction

Fusarium head blight (FHB) is a major constraint in wheat and barley production. Several approaches have been used to manage FHB in wheat, among which the use of FHB resistant cultivars is considered to be the most efficient, economic and environmental friendly method (Bai and Shaner, 2004). More than 200 QTL have been identified, including 52 QTL associated with rachis resistance based on single floret inoculation (Buerstmayr et al., 2009). Among these, QTL-2DL is one of the major and the most stable QTL across different genetic backgrounds and environments (Buerstmayr et al., 2009). This was first identified from Wuhan-1, a Chinese genotype, in which it explained up to 28% of the total phenotypic variation (Somers et al., 2003). However, genetic determinants underlying these QTL still remain largely unknown. Thus, the identification and functional elucidation of genes from these QTL are very important for their use in breeding.

The QTL-Fhb1conferring rachis resistance was fine to 261 kb region on chromosome arm 3BS (Liu et al., 2008). A positional cloning of QTL-Fhb1 region of chromosome 3B disclosed seven novel genes underlying 261 kb region. Transgenic wheat lines were developed for four of these genes, but none of the transgenic lines carrying these genes exhibited rachis resistance (Liu et al., 2008). The QTL-Fhb1 resistance, derived from Sumai-3 cultivar, was claimed to be due to the conversion of deoxynivalenol (DON) to non-toxic DON-3-O-glucoside based on toxin analysis in segregating populations (Lemmens et al., 2005). However, sequencing and physical mapping of QTL-Fhb1 failed to reveal a UDP-glucosyl transferase gene in the QTL region (Choulet et al., 2010). Furthermore, contrasting results were found in a metabolomic analysis of Nyubai-derived QTL-Fhb1, where the resistance was considered to be mainly due to cell wall reinforcement through deposition of HCAAs with no significant variation in DON or its detoxification product, DON-3-O-glucoside (Gunnaiah et al., 2012). Apart from this, transcriptome studies reported numerous differentially expressed genes involved in FHB resistance (Bernardo et al., 2007; Jia et al., 2009; Schweiger et al., 2013; Xiao et al., 2013). Interestingly, a recent transcriptomic study of NILs containing QTL-2DL attempted to identify

candidate genes, but failed to identify QTL specific genes for resistance to FHB (Long et al., 2015). Therefore, functional analysis of mapped QTL using alternative disciplines like metabolomics is considered to be one of the promising tools to identify the underlying genes (Kushalappa and Gunnaiah, 2013). Semi-comprehensive metabolite profiling of barley (Bollina et al., 2010; Bollina et al., 2011; Chamarthi et al., 2014; Kumaraswamy et al., 2011a; Kumaraswamy et al., 2011b) and wheat (Gunnaiah and Kushalappa, 2014; Gunnaiah et al., 2012; Hamzehzarghani et al., 2005; Hamzehzarghani et al., 2008) genotypes with varying levels of resistance to FHB has led to the identification of several RR metabolites and their role in resistance. Recently, a semi-comprehensive metabolomics study of barley genotypes, resistant and susceptible to FHB, identified a transcription factor, *HvWIN1,* that regulated downstream resistance genes to biosynthesize fatty acids that were deposited to reinforce the cuticle to contain *F. graminearum* infection (Kumar et al., 2016). In potato, RR metabolites and their biosynthetic enzymes were identified (Pushpa et al., 2013; Yogendra and Kushalappa, 2016; Yogendra et al., 2014) and functionally validated for late blight disease (Yogendra et al., 2015). Resistance in plants against biotic stress is considered to be due to hierarchies of resistance *R* genes with regulatory roles, such as elicitor/effector recognition receptors (R_{ELRR} and/or R_{ERR}), phytohormone biosynthetic genes (R_{PHR}), mitogen-activated protein kinase (R_{MAPK}), and transcription factors (R_{TF}), which regulate metabolic pathway network genes that biosynthesize resistance related metabolites (R_{RRM}) and/or RR proteins (R_{RRP}) (Kushalappa et al., 2016).

Plants modulate themselves to a specific stress by regulating functional genes involved in biosynthesizing a wide variety of metabolites (Gong et al., 2015). Phosphatidic acids (PAs) are a group of important lipid molecules in plants that are involved in various biotic (e.g. pathogens) and abiotic (e.g., osmotic, temperature) stress responses (Arisz et al., 2009; Munnik, 2001). PAs and their derivatives are secondary messengers and play a central role in the general stress-signaling (Gómez-Merino et al., 2004; Munnik, 2001). They are involved in structural fortification of plant cell walls (Arisz et al., 2009; Khajuria et al., 2013) and also help in reducing cell death (Zhang et al., 2003). PAs are biosynthesized either through direct enzymatic activity of diacylglycerol kinase (DGK) on diacylglycerol molecules (Arisz et al., 2009; Munnik, 2001), or through an indirect activity of glycerol kinase (GLI1) on glycerol via glycerol metabolism (Chanda et al., 2008; Mandal et al., 2011). HCAAs are a class of complex secondary metabolites produced in the phenylpropanoid pathway that are induced in plants in response to pathogens

(Gunnaiah et al., 2012; Muroi et al., 2009; Muroi et al., 2012; von Röpenack et al., 1998). They reduce pathogen advancement through their antimicrobial and cell wall reinforcement properties (Ishihara et al., 2008; Keller et al., 1996; Miyagawa et al., 1995; Schmidt et al., 1998). Agmatinecoumaroyl transferase (ACT) is a rate limiting enzyme involved in the biosynthesis of these metabolites (Burhenne et al., 2003; Muroi et al., 2009; Muroi et al., 2012).

WRKYs are one of the largest families of transcriptional regulators in plants and are involved in biotic and abiotic stress responses, such as metabolite biosynthesis, cell wall formation, senescence, trichome development, and hormone responses (Guillaumie et al., 2010; Rushton et al., 2012; Rushton et al., 2010; Zou et al., 2004). WRKY proteins have either one or two WRKY DNA binding domains with the consensus amino acid sequence, WRKYGQK at the N-terminal end and a zinc-finger motif at their C-terminal end (Eulgem et al., 1999; Rushton et al., 2010). WRKY TFs regulate target gene expression through specific binding to the DNA sequence motif (T)(T)TGAC(C/T), which is known as the W-box (Eulgem et al., 1999).

In wheat, despite huge efforts, the elucidation of molecular functions of WRKY genes is still limited. In this study, we identified and characterized *TaWRKY70* TF from bread wheat. The *TaWRKY70* gene was confirmed to be located within the QTL-2DL region, and imparted resistance to FHB by activating PA and HCAA biosynthesis through regulating downstream resistance genes, *TaDGK*, *TaGLI1*, and *TaACT*.

4.3 Materials and methods

4.3.1 Plant production and experimental design

We used NILs, derived from a BW301 X HC374 cross (McCartney et al., 2007; Somers et al., 2003). BW301 is an FHB susceptible hard red spring wheat line from western Canada and HC374 is resistant to FHB (derived from the cross Wuhan1 x Nyubai). NILs were genotyped with microsatellite markers. Homozygous lines with susceptible background, differing only in the alleles of the QTL-2DL locus, with no other known FHB resistance QTL located on chromosome 3B, 4B, 5A and 6B were selected (Somers et al., 2005; Hamzehzarghani et al., 2008). The seeds of NILs with FHB susceptible and resistant alleles of QTL-2DL were obtained from Dr. McCartney, AAFC, Morden, Canada. Three plants per pot were maintained and the experiment was laid out in randomized complete block design (RCBD) with two genotypes

(resistant and susceptible NILs), two inoculations (pathogen and mock-solution) and five replications over time. Plants grown in the greenhouse were maintained at 23±2 °C, photoperiod 16 h, and relative humidity 70 ± 10 %, throughout the growing period.

4.3.2 Pathogen production and inoculation

The *F. graminearum* isolate GZ-3639 was grown on potato dextrose agar at 26 °C for 4 days. For spore production, *F. graminearum* was sub-cultured on Rye B agar media and kept inverted by exposing the plates to the UV light for 3 days. From a seven day old culture macroconidia were harvested and spore count was adjusted to 1×10^5 macroconidia ml^{-1} using a hemocytometer (American Scientific Products, USA) (Bollina et al., 2010). Three alternate pairs of wheat spikelets at 50 % anthesis stage were point inoculated with 10 µl either macroconidial suspension or mock-solution using a syringe (GASTIGHT 1750 DAD, Reno, USA). Plants were covered with clear plastic bags sprayed with water to maintain high moisture. Bags were removed at 48 hours post inoculation (hpi).

4.3.3 Sample collection, metabolite analysis using liquid chromatography-high resolution mass spectrometry (LC-HRMS) and data processing

At 72 hpi, the spike region with 3 inoculated and 3 alternate uninoculated pairs of spikelets, was harvested. Spikelets and rachis were collected separately and frozen immediately in liquid nitrogen and stored at -80 °C until use. Metabolites were extracted from rachis samples in 60% ice cold aqueous methanol. A 5 µl of liquid clear sample extract was used for metabolite analysis based on LC-HRMS (at IRCM, Montreal, Canada) as described previously (Bollina et al., 2010).

The LC-HRMS output Xcalibur RAW files were converted into mzXML format. Data was analyzed using MZMine2, and peaks were identified as metabolites based on monoisotopic mass and fragmentation match with databases and available literature (Bollina et al., 2010; Bollina et al., 2011; Gunnaiah and Kushalappa, 2014; Gunnaiah et al., 2012; Pushpa et al., 2013; Yogendra et al., 2014). Relative peak intensities of monoisotopic masses of metabolites were subjected to Students *t*-test (SAS v 9.3). Peaks significant at $P<0.05$ (Kushalappa and Gunnaiah, 2013), and false discovery rate threshold of 0.05 (Vinaixa et al., 2012) were retained. The false discovery rate of peaks depends mainly on the signal/noise (S/N) ratio; the lower the ratio, the higher the false discovery rate. Therefore, S/N ratio was kept high to minimize false discovery (Kumar et

al., 2016). Metabolites significantly higher in abundance in resistant than susceptible NIL were considered as RR metabolites. Further, these metabolites were grouped into RR constitutive (RRC=RM>SM) and RR induced (RRI = (RP>RM) > (SP>SM)) metabolites. The fold-change in abundance of metabolites in NIL-R was calculated relative to NIL-S (NIL-R/NIL-S) (Gunnaiah et al., 2012). Only the high fold-change (>2) RRI metabolites were prioritized for further candidate gene identification.

4.3.4 Disease severity and fungal biomass assessment

To evaluate rachis resistance in wheat genotypes, 2 NILs with resistant and susceptible alleles, were planted in a RCBD with 3 replications at 3 day intervals. Disease severity in NILs was quantified as a proportion of spikelets diseased (PSD), from which the area under the disease progress curve (AUDPC) was calculated (Hamzehzarghani et al., 2008). PSD was analyzed for significance based on the ANOVA using SAS (SAS v 9.3).

Rachis samples were harvested at 6 days post inoculation (dpi) and immediately put in liquid nitrogen and stored at -80 °C until further use. Genomic DNA was extracted and fungal biomass was quantified using real-time qPCR by measuring the relative copy number of the fungal housekeeping gene *tri6* normalized with *TaActin*. The relative gene copy number based on real-time qPCR was used to estimate the amount of fungal biomass (Kumar et al., 2015).

4.3.5 Candidate gene identification, based on high fold-change RR metabolites and their physical localization within QTL-2DL

The RRI metabolites with high fold-change in abundance were mapped on metabolic pathways to find their catalytic enzymes, and the corresponding genes were identified using genomic databases (such as KEGG, MetaCyc, PlantCyc and *Arabidopsis* Acyl metabolism pathways) and available literature. The SSR markers, WMC245, GPW8003, GWM539 and GWM608 were used to define the interval for QTL-2DL. These markers were sequenced and subjected to BLASTN (Altschul et al., 1990) search in International Wheat Genome Sequencing Consortium (IWGSC) database to physically localize the QTL-2DL region. The candidate genes identified based on high fold-change RRI metabolites were BLAST searched against the IWGSC database to confirm co-localization within the mapped QTL-2DL region. Contigs identified as best hits were retrieved from the database and gene prediction was performed using SoftBery –

FGENESH (http://linux1.softberry.com/berry.phtml?topic=fgenesh&group=programs&subgroup=gfind) program to study gene structure. The identified gene was amplified using gene specific primers designed using the NCBI Primer-BLAST tool (http://www.ncbi.nlm.nih.gov/tools/primer-blast/). Synteny mapping was also performed with rice and brachypodium to predict and locate other putative genes in the QTL-2DL region.

4.3.6 Gene cloning, sequencing and sequence analysis

A full length *TaWRKY70* gene was amplified from genomic DNA using primer pairs TaWRKY_F and TaWRKY_R, from NILs. Gene amplification was conducted using a thermal cycler (Bio-Rad, Mississauga, ON, Canada) with the following steps: initial denaturation at 95 °C for 5 min, followed by 35 cycles of 94 °C for 30 s, 55°C for 1 min, 72 °C for 2 min, followed by final extension at 72 °C for 10 min. PCR products were separated by electrophoresis through 1 % agarose gel. A band size corresponding to ~1300 bp was then purified from the gel, cloned into the pGEM®-T Easy vector (Promega, USA), and sequenced on ABI Automated DNA sequencer in Genome Quebec. DNA sequences were translated to amino acid sequences using the ExPASy Translate Tool (http://web.expasy.org/translate/). The NCBI Conserved Domain Database (NCBI CDD) was used to search for functional domains present in deduced amino acid sequence. These results were confirmed using the PROSITE tool (http://www.expasy.ch/prosite) and the MOTIF Search tool (http://www.genome.jp/tools/motif/). Multiple sequence alignment was performed using MultAlin (http://multalin.toulouse.inra.fr/multalin/) and phylogenetic relationships were determined using Phylogey.fr (http://www.phylogeny.fr/) program

4.3.7 RNA isolation and gene expression based on qPCR

For relative quantification of transcript expression, total plant RNA was isolated from 5 biological replicates using an RNeasy plant mini kit (Qiagen Inc.). Purified total RNA (1-2 µg) was used to reverse transcribe RNA into cDNA using an iScript cDNA synthesis kit (BioRad, ON, Canada). Using an equal quantity of cDNA (20 ng) of each sample, real-time qPCR was performed using Qi SYBR Green supermix (BioRad, Canada) in a CFX384TM Real-Time system (BioRad, Canada). The target mRNA abundance was normalized to the *TaActin* transcript level. PCR results were analyzed using comparative Δ-Δ Ct method ($2^{-\Delta\Delta CT}$) (Livak and Schmittgen, 2001).

4.3.8 Nuclear localization assay

The LocSigDB (http://genome.unmc.edu/LocSigDB/) was used for nuclear localization signal (NLS) prediction. The full-length coding region of *TaWRKY70* was amplified and cloned into pCX-DG vector containing green fluorescence protein (GFP) and the *Cauliflower Mosaic Virus* (*CaMV*) 35S promoter (Chen et al., 2009). For subcellular localization study, TaWRKY70+GFP fusion and GFP alone as a control were transfected into potato protoplasts using a polyethylene glycol-calcium method (Yoo et al., 2007). Transfected protoplasts were incubated at 23 °C for 16 h and analyzed for GFP fluorescence by fluorescence microscopy.

4.3.9 Luciferase (LUC) transient expression assay

The coding region of *TaWRKY70* and the promoters of *TaACT, TaDGK* and *TaGLI1* from the resistant genotype were amplified, cloned into pGEM®-T Easy vector (Promega, USA), and confirmed by sequencing. This was followed by subcloning into the FU63 (CD3-1841) vector (Wang et al., 2013). For LUC transient expression assays, reporter plasmids (ACTp-LUC or DGKp-LUC or GLI1p-LUC or DNA fragment (30 bp) without W-box as control), effector constructs containing *TaWRKY*, and 35S::β-glucuronidase (GUS) internal control (Fig. 4.7a) were co-transformed into potato protoplasts. The protoplasts were pelleted and re-suspended in 1× cell culture lysis reagent (Promega, USA). GUS fluorescence was measured using a Modulus luminometer/fluorometer with a UV fluorescence optical kit (Fluorescence Microplate Reader; BioTek, USA). The experiment was carried out in 3 replicates; each replicate contained 20 µl protoplast lysate and 100 µl LUC mix. LUC activity was detected with a luminescence kit using LUC assay substrate (Fluorescence Microplate Reader). The relative reporter gene expression levels were expressed as LUC/GUS ratios, which were used to discriminate treatments.

4.3.10 Construction of BSMV vectors and virus-induced gene silencing of *TaWRKY70*

For transient gene silencing, a 283 bp fragment of *TaWRKY70* was selected with efficient siRNA generation and no off-target genes into the modified viral genome using the siRNA Scan tool (http://bioinfo2.noble.org/RNAiScan.htm), and a BLAST search of fragment against GenBank database. We chose the most divergent sequence containing (3` UTR region) to increase the specificity (Fig. 4.11a). The fragment was amplified from cDNA using the primers listed in Table 4.3 and cloned into the pGEM®-T Easy Vector (Promega Corp., WI, USA) and sequence

was confirmed. Plasmid DNA was digested using *NotI* (New England Biolabs, MA, USA) and the cDNA fragment was subsequently ligated to pSL038-1 vector, a plasmid encoding a modified BSMV γ genome segment with a cloning site downstream of the γb gene (Cakir et al., 2010) (Fig. 4.11b and c). The pSL038-1 vector carrying either *phytoene desaturase (PDS)* or without any genes served as positive and negative control respectively. Plasmids BSMV α, p γSL038-1 were linearized with *Mlu1* restriction enzyme, whereas, BSMV β was linearized by with *Spe1*. Linearized plasmids were converted into capped in-vitro transcripts using mMessagem Machine™ T7 in-vitro transcription kit (Ambion, Inc., Austin, TX, USA), following the manufacturer's protocol. The plants were grown as explained in the plant production and experimental design section, in 5 replicates. Five plants were selected from each replicate and inoculated with all 3 in-vitro transcripts (α, β and γ BSMV) in 1:1:1 ratio (1 µl of each), along with 22.5 µl inoculation buffer that facilitated viral infection (1% sodium pyrophosphate, 1% bentonite, 1% celite in 0.1 M glycine, 0.06 M dipotassium phosphate). Flag leaf and spikelets were inoculated as described earlier (Scofield et al., 2005).

4.3.11 Confirmation of gene silencing by qPCR, and estimation of fungal biomass and targeted metabolites

At 12 dpi with the virus, 3 alternate spikelets in 5 spikes per replicate were inoculated with 10 µl *F. graminearum* spore suspension and covered with water-sprayed plastic bags. The bags were removed after 48 hpi and samples were collected at 72 hpi for qPCR and metabolite analysis. Similarly, at 6 dpi, samples were collected for the relative quantification of fungal biomass as the relative gene copy number of the fungal housekeeping gene *tri6*.

4.4 Results

4.4.1 Fungal biomass quantification

The disease severity of NILs with alternative alleles for resistance at QTL-2DL was assessed by inoculating a pair of spikelets in the mid region of the spike with *F. graminearum*. The AUDPC was significantly higher in susceptible NIL (NIL-S) (2.33) compared to resistant NIL (NIL-R) (1.48). The fungal biomass, estimated as the relative gene copy number of *tri6* based on real-time qPCR, was also significantly higher (5.8 fold-change) in NIL-S compared to NIL-R in rachis as

we seen in Chapter III. This clearly showed high level of rachis resistance against FHB associated with QTL-2DL.

4.4.2 Metabolite profiles of NILs

Semi-comprehensive metabolomics of rachis samples collected at 72 hpi identified several differentially accumulated RR metabolites in NILs with contrasting alleles for resistance at QTL-2DL. The significant metabolites categorized into RRC and RRI. RRI metabolites with fold-change in abundance were includes PAs and HCAAs: phosphatidic acids and derivatives (PAs) [(1-heptadecanoyl,2-(5Z,8Z,11Z,14Z-eicosatetraenoyl)-sn-glycero-3-phosphat = PA(17:0/20:4(5Z,8Z,11Z,14Z) (fold-change=54.3)), (1-pentadecanoyl-2-(8Z,11Z,14Z-eicosatrienoyl)-glycero-3-phosphate=(PA(15:0/20:3(8Z,11Z,14Z) (fold-change=9.5)) and (1-(9Z-nonadecenoyl)-2-(13Z,16Z-docosadienoyl)-glycero-3-phosphate = (PA(19:1(9Z)/22:2 (13Z,16Z)(fold-change =2.3))], p-coumaroylagmatine (fold-change=28.7), p-coumaroyputrescine (fold-change=9.5) (Table 4.1).

4.4.3 Identification of candidate genes in QTL-2DL

Putatively identified high fold-change RRI metabolites were mapped to metabolic pathways and the candidate genes (R_{RRM}) encoding the enzymes that biosynthesize these RRI metabolites were identified from public databases and available literature. Agmatinecoumaroyl transferase (*ACT*) is the rate limiting enzyme in the biosynthesis of HCAAs such as coumaroylagmatine and coumaroylputrescine (Burhenne et al., 2003; Muroi et al., 2009). Diacylglycerol kinase (*DGK*) and glycerol kinase (*GLI1*) are important enzymes in the biosynthesis of PAs in plants (Cai et al., 2009; Chanda et al., 2008; Gómez-Merino et al., 2004; Testerink and Munnik, 2005). BLAST analysis positioned the closest gene matches for these enzymes within the QTL interval on 2DL (Fig. 4.1). *TaACT* and *TaDGK* including their promoters were sequenced and the sequences were deposited in the NCBI database. Sequence comparison of *TaACT* and *TaDGK*, in contrasting NILs revealed that only the *TaACT* was polymorphic. This led us to suspect a possible involvement of a TF in regulating the PA pathway. While searching for other candidate genes, a WRKY-like TF was found in the QTL-2DL region. A list of other predicted genes present in QTL-2DL based on comparative study with rice and brachypodium is given in the supplementary data (Table 4.4), but their roles in FHB resistance are unknown.

4.4.4 *TaWRKY* gene sequencing and sequence analysis

WRKY TFs are involved in regulating plant responses to biotic and abiotic stresses. Therefore, we sequenced the predicted full length *WRKY* gene from genomic DNA of NILs. Sequence analysis based on FGENESH suggested that *WRKY* has three exons and two introns (Fig. 4.2a) and the intron-exon boundaries were confirmed to be AG and GT at the acceptor and donor sites, respectively, through FSPLICE (http://linux1.softberry.com/berry.phtml?topic=fsplice& group=programs& subgroup=gfind). The full length sequence of *TaWRKY* was 1288 bp containing an open reading frame (ORF) of 1165 bp, a 96 bp 3´ untranslated region (UTR) and 27 bp 5´ UTR (Fig. 4.2a). Plant canonical polyadenylation signal, a six-nucleotide near-upstream element (NUE - AAATAA), was found in the 3´ UTR at 1251 to 1257 bp (Fig. 4.2a) (Loke et al., 2005). The complete genomic sequence was submitted to NCBI (KU562861). The putative protein encoded by *TaWRKY* consisted of 290 amino acids. It has a conserved characteristic DNA-binding domain comprising a single WRKY domain and Cys2-His-Cys type zinc-binding motif spanning position 98 to 166 amino acids (Fig. 4.2b & c). Group III WRKYs differ from groups I and II in an altered C2-HC zinc finger motif C-X7-C-X23-HX-C (Kalde et al., 2003) (Fig. 4.2c). Multiple sequence alignment and phylogenetic analyses indicated that TaWRKY is a Group III type of WRKY (Fig. 4.3). TaWRKY showed 99% identity with *Aegilops tauschi* putative WRKY70. Here onwards we designated TaWRKY as TaWRKY70 like TF (=*TaWRKY70*).

4.4.5 Sequence variation of *TaWRKY70* between NILs and differential gene expression during *F. graminearum* infection

Multiple sequence alignment of *TaWRKY70* between NILs and *T. aestivum* cv. Chinese Spring revealed single nucleotide polymorphisms (SNP) in NIL-S at 294 bp position (Fig. 4.4a), which is exactly at the first exon-intronic junction. This resulted in a 14 amino acid deletion in predicted protein sequence by activating cryptic splice site at 42 bp upstream in the first exon of *TaWRKY70* transcript (Fig. 4.4b). However, additional experimental proof is needed to confirm the mutation and to know how it induces the truncated protein in-vivo and alters the transcriptional activity of TaWRKY70, ultimately affecting resistance potential to FHB.

The relative expression of *TaWRKY70* following *F. graminearum* inoculation was significantly (P<0.05) higher (2.3 fold-change at 48 hpi and 2.0 fold-change at 72 hpi) in pathogen treated NIL-R compared to pathogen treated NIL-S. Similarly, its expression was high in pathogen treated NIL-R compared to mock treated samples of both the NILs at both time points (48 hpi and 72 hpi), though the expression levels were slightly lower at 72 hpi (Fig. 4.5a), suggesting *TaWRKY70* has a potential role in the early stages of defense activating downstream genes against *F. graminearum*.

4.4.6 Gene expression, promoter analysis of RR metabolite biosynthetic genes and their physical interaction with R_{TaWRKY}

At 72 hpi, relative expression levels of the downstream R_{RRM} genes *TaDGK* (2.4 fold-change), *TaGLI* (2.0 fold-change), and *TaACT* (3.3 fold-change) were significantly (P<0.01) higher in NIL-R than in NIL-S after *F. graminearum* inoculation, similar to *TaWRKY70* (Fig. 4.5b). To further study the downstream R_{RRM} targets of *TaWRKY70*, we did promoter analysis of R_{TaACT}, R_{TaDGK} and R_{TaGLI1}. The promoter sequences from -1 bp to -1000 bp upstream of the ATG start site were considered for analysis using a PLACE database (http://www.dna.affrc.go.jp/PLACE/) and a manual search. Promoter analysis of these genes revealed the presence of a putative W-box sequence in their promoters within -500 bp (Table 4.2). We confirmed the potential interaction of *TaWRKY70* with these downstream R_{RRM} genes using *Arabidopsis* as a search organism in GeneMANIA software (http://www.genemania.org/). Resulting networks showed a clear interaction between *TaWRKY70* and the R_{RRM} genes *TaACT*, *TaDGK* and *TaGLI1* (Fig. 4.6). Physical interaction *in-vivo* was confirmed based on luciferase assay. Reporter and effector constructs were transformed into potato protoplasts to check the expression of LUC reporter. We found drastic increases in the expression of the LUC reporter in *TaACT* (34.7), *TaDGK* (32.9) and *TaGLI1* (31.6) promoters compared with control without W-box (4.5) (Fig. 4.7b), suggesting the transcriptional regulation of *TaDGK*, *TaGLI1* and *TaACT* to biosynthesize PAs and HCAA, thus confirming their *in-silico* predicted interaction.

4.4.7 Nuclear localization of TaWRKY70 protein

To investigate the subcellular localization of TaWRKY70, we used LocSigDB (http://genome.unmc.edu/LocSigDB/) with default setting. We found three conserved amino acid

region (KRK) potentially acting as nuclear localization signal (NLS) for TaWRKY70 (Fig. 4.8a). Additionally, we used a transient expression system in potato protoplasts to characterize the subcellular localization of TaWRKY70. The TaWRKY70+GFP fusion protein was localized in the nucleus, while the control vector (GFP alone) was expressed in the cytosol and nucleus (Fig. 4.8b). These results agreed with the subcellular localization prediction, suggesting that TaWRKY70 is a nuclear protein.

4.4.8 Response to *F. graminearum* infection after knocking down of *TaWRKY70* in wheat

Based on changes in *TaWRKY70* expression after *F. graminearum* inoculation, the BSMV-VIGS system was employed to knock down the transcription of *TaWRKY70* and to further investigate its function in response to *F. graminearum* infection. The feasibility and silencing efficiency of the BSMV-VIGS system in NIL-R was tested using wheat phytoene desaturase (*TaPDS*) as a positive control. At 12 dpi with *BSMV:TaPDS*, photo-bleaching symptoms started appearing on wheat spikes when *TaPDS* was silenced. Therefore, the BSMV-VIGS system was used to assess the potential roles of *TaWRKY70* in wheat resistance against *F. graminearum* infection. Under the same conditions, the *BSMV:TaWRKY70* (test/silenced) and *BSMV:00* (control/non-silenced) recombinant vectors were rub-inoculated onto the NIL-R.

To study the efficiency of silencing of *TaWRKY70* in NIL-R plants that had been infected with recombinant BSMV vectors, the relative expression levels in rachis were detected by real time qPCR. The relative expression of *TaWRKY70* was significantly (P<0.001) reduced by 86.04% in plants infected with *BSMV:TaWRKY70* compared to *BSMV:00* infected plants at 72 hpi with *F. graminearum*, confirming the silencing of target gene in wheat rachis (Fig. 4.9a). To further determine whether silencing of *TaWRKY70* in NIL-R, compromised resistance to *F. graminearum* infection, the fungal biomass of *F. graminearum* was estimated by measuring the relative transcript levels of the *F. graminearum* housekeeping gene. Fungal biomass was significantly higher (P<0.001) in silenced plants as compared to control plants (Fig. 4.9b). From these results it is confirmed that the enhanced susceptible phenotypes observed in NIL-R inoculated with the *F. graminearum* were due to the silencing of *TaWRKY70*.

4.4.9 Silencing of *TaWRKY70* affected transcriptional response of R_{RRM} genes and RR metabolite accumulation

It is evident from the presence of W-Box in the promoter, GeneMANIA analysis, and the luciferase assay that *TaWRKY70* physically interacts with the downstream targets *TaACT*, *TaDGK* and *TaGLI1*. To check whether knocking down *TaWRKY70* expression affects transcription of downstream genes, the relative expression levels of these genes were estimated using qPCR. The expression levels of *TaACT* (fold-change =3.44), *TaDGK* (fold-change =1.36) and *TaGLI1* (fold-change =1.88) in silenced samples were significantly down-regulated compared to non-silenced samples, further confirming these genes as potential targets of *TaWRKY70* (Fig. 4.9c). To prove the biochemical and molecular mechanisms of the involvement of *TaWRKY70* to resist FHB, metabolite profiling was performed in silenced and non-silenced NIL-R plants. In NIL-R silenced plants, the abundances of candidate RR metabolites such as PAs (PA(17:0/20:4(5Z,8Z,11Z,14Z)), PA(15:0/20:3(8Z,11Z,14Z)) and PA(19:1(9Z)/22:2(13Z,16Z)) with fold-change = 8.3, 2.5 & 1.6, respectively), p-coumaroylagmatine (fold-change =6.7) and p-coumarolyputrescine (fold-change =3.5) were significantly (P<0.005) reduced compared to non-silenced plants (Fig. 4.9d). This clearly implied the potential involvement of *TaWRKY70* in down-regulating the transcriptional response of candidate genes in NIL-R, thereby reducing secondary metabolite production and causing compromise FHB resistance in silenced NIL-R plants.

4.5 Discussion

Resistance in plants against pathogen attack is controlled by several hierarchies of resistance genes that eventually biosynthesize RR metabolites and proteins that directly suppress and/or contain the pathogen to initial infection through their antimicrobial or cell wall reinforcement properties (Kushalappa et al., 2016). Plant R_{ELRR} genes recognize pathogen produced elicitors and trigger downstream R_{MAPK} and R_{TF} genes which regulate the R_{RRM} and R_{RRP} genes that biosynthesize RR metabolites and proteins. It is important to map the network of plant genes involved in the hierarchy to resist the pathogen. Some of these genes have major while others have minor effects on resistance. In this study, we report a wheat TF as one of a candidate gene with significant FHB resistance effects, through regulation of several downstream R_{RRM} genes that biosynthesize RRI metabolites that directly suppress and/or contain pathogen advancement.

Metabolites are the end products of genes and thus they better represent the phenotype, than transcripts. Accordingly, metabolite profiling was used as tool to reveal R_{RRM} genes involved in

NILs with contrasting levels of FHB resistance at QTL-2DL. Only the high fold-change RRI metabolites were considered to explore the R_{RRM} genes. PAs and HCAAs were the major RRI metabolites found in wheat rachis after pathogen invasion. PA is the essential intermediate in the *de-novo* biosynthesis of all glycerolipids (Okazaki and Saito, 2014). PAs and their derivatives are involved in signaling and structural fortification of the cell wall through deposition of glycerol 3-phosphates (Arisz et al., 2009; Khajuria et al., 2013). This also helps in the suppression of cell death induced by hydrogen peroxide (Zhang et al., 2003). HCAAs are phytoalexins that suppress pathogens due to their antimicrobial activity and as well contain the pathogen to initial infection by cell wall reinforcement (Ishihara et al., 2008). We mapped these metabolites on to their metabolic pathways to identify their biosynthetic genes. Genes involved in biosynthesizing these RRI metabolites were *TaACT, TaDGK* and *TaGLI1*. Several studies have reported the biotic stress resistance roles of *ACT* (Burhenne et al., 2003; Muroi et al., 2009; Muroi et al., 2012), *DGK* (De Jong et al., 2004; Zhang et al., 2003) and *GLI1* (Chanda et al., 2008; Mandal et al., 2011; Yang et al., 2013). While searching for other genes in the QTL-2DL region, we found a gene encoding a WRKY-like protein. WRKY proteins are regulatory in nature and have a role in plant biotic and abiotic stress resistance by controlling the transcription of downstream *R* genes by binding to W-Box cis-elements present in their promoters (Rushton et al., 1996). Sequence analysis of *TaWRKY70* gene revealed SNP between NILs. The SNP in NIL-S at the position of 294 bp in first exon-intron junction led to a shift of ORF, which resulted in a truncated protein. How it affects protein structure and function requires additional studies. The levels of gene expression of *TaACT, TaDGK, TaGLI1* and *TaWRKY70* were higher in NIL-R compared to its susceptible counterpart. Further, the disease severity and fungal biomass in NIL-R were significantly lower than in NIL-S, as confirmed in our previous study. Taken together, these results demonstrate the potential role of these candidate genes in FHB resistance in wheat.

Sequence comparison of *TaDGK* in NILs revealed the absence of sequence variation both in the coding and promoter regions. In spite of this, transcript expression levels were higher in NIL-R than in NIL-S. We sequenced and analyzed the promoter regions of *TaACT, TaDGK* and *TaGLI1,* which revealed the presence of W-Box *cis*-element in their promoter, giving a clue about involvement of TaWRKY70 protein in regulation of downstream R_{RRM} genes transcription. Subcellular localization study showed TaWRKY70 to be a nuclear protein. Further, the bioinformatics analysis of protein-DNA interaction networks using GenMANIA software

showed that TaWRKY70 interacts with all the R_{RRM} genes (*TaACT, TaDGK* and *TaGLI1*) that biosynthesize the candidate RRI metabolites identified here. Further, their physical interaction was supported based on luciferase assay *in-vivo*. These results present compelling evidence on the involvement of *TaWRKY70* in FHB disease resistance, by regulating downstream genes that produced RRI metabolites with signaling, antimicrobial and cell wall reinforcement properties.

An association of RRI metabolites with R_{RRM} genes alone is not enough to claim the role of *TaWRKY70* in FHB resistance, and they need to be functionally validated. Among several tools available, such as mutagenesis, RNAi and VIGS, VIGS is considered to be the most appropriate for its easy and rapid knockdown ability of genes during plant development, as it enables assessment of the lack of resistance effect induction by the pathogen (Ramegowda et al., 2014). There are several reports on the successful use of VIGS in functional genomics in tobacco, tomato, *Arabidopsis*, potato, wheat and barley, as these plants have well established vectors for gene silencing. Therefore, we used VIGS as a tool in functional characterization of *TaWRKY70* in NIL-R. Knocking down of the expression of *TaWRKY70* in NIL-R resulted in reduced transcript abundance of *TaACT, TaDGK* and *TaGLI1*, which in turn, decreased the abundances of their biosynthetic RRI metabolites, resulting in increased fungal biomass. The silenced NIL-R phenotype was quite similar to NIL-S phenotype, as determined based on the fungal biomass. These results indicate that *TaWRKY70* TF modulates the expression of several R_{RRM} genes, of which *TaACT, TaDGK* and *TaGLI1* may be a subset. PA biosynthetic genes were regulated by TFs in *Nannochloropsis* spp., a group of oleaginous microalgae (Hu et al., 2014). Knock-down of *FcWRKY70* in kumquat down-regulated *ADC* (arginine decarboxylase) abundance and decreased putrescine levels, accompanied by compromised dehydration tolerance (Gong et al., 2015). Late blight pathogen infection in potato induced HCAA biosynthetic genes, regulated by *StWRKY1*, and the promoter region sequence analysis of 4-coumarate:CoA ligase (*St4CL*) and tyramine hydroxycinnamoyl transferase (*StTHT*) revealed the W-box sequence, demonstrating the WRKY binding activity (Yogendra et al., 2015). Whitefly infestation in *Arabidopsis* also induced *AtWRKY* and regulated *At4Cl4* expression by binding to W-box present in its promoter (Hahlbrock et al., 2003). Similarly, in wheat, aphid infestation induced *TaWRKY53*, silencing of which significantly reduced the expression of *PAL* gene (Van Eck et al., 2010), suggesting that the network of these genes are involved in imparting resistance to several biotic stresses.

In summary, we have identified and isolated Group III stress-responsive WRKY gene, designated as *TaWRKY70* from wheat, which acts as a positive regulator of FHB resistance. The NILs containing alleles for genes in the QTL-2DL region, accumulated high amounts of RRI metabolites whereas, the silenced plants had reduced amounts. The R_{RRM} genes such as *TaACT*, *TaDGK* and *TaGLI1* along with R_{TF} gene *TaWRKY70* were localized within the QTL-2DL region. Promoter analysis of the R_{RRM} genes contained W-box elements and their physical interaction based on luciferase assay, which were shown to be regulated by *TaWRKY70*, indicating *TaACT, TaDGK* and *TaGLI1* genes as direct targets of *TaWRKY70*. Collectively, these results indicated that *TaWRKY70* functioned in mediating FHB resistance by elevating PAs and HCAAs by regulating downstream *TaACT, TaDGK* and *TaGLI1* genes (Fig. 4.10). The establishment of $R_{TaWRKY70}$*(R_{TaACT}+ R_{TaDGK}+ R_{TaGLI1}), a major network provides a crucial knowledge about the mode of action of *TaWRKY70* in FHB resistance. In conclusion, taken together, the *TaWRKY70* gene in the QTL-2DL governs major resistance effect against *F. graminearum*. This gene can be used in FHB resistance breeding programs or for genome editing of susceptible cultivars, if these genes are non-functional, to enhance resistance in wheat against FHB.

Table 4.1: List of high fold-change resistance related induced (RRI) metabolites identified in NILs with contrasting FHB resistance alleles at QTL-2DL

RRI			
Observed mass	**Name**	**Fold change**	**Category**
710.4887	PA(17:0/20:4(5Z,8Z,11Z,14Z))	54.3***	Glycerophospholipids
276.1592	p-Coumaroylagmatine	28.7***	HCAA
234.1373	p-Coumaroylputrescine	9.5**	HCAA
684.4729	PA(15:0/20:3(8Z,11Z,14Z))	9.5**	Glycerophospholipids
768.5699	PA(19:1(9Z)/22:2(13Z,16Z))	2.3*	Glycerophospholipids

Significance (t-test): *P<0.05, **P<0.01, *** P<0.001.

Table 4.2: Promoter analysis of R_{RRM} genes regulated by *TaWRKY70*.

Genes	GenBank accession no.	W-BOX sequence	Position (bp)
TaACT	KT962210	TCGCTGGTGA**TGACT**AGAGGCGGCC	-464
TaDGK	KU562862	ATTATACTTA**TTGACT**TTGCATCAAG	-281
TaGLI1	KC244204	GTGATAGTCA**TTGACT**TCCACGCCCA	-250

Table 4.3: List of primers used in this study

		Primers	
Experiments	**Name**	**Forward**	**Reverse**
Gene sequencing	*TaWRKY*	GGAGCAGGAGAGTGTTCGAG	CAACCGGGAAGATCGAAGAT
VIGS Fragment amplification	*TaWRKY_VIGS*	CGCATGCTCCTCACCTCACCGG	CCGTCGCAGCAGCGTCGTCGA
VIGS gene expression	*TaWRKY-VIGSqPCR*	TCGACGACGCTGCTGCGACG	GCAGAGCTCCCTGGCGTGC
Gene sequencing	*TaDGKq*	CGGCCCGCATGACTTGCT	TGGAATGCGGTAGTCCGACA
	TaGLI1q	TCAAGCAGCACTACCCG	CAAACCAGCATCCACATTA
	TaWRKYqPCR	TCGACGACGCTGCTGCGACG	GCAGAGCTCCCTGGCGTGC
	TaACTqPCR	ACCACGCGATCCGCCGCGAG	CGGCGTGGCGTTCGTCGTCGTT
	TaACTIN	ACCTTCAGTTGCCCAGCAAT	CAGAGTCGAGCACAATACCAGTTG
	Tri6	TCTTTGTGAGCGGACGGGACTTTA	TGTTGGTTTGTGCTTGGACTCAT
Promoter sequencing	*TaACTp*	GCCGCCACCCAGATCCAATC	GGCGACAAGTGCAAGGTTA
	TaDGKp	GTTGCCGTGTTGCCGAGGGT	GCCAGAACCGTTAGAACCAATTGC
	TaGLI1p	TCAGGTCAATTGGACTCCGTTTG	CTGGGAAGCAGTTGGGAGCGG
NLS Assay	*TaWRKYNLS*	ATCCCCAATACTATGTCCATGGCG	GATCCCCAATACTCAATGGTCGAG
LUC Assay	*WRKY_LUC*	GAATCCATGTCCATGGCGCCGTACGAG	GAGCTCCTGCTCAGCACCTCCTCCT
	ACT_LUC	CTCGAGGCCGCCACCCAGATCCAATC	GCGGATCCGGCGACAAGTGCAAGGTTA
	DGK_LUC	CTCGAGGTTGCCGTGTTGCCGAGGGT	GGATCCGCCAGAACCGTTAGAACCAATTGC
	GLI1_LUC	CTCGAGTCAGGTCAATTGGACTCCGTTTG	GGATCC CTGGGAAGCAGTTGGGAGCGG

Table 4.4: Predicted genes present in the QTL-2DL based on *in-silico* gene prediction and synteny with Brachypodium and Rice.

S.N	Gene on chromosome 4 of Rice	Gene ID	Wheat scaffold
1	Cysteine-rich receptor-like protein kinase 7 precursor, putative	LOC_Os04g01860	IWGSC_chr2DL_ab_k71_contigs_longerthan_200_9734312
2	Dihydrodipicolinate synthase, chloroplast precursor, putative, expressed	LOC_Os04g18200.1	IWGSC_chr2DL_ab_k71_contigs_longerthan_200_9763750
3	ABC transporter - CER5	EU127477.2	IWGSC_chr2DL_ab_k71_contigs_longerthan_200_9821167
4	Phenylalanine ammonium transferase - PAL	LOC_Os04g43800.1	IWGSC_chr2DL_ab_k71_contigs_longerthan_200_9823366
7	Glycerol-3-phosphate acyltransferase - GPAT3	EMT04881.1	IWGSC_chr2DL_ab_k71_contigs_longerthan_200_9834552
8	Translation initiation factor IF-1, chloroplast, putative	LOC_Os04g16834.1	IWGSC_chr2DL_ab_k71_contigs_longerthan_200_9837111
9	NADPH-dependent oxidoreductase, putative, expressed	LOC_Os12g12470.1	IWGSC_chr2DL_ab_k71_contigs_longerthan_200_9853575
11	Serine/threonine-protein kinase receptor precursor, putative, expressed	LOC_Os04g01310.1	IWGSC_chr2DL_ab_k71_contigs_longerthan_200_9860267
13	Protein kinase, putative, expressed	LOC_Os04g01874.1	IWGSC_chr2DL_ab_k71_contigs_longerthan_200_9865552
14	Pectin lyase-like superfamily protein	LOC_Os04g52320.1	IWGSC_chr2DL_ab_k71_contigs_longerthan_200_9714859
15	Cell wall invertase 2	LOC_Os04g33740.1	IWGSC_chr2DL_ab_k71_contigs_longerthan_200_9733491
16	Succinate dehydrogenase 5	Bradi5g09750.1 LOC_Os04g34100.1	IWGSC_chr2DL_ab_k71_contigs_longerthan_200_9821901

17	Auxin signaling F-box 2	Bradi5g08680.1	IWGSC_chr2DL_ab_k71_contigs_longerthan_200_9848890
18	NB-ARC domain-containing disease resistance protein	Bradi5g15560.1 LOC_Os04g43440.1	IWGSC_chr2DL_ab_k71_contigs_longerthan_200_9861014

*__Gene ID containing:__ LOC (locus) – Rice, Bradi – Brachypodium, others - wheat

Figure 4.1: Physical map of the QTL-2DL on the long arm of wheat chromosome 2D. Location of the flanking markers (red color) reported in different studies are shown on left side and location of candidate genes (green color) identified within the QTL-2DL are shown on the right side.

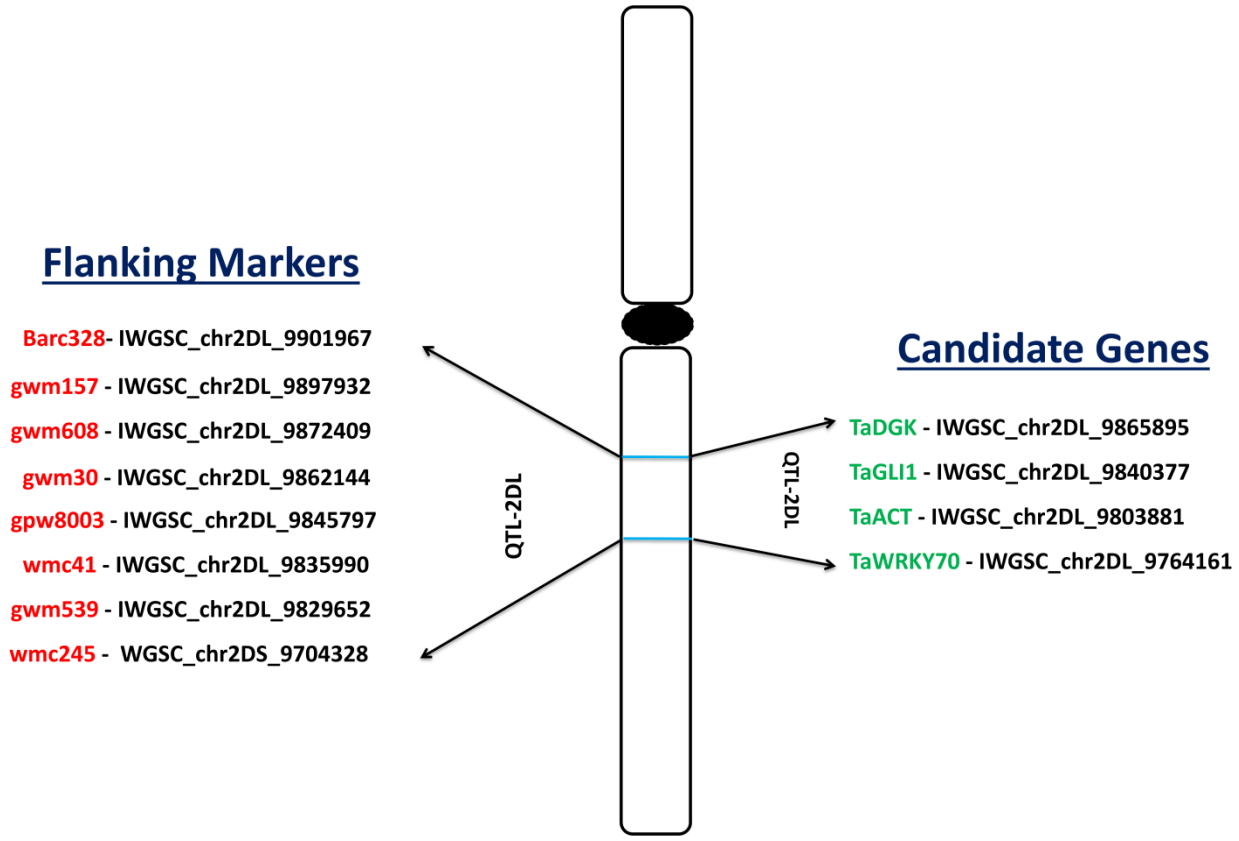

Figure 4.2: *In-silico* analysis of *TaWRKY70*. (a) Schematic diagram depicting the *TaWRKY70* gene structure containing exon, intron and coding regions; (b) Conserved domain predicted based on NCBI Conserved Domain Database Search, it shows presence of conserved WRKY domain; (c) Figure showing the characteristic features of Group III WRKY transcription factors, showing the DNA binding domain containing 69 amino acids underlined. It has WRKYGQK and C2HC, WRKY and zinc finger conserved motifs, respectively.

A)

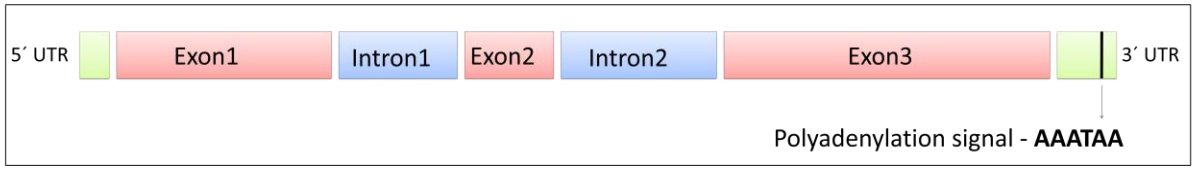

B)

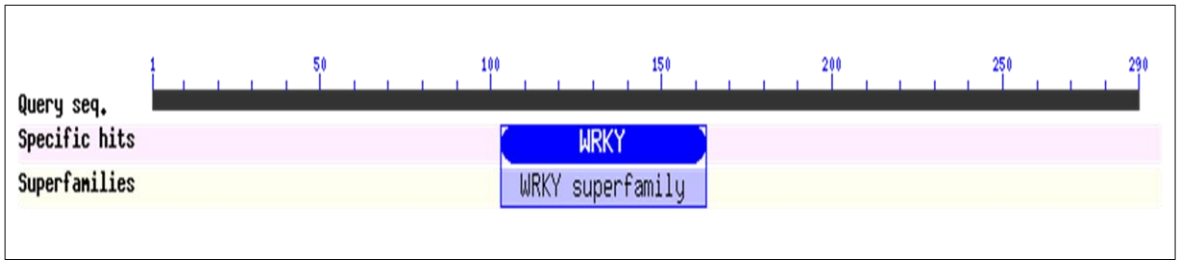

C)

TaWRKY70 Protein

MSMAPYEKVMDDLAKGQQFATQLQGLLRDSPKAGHIMDQILHTFSRAIHAAKAAAAASASESEVTDGASSGGKRKSA
AGGGPRKACRTRTQDSSVVTKNMKSLEDGQTWRKYGQKEIQNSKHSKAYFRCTHKYDQQCMARRQAQRCDDDPDTF
RVTYIGVHTCRDPAAAVAPHAPHLTGTAAGCHLISFAPAAAHGTTTTTNTNLVDDAAATGSGLQLPGLKLEGGDQEEVLS
SRTPGSSALYGAAAAAAWPDQGDVTSTLQYGGAGAFGGGLFDGYPYLEDLLSYDLDH

Figure 4.3: Phylogenetic relationships of *TaWRKY70* (in red box) with other plant *WRKY* sequences obtained from NCBI database for wheat (*TaWRKY1A*, *TaWRKY19A*, *TaWRKY74a*, *TaWRKY53a*, *TaWRKY71*, *TaWRKY74b*, and *TaWRKY19b*), rice (*OsWRKY45* and *OsWRKY32*), arabidospsis (*AtWRKY18*, *AtWRKY6*, *AtWRKY70* and *AtWRKY4*), barley (*HvWRKY32*), *Aegilops tauschii* (*WRKY70*), *Triticum urartu* (*WRKY70*). Maximum likelihood tree representing relationships among WRKY proteins from different plant species. Numbers in red color represents branch length.

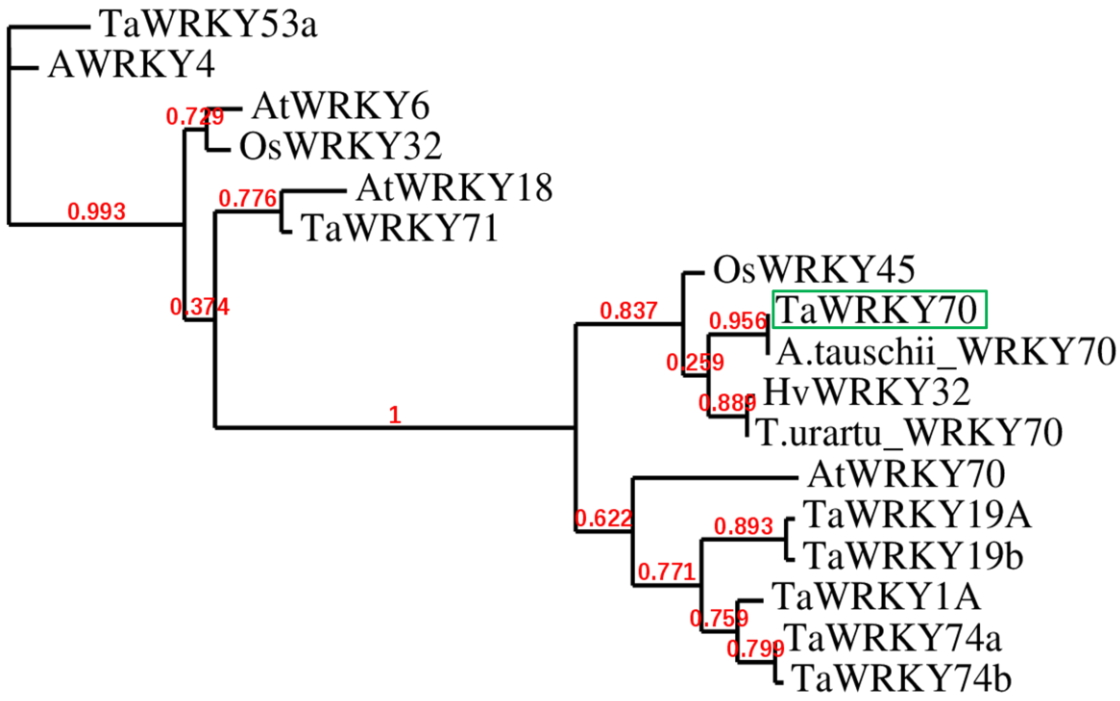

Figure 4.4: a) Comparison of DNA sequence variation between NIL-R, NIL-S and Chinese spring *TaWRKY70.* There is a SNP at exon-intron junction.

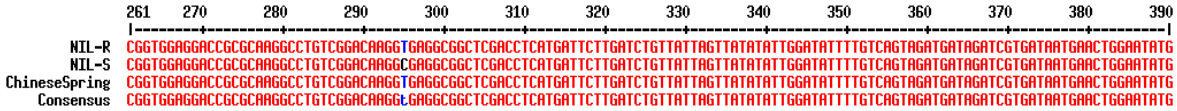

b) Comparison of protein sequence variation between NIL-R, NIL-S and Chinese spring *TaWRKY70.* The box shows the predicted nuclear localization signal.

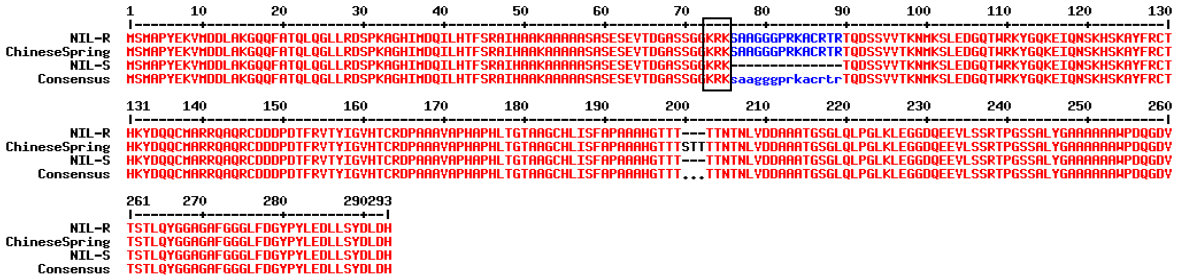

Figure 4.5: Relative transcriptional changes of *TaWRKY70* and its downstream genes induced by *Fg* and mock (water) inoculation based on qRT-PCR. Here target gene expression is normalized to reference gene *TaActin.* (a) Relative transcriptional changes of *TaWRKY70* at 48 and 72 hpi; (b) Gene expression of *TaDGK* and *TaGLI1* and *TaACT* (which did not show any expression in mock treated samples) at 72 hpi. RP = Resistant pathogen, RM = Resistant mock, SP = Susceptible pathogen and SM = Susceptible mock. Significant differences in expression levels of RP as compared to SP using Students *t*-test: **P*<0.05; ***P*<0.01.

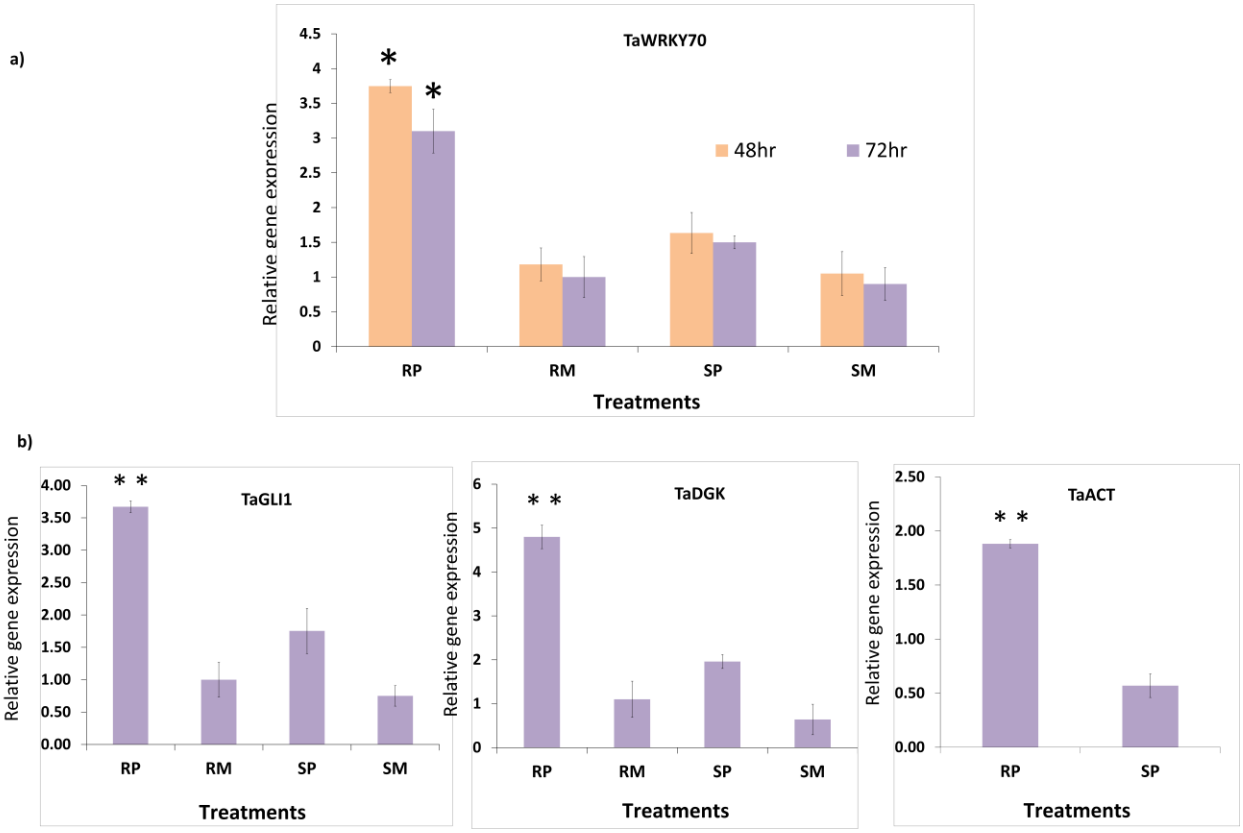

Figure 4.6: In-silico DNA-protein interaction using GeneMANIA server. Here dark colored rounds indicate target genes, DGK8 (*TaDGK*), HCT (*TaACT*), WRKY70 (*TaWRKY70*) and NHO1 (*TaGLI1*).

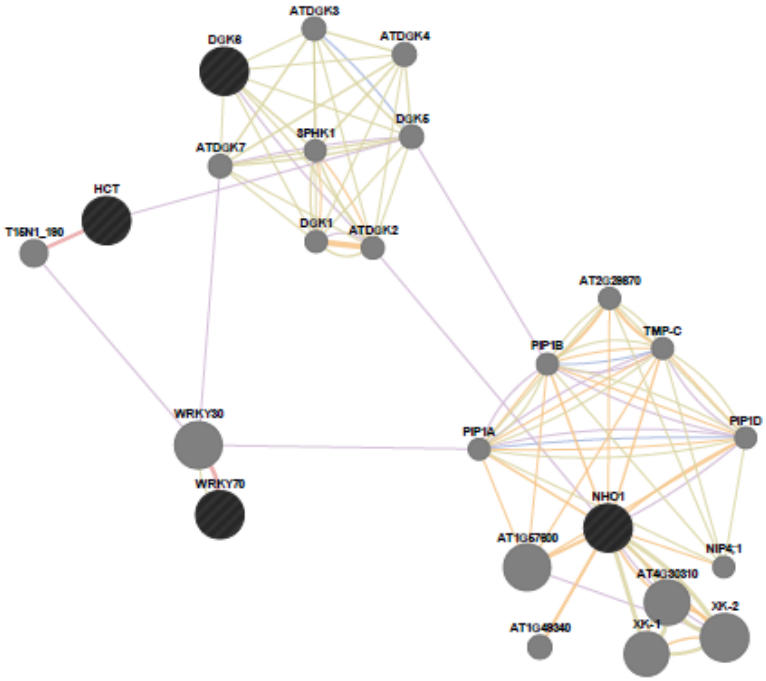

Figure 4.7: Transcriptional regulation of RRI metabolite biosynthetic genes by *TaWRKY70*: (A) constructs used in the transient expression assay and (B) relative luciferase (LUC) reporter activity by *TaWRKY70*. The relative reporter gene expression levels were expressed as LUC/GUS ratios. Values are averages of three replicates. Significant differences in expression levels in promoters compared with vector (DNA without w-box) based on Student's *t*-test: ***P*<0.01.

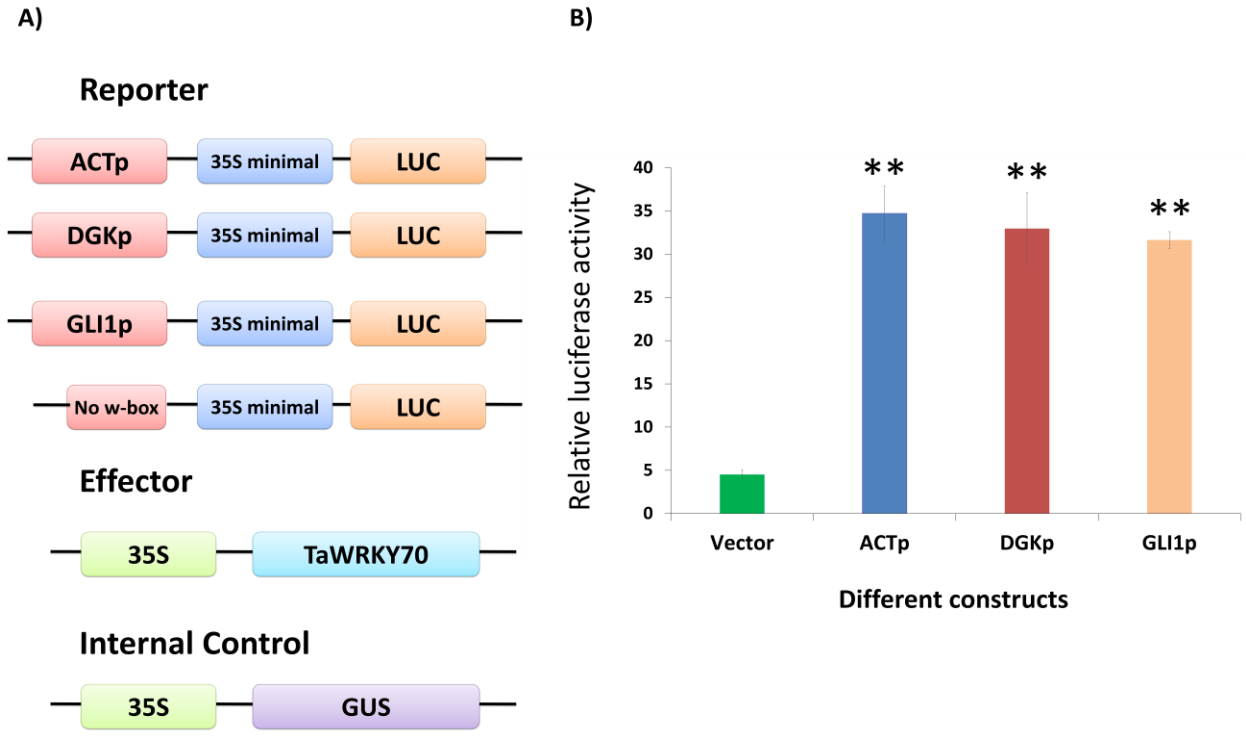

Figure 4.8: Nuclear localization of TaWRKY70 protein. (a) Nuclear localization signal (NLS) predicted. Red colored amino acid region in bold font and underlined is a NLS; (b) Nuclear localization analysis. Constructs consisting of either TaWRKY70-GFP fusion or GFP alone were used to transiently transform into potato protoplasts. Free GFP and TaWRKY70-GFP fusion proteins were transiently expressed in potato protoplast and observed with a fluorescence microscope. Here, the extreme left panel (GFP fluorescence), the middle panel (bright field) and the right panel (merged view of two images). Transient expression assays were conducted at least three times.

a)

MSMAPYEKVMDDLAKGQQFATQLQGLLRDSPKAGHIMDQILHTFSRAIHAAKAAAAASASESEVTDGASSGG**KRK**SAAGGGPRK
ACRTRTQDSSVVTKNMKSLEDGQTWRKYGQKEIQNSKHSKAYFRCTHKYDQQCMARRQAQRCDDDPDTFRVTYIGVHTCRDPAA
AVAPHAPHLTGTAAGCHLISFAPAAAHGTTTTTNTNLVDDAAATGSGLQLPGLKLEGGDQEEVLSSRTPGSSALYGAAAAAAWPDQ
GDVTSTLQYGGAGAFGGGLFDGYPYLEDLLSYDLDH

b)

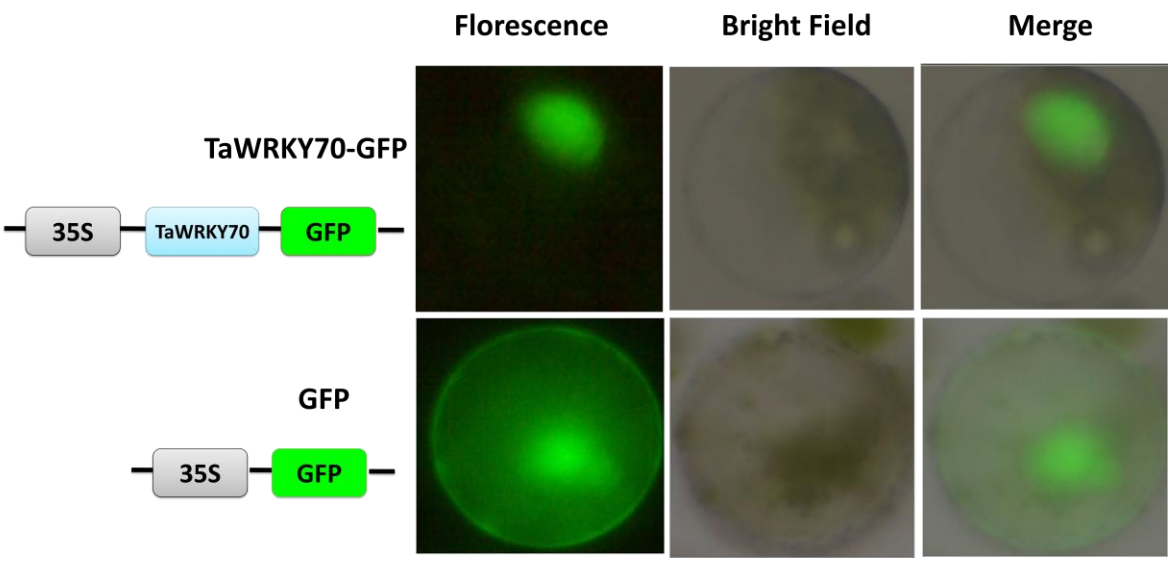

Figure 4.9: Effect of *TaWRKY70* silencing in FHB resistant near-isogenic line (NIL-R), inoculated with *F. graminearum* or mock-solution. (A) Confirmation of knocking down of *TaWRKY70* by assaying relative transcript expression of *TaWRKY70* normalized to reference gene *TaActin* in silenced plant (BSMV:*TaWRKY70*) compared to non-silenced (BSMV:00) at 3 dpi after *Fg* inoculation; (B) Fungal biomass in BSMV-infected plants at 6 dpi with *Fg*. Relative copy number of *tri6* fungal housekeeping gene (=fungal biomass) was quantified in *TaWRKY70* knocked down (BSMV:*TaWRKY70*) plants and compared with control (BSMV:00). Here relative target gene copy number is normalized to reference gene *TaActin*; and (C) Relative transcript levels of *TaDGK*, *TaACT* and *TaGLI1* assayed individually in *TaWRKY70* knocked down (BSMV:*TaWRKY70*) plants compared to non-silenced (BSMV:00) at 3 dpi after *Fg* inoculation. Here target gene expression is normalized to reference gene *TaActin*; (D) Relative metabolite abundances of RRI metabolites in silenced (BSMV:*TaWRKY70*) and non-silenced (BSMV:00) NIL-Rat 3 dpi after *Fg* inoculation. PA-1 – PA(17:0/20:4(5Z,8Z,11Z,14Z)), PA-2 – PA(15:0/20:3(8Z,11Z,14Z)), PA-3 – PA(19:1(9Z)/22:2(13Z,16Z)), Cou-Ag – p-coumaroylagmatine and Cou-put – p-coumaroylputrescine. Significant differences in expression levels as compared in silenced (BSMV:*TaWRKY70*) with non-silenced (BSMV:00) using Students *t*-test: **P*<0.05; ***P*<0.01.

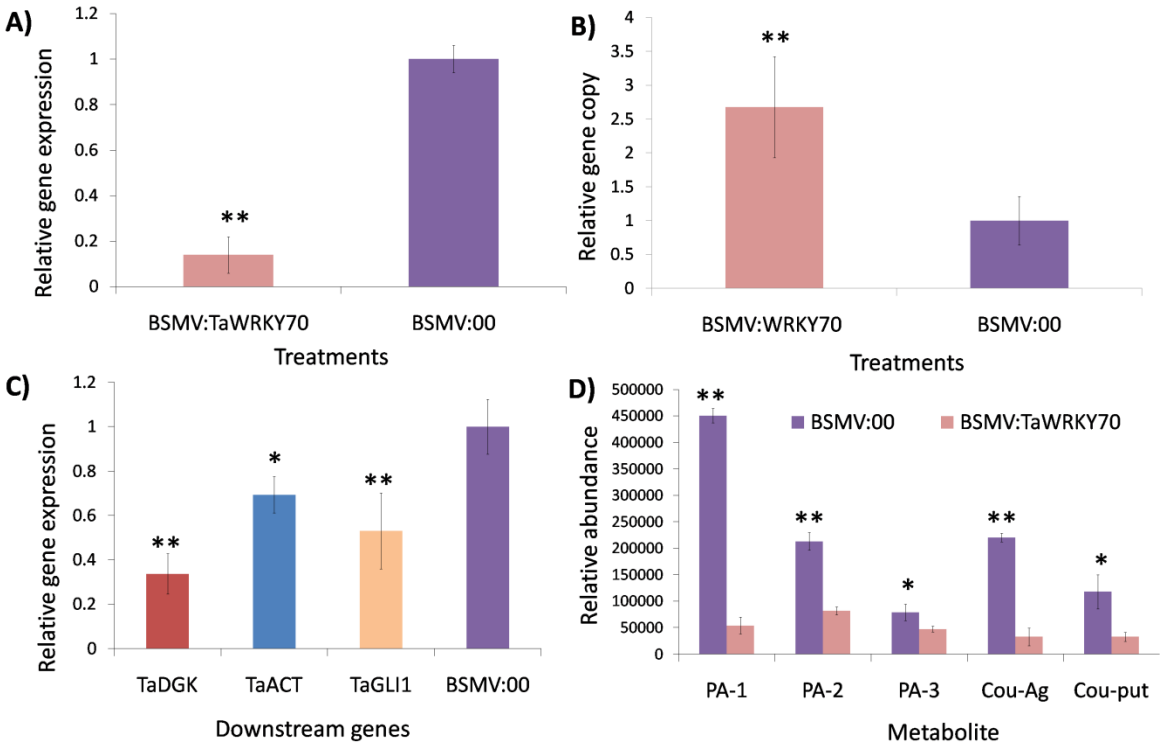

Figure 4.10: A proposed model showing *TaWRKY70* regulating downstream genes involved in the biosynthesis of hydroxycinnamic acid amides (HCAAs) and phosphotidic acid and derivatives (PAs) to resist the pathogen through cell wall fortification, intensified signaling and reduced cell death. After pathogen perception, *TaWRKY70* gets activated by unknown pathways (ex: MAP kinase) and this intern regulates the transcript expression of downstream genes involved in biosynthesis of resistance related induced (RRI) metabolites.

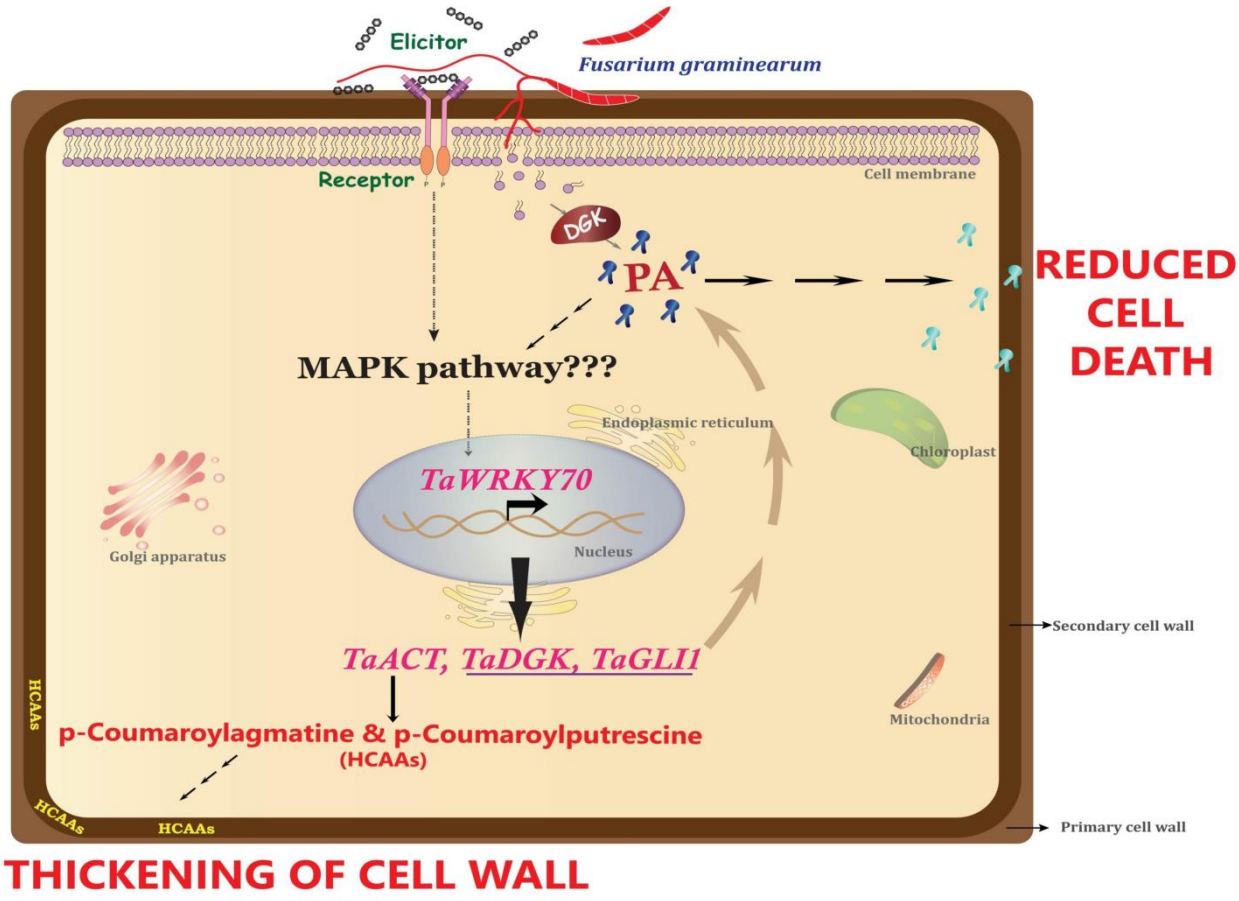

Figure 4.11: a) Primers designed for knocking down *TaGLI1* gene. Virus-induced gene silencing (VIGS) fragments were designed to specifically knock-down the *TaGLI1* gene. The knock-down fragment is boxed; b) Representation of typical BSMV based VIGS vectors and c) The *TaWRKY70* cDNA fragment was cloned to pSL038-1 vector (Test, in the top) downstream of the γb gene. pSL038-1 vector carrying either *phytoene desaturase* (*PDS*) gene (BSMV:*TaPDS*, in the middle) or without any plant gene (BSMV:00, in the down) served as positive control and negative controls, respectively.

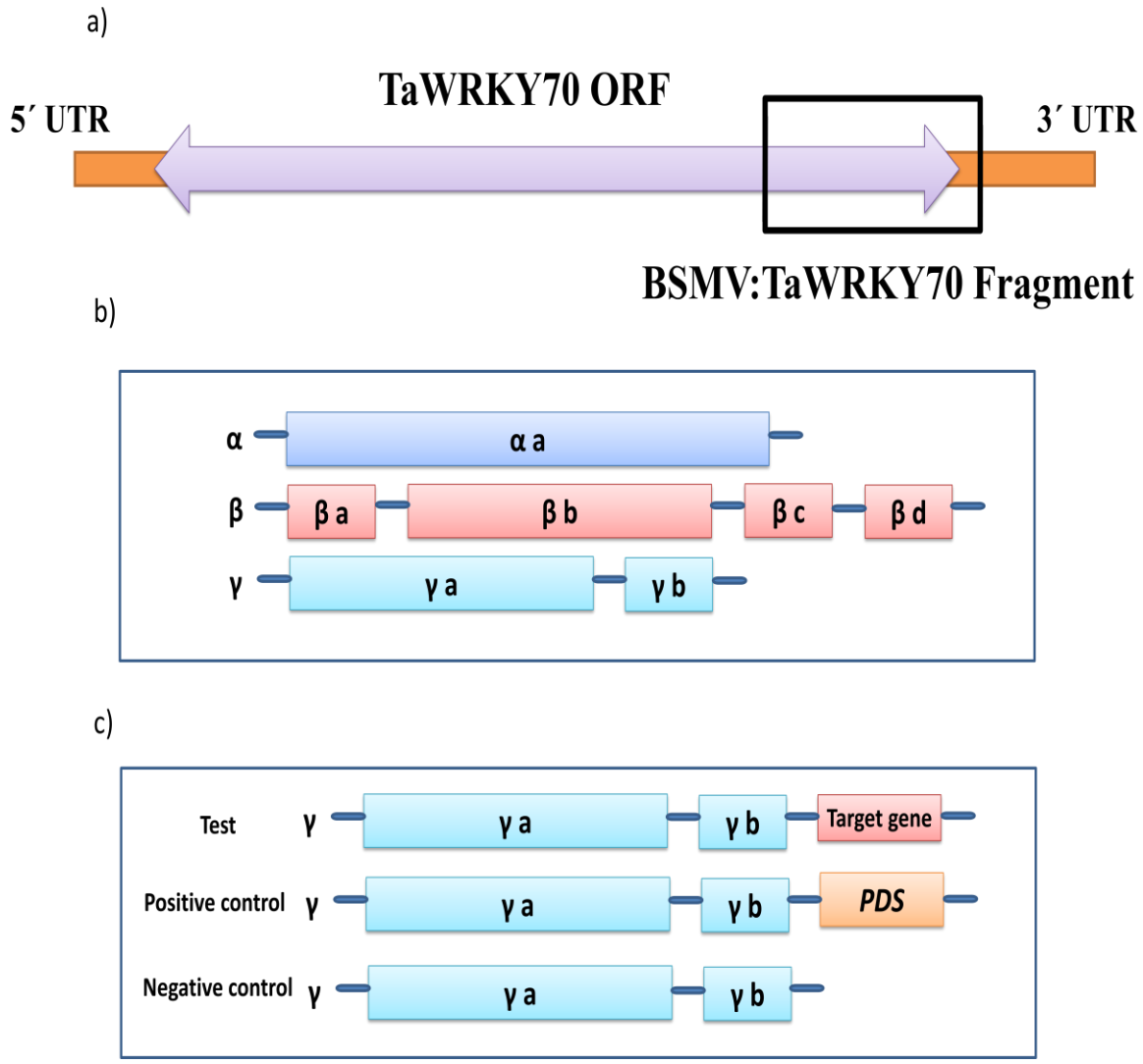

Connecting statement for Chapter V

Chapter V, entitled "Liquid chromatography and high resolution mass spectrometry-based metabolomics to identify quantitative resistance-related metabolites and genes, in spikelets of wheat NILs with QTL-2DL against Fusarium head blight" authored by Udaykumar Kage, Shivappa Hukkeri and Ajjamada C. Kushalappa, will be submitted to the peer reviewed scientific journal for publication.

It is evident that QTL-2DL is one of the major QTL responsible for rachis resistance to FHB in wheat. In chapter III and IV, it was revealed that the resistance to spread of pathogen is mediated by mechanisms located in the rachis tissue. It was also proved that QTL-2DL exhibits spikelet resistance based on spray inoculation in field condition (McCartney et al., 2007). A Reduced fungal biomass accumulation in inoculated spikelets of resistant NIL relative to susceptible during initial few days after infection and also a reduced spread of infection to adjacent spikelet during later stages was reported (Long et al., 2015). FHB is evaluated based on spray inoculation under field conditions, but this method lead to experimental error due to uneven distribution and variable inoculum quantity reaching spikelets and interaction with environmental conditions. An improved method based on inoculation of three alternate spikelets and assessment of fungal biomass significantly reduced experimental error, and enabled discrimination of both spikelet and rachis resistance (Kumar et al., 2015). Resistance mechanisms to FHB are organ specific and biochemical resistance mechanisms in spikelet are not clearly understood. We hypothesized that QTL-2DL exhibits novel resistance mechanisms at the spikelet for resistance to FHB, and the near-isogenic lines (NILs) with resistance and susceptible QTL-2DL alleles would differentially accumulate metabolites. The present study was undertaken to understand the spikelet resistance mechanisms to FHB in wheat.

Chapter V

Liquid chromatography and high resolution mass spectrometry-based metabolomics to identify quantitative resistance-related metabolites and genes, in spikelets of wheat NILs with QTL-2DL, against *Fusarium graminearum*

Udaykumar Kage, Shivappa Hukkeri and Ajjamada C. Kushalappa*

Plant Science Department, McGill University, Sainte-Anne-de-Bellevue,
Quebec, Canada H9X 3V9

5.1 Abstract

Metabolomics has become a widely used tool in plants to phenotype different genotypes with varying levels of resistance to stresses. Two near-isogenic lines (NILs) of wheat QTL-2DL, with contrasting levels of resistance to Fusarium head blight (FHB), were grown under greenhouse conditions, spikelets were individually inoculated, fungal biomass quantified and the metabolite profiling was done. The NILs significantly varied in resistance to FHB. The metabolites in phenylpropanoid, fatty acid and glycerophospholipid pathways were highly induced in NIL-R (resistant NIL) relative to NIL-S (susceptible NIL), upon *Fusarium graminearum* inoculation. Key genes, involved in the biosynthesis of high fold-change resistance related (RR) metabolites, such as glyceraldehyde 3-phosphate acyltransferase (*GPAT*), eceriferum 5 *(CER5)*, an ABC transporter, and phenylalanine ammonium lyase (*PAL*) were identified from the QTL-2DL region based on wheat genome survey sequence. Concurrently, relative transcript expressions of these candidate genes were also up-regulated in NIL-R after pathogen inoculation, confirming their potential involvement in the biosynthesis of high fold-change RR metabolites. The spikelet resistance to FHB observed in this study was mainly associated with cell wall remodelling through deposition of cutin and suberin molecules.

5.2 Introduction

Fusarium head blight is one of the devastating diseases of wheat and barley. The coincidence of anthesis and early grain-filling stage with warm and wet weather is very congenial for FHB infection (Bai et al., 2001). Infected crop is contaminated with toxic fungal secondary metabolites known as mycotoxins such as deoxynivalenol (DON), nivalenol (NIV) and zearalenone. These toxins affect milling and baking quality and they are very harmful to human and animal health (Dexter et al., 1996).

Through fungicide application the severity of FHB can be reduced by 50 to 60 %, however, this approach is not environmentally sustainable and also the effectiveness is variable, depending on the environmental conditions (Stack, 2000). Therefore, development and cultivation of FHB resistant varieties is one of the promising strategies in FHB management. The FHB resistance is generally evaluated based on five types of resistance, of these, resistance to initial infection (type I), resistance to spread of infection through rachis (type II) and resistance to mycotoxins in grains (type III) are commonly used (Schroeder and Christensen, 1963). Resistance to FHB is evaluated based on spray inoculation under field conditions, but this method leads to high experimental errors due to uneven distribution and variable inoculum quantity reaching spikelets and interaction with environmental conditions. Single floret inoculation in a spike has been successfully used in greenhouse and field conditions to evaluate rachis resistance in wheat (Cheng et al., 2015). However, single floret inoculation to assess spikelet resistance in barley, which generally has a very high level of rachis resistance, under greenhouse conditions was unable to discriminate small phenotypic variations in FHB severity based on visual assessment (Smith et al., 2004; Yli-Mattila et al., 2008). An improved method based on inoculation of three alternate individual spikelets and assessment of fungal biomass significantly reduced experimental errors, and enabled discrimination of both spikelet and rachis resistance (Kumar et al., 2015). Among several quantitative trait loci (QTL) identified for FHB resistance, QTL-2DL is one of the major ones exhibiting both spikelet and rachis resistance (Somers et al., 2003; McCartney et al., 2007). Despite being a major QTL for FHB resistance, genetic components underlying this QTL are still largely unknown, especially for spikelet resistance. The spikelets are generally resistant to *F. graminearum* infection because of a thick

wax layer. Pathogen enters through anthers or space between a lemma and palea, eventually gaining access through stomata on the inner sides of the lemma and palea.

Plants resist pathogens through synthesizing metabolites and proteins, following pathogen invasion. The RR metabolites and proteins can be constitutive (RRC) or induced (RRI) and the resistance is due to their antimicrobial properties or they are deposited to reinforce cell walls, forming structural components, thus containing the pathogen (Kushalappa and Gunnaiah, 2013). By comparing the metabolite composition between two individuals at a particular growth stage or time, differences in functionality can be assessed. Semi-comprehensive metabolite profiling of barley and wheat genotypes with varying levels of resistance to FHB has led to the identification of several resistance related (RR) metabolites (Bollina et al., 2010; Bollina et al., 2011; Hamzehzarghani et al., 2005; Hamzehzarghani et al., 2008; Kumaraswamy et al., 2011a; Kumaraswamy et al., 2011b). The FHB resistance mechanism controlled by the QTL-Fhb1 has been associated with cell wall thickening, through deposition of hydroxycinnamic acid amides (HCAAs) and flavonoids in FHB resistance (Gunnaiah et al., 2012). Thus, it is possible to decipher the mechanisms of resistance in QTL-2DL based on metabolite profiling of NILs, which have the same genetic background (susceptible) except for the alleles at the QTL region. Metabolite profiling based on liquid chromatography and high resolution mass spectrometry (LC-HRMS) is essential to phenotype resistance as it can identify a wide range of metabolites, whereas, using gas chromatography and mass spectrometry (GC/MS) nonvolatile metabolites cannot be detected (Bedair and Sumner, 2008; Schauer and Fernie, 2006).

In our previous studies, first we employed GC/MS (Hamzehzarghani et al., 2008) for metabolite profiling of pooled samples of spikelets and the rachis of NILs with QTL-2DL. In a recent study, we employed LC-HRMS for metabolite profiling of only rachis samples, which revealed a high fold induction of HCAAs and phosphatidic acids in rachis tissues to be responsible for cell wall thickening and antimicrobial effects against FHB spread, imparting rachis resistance (Chapter III and IV). We build on this study and now performed metabolite profiling of only spikelet samples of NILs with QTL-2DL using LC-HRMS, to gain an in-depth understanding of spikelet resistance mechanisms and the genes responsible for resistance to FHB. By considering all the above facts, the present study used the inoculation of individual spikelets and metabolite profiling of NILs based on LC-HRMS. The dissection of QTL-2DL using flanking marker

sequences and integration of metabolite profile and transcript expression information identified *GPAT*, *CER5* and *PAL* as putative candidate genes, appears to be acting cumulatively to reinforce cell walls through deposition and cross-linking of fatty acids and phenolics.

5.3 Material and Methods

5.3.1 Plant material

The NILs with FHB susceptible/resistant alleles at QTL-2DL (Somers et al., 2003) were derived from a cross between BW301 X HC374 (McCartney et al., 2007; Somers et al., 2005). The BW301 is FHB susceptible hard red spring wheat line from western Canada and HC374 is resistant to FHB. Microsatellite markers were used for genotyping NILs, the homozygous lines except for alleles of a QTL-2DL locus with susceptible background were selected (Somers et al., 2005). The seeds of resistant and susceptible NILs were obtained from Dr. McCartney, AAFC, Morden, MB. In each pot five seeds were sown and later three plants per pot were maintained under greenhouse conditions (at 16 h light and eighth dark, and 23 ± 2 °C ambient temperature).

5.3.2 Pathogen production and inoculation

Fusarium graminearum, a DON-producing isolate GZ-3639 (Proctor et al., 1995) culture, was maintained on potato dextrose agar (PDA) media. From this, a fresh culture was grown on rye B agar media, at 26 °C, for four days. For spore production, the pathogen was further sub-cultured on rye B agar plates and exposed near to UV light, for eight h dark and 16 h light over four days. From a seven-day old culture, macroconidia were harvested, spore concentration was adjusted to 1×10^5 macroconidia ml^{-1}. At 50 % anthesis stage (Growth stage = 55) five wheat spikes per replication were selected and the middle three alternate spikelet pairs were inoculated with 10 µl macroconidial suspension (approximately 1000 spores/spikelet) or mock solution using a syringe (GASTIGHT 1750 DAD, Reno, USA). Inoculated plants were covered with water sprayed white plastic bags to maintain high moisture and they were removed at 48 hours post inoculation (hpi).

5.3.3 Experiment layout, sample collection, metabolite analysis, and data processing

The experiment was laid out in a randomized complete block design with two genotypes (resistant and susceptible NILs), two inoculations (pathogen and mock) and five replications over time. At 72 hpi, the mid 6 pairs of spikelet region, including three pairs of inoculated

spikelets, was cut, the spikelets and rachis were separately collected, frozen in liquid nitrogen and stored at -80 °C until further use. The spikelets samples were ground in liquid nitrogen and metabolites were extracted in 60 % aqueous solution of methanol, centrifuged and the 5 µl of supernatant was used for metabolite analysis. Metabolites were analyzed by injecting aliquots of sample extracts to liquid chromatography and high resolution mass spectrometry (LC-HRMS; LC-LTQ-Orbitrap, Thermo Fisher Electron Corporation) as previously reported (Bollina et al., 2010). The output data file from LC-HRMS was imported into the Bioinformatics tool MZmine2 for peak deconvolution, peak detection, and spectral filtering. The MZmine2 processing and statistical analyses were performed as described previously (Gunnaiah et al., 2012).

5.3.4 Putative metabolite identification

The RR metabolites were putatively identified based on three criteria: i) Accurate mass match with the metabolites reported in several databases, such as PlantCyc, METLIN, KNApSAcK, LIPID MAPS, NIST and KEGG with an accurate mass error, AME ≤ 5 ppm (Kushalappa and Gunnaiah, 2013; Tohge and Fernie, 2010); ii) Fragmentation pattern mass match with databases and literature (Matsuda et al., 2009); iii) *In-silico* confirmation of fragmentation based on Masspec scissor in ChemSketch (ACD labs, Toronto) (Matsuda et al., 2009).

The relative peak intensities of monoisotopic masses of metabolites were subjected to Students *t*-test (SAS v 9.3). The peaks significant at $P<0.05$ (Kushalappa and Gunnaiah, 2013), and false discovery rate threshold of 0.05 (Vinaixa *et al*., 2012) were retained. The false discovery rates of peaks are higher at low signal/noise (S/N) ratio and/or at low abundances, therefore we used a high S/N ratio and abundances of metabolites (Kumar et al., 2016). The metabolites with significantly higher abundances in NIL-R than in NIL-S, based on a *t*-test, were considered as RR metabolites. These were further grouped into RR constitutive (RRC= RM>SM) and RR induced (RRI= (RP>RM)> (SP>SM)) metabolites. The significant peaks based on *t*-test from all the treatments were subjected to hierarchical cluster analysis (HCA) and canonical discriminant analysis (CDA) to classify the observation based on canonical scores, using CANDISC and PROC GLM procedures of SAS 9.4 program (Hamzehzarghani et al., 2008). The canonical (CAN) scores were used for HCA for unsupervised classification of the treatments. The Euclidian distance between group centers in CAN space was used to construct dendgrogram. Metabolites only with significant fold-change ≥ 2 were considered for further study.

5.3.5 Relative quantification of fungal biomass

Three alternate pairs of spikelets in five spikes per replication, from five replicates, were inoculated with macroconidial suspension using a syringe (GASTIGHT 1750 DAD, Reno, USA). At six days post inoculation (dpi), three pairs of inoculated and three alternate pairs of un-inoculated spikelets were harvested, ground and the genomic DNA was isolated using DNeasy Plant Mini Kit (Qiagen, Canada). An equal quantity of DNA (20 ng) was taken and the fungal biomass was estimated based on the number of relative gene copies of fungal housekeeping gene *Tri6* (Fusarium trichothecene-producing gene) using real-time qPCR. The abundance of *Tri6* gene was normalized with *TaActin* and the qPCR readings were used to estimate the fungal biomass in NILs (Kumar et al., 2015).

5.3.6 Identification of candidate genes in FHB QTL-2DL

The presence of SSR markers, WMC245, GPW8003, GWM539, and GWM608 was used to define the interval for QTL-2DL. These markers were sequenced and subjected to BLASTN (Altschul et al., 1990) search on the International Wheat Genome Sequencing Consortium (IWGSC) wheat genome database to physically localize the QTL-2DL. Based on previous studies the genes involved in the biosynthesis of high fold-change RRI metabolites were selected from different crop species and BLAST searched in Wheat URGI BLAST (https://urgi.versailles.inra.fr/blast/?dbgroup=wheat_survey &program=blastn) tool to check whether they were located in QTL-2DL region. Best hit contigs were downloaded and genes were predicted using SoftBerry–fgenesh program (http://linux1.softberry.com /berry.phtml?topic=fgenesh&group=programs&subgroup=gfind) to study the gene structure. DNA sequence was converted to protein sequence using ExPASy Translate Tool (http://web.expasy.org/translate/). The MOTIF search tool (http://www.genome.jp/tools/motif/) was used for domain prediction in deduced amino acid sequence.

5.3.7 RNA isolation, cDNA synthesis and qPCR analysis

For real-time quantification of gene expression, total plant RNA was isolated from five biological replicates of spikelets using the RNeasy plant mini kit (Qiagen Inc.). From purified total RNA, 1-2 μg was used to reverse transcribe RNA into cDNA using iScript cDNA synthesis kit (BioRad, ON, Canada). With the help of Qi SYBR Green supermix (BioRad) in a

CFX384TM Real-Time system (BioRad, ON, Canada), qPCR was performed. The mRNA abundance was normalized with *TaActin.* PCR results were analyzed using comparative delta-delta Ct method ($2^{-\Delta\Delta CT}$) (Livak and Schmittgen, 2001). Primers used for qPCR are given in Table 5.2.

5.4 Results

5.4.1 Fungal biomass varied between NILs

The fungal biomass was quantified at six dpi in NIL-R and NIL-S, based on relative gene copy numbers of fungal *Tri6* gene. The amount of fungal biomass in spikelets was significantly (2.5 - fold) lower in NIL-R than in NIL-S (Fig. 5.1). Thus, proving that the NILs were distinctly vary in spikelet resistance.

5.4.2 Clustering of observations based on multivariate analysis

A total of 49 significant metabolites, excluding isotopes and adducts, common to all the five replicates, were subjected to canonical discriminant analysis to classify samples and to identify possible biological functions associated with them. The CAN vectors were able to separate the clusters, where, the CAN1 vector explained 21.7 % variance, and it identified resistance function, successfully discriminating NIL-R from NIL-S. The CAN2 vector explained 20.6% of variance and it identified pathogenesis function, separating pathogen treated from mock treated observations (Fig. 5.2). Further, the hierarchical cluster analysis showed, replicates and treatments were distinctly clustered and the replicates were classified within the treatments with small difference among them (Fig. 5.3).

5.4.3 Resistance related metabolites associated with spikelets with varying alleles at QTL-2DL

To assess the impact of *Fusarium* infection on wheat metabolite expression, a semi-comprehensive metabolomics was used to see the differential metabolite profiles between two wheat NILs with resistant and susceptible alleles of QTL-2DL. The pathogen inoculated spikelet samples were collected at 72 hpi and metabolites were analyzed based on LC-HRMS. After filtering of isotopes and adducts a total of 2231 consistent monoisotopic peaks were detected in this study, among which 1225 were RRC and 789 were RRI metabolites. Out of these, 23 RRC

and 24 RRI (including RRIq, which were detected only in NIL-R but not in NIL-S, after pathogen inoculation) metabolites were putatively identified (Table 5.1, Fig 5.4a). The RRC metabolites identified belonged to major chemical groups, such as, flavonoids (39.13%), fatty acids (21.73%), glycerophospholoipids (21.73%) and terpines (13.04%) (Fig. 5.4b). Whereas, the RRI metabolites belonged to fatty acids (47.6%), glycerophospholoipids (33.3%), phenylpropanoids (14.2%) and gingerglycolipid A, a lipid (Fig. 5.4c).

The RR metabolites with only fold-change ≥2 were considered for downstream studies to identify candidate genes and to correlate with gene expression, assuring increased confidence, which is away from the technical precision of a typical semi-comprehensive metabolomics workflow. The number of significant (P<0.005) RR metabolites in fatty acid, glycerophospholipid and phenylpropanoid pathways were higher in NIL-R than in NIL-S. Induction of these metabolites in spikelets after challenging with fungus indicated their likely role in spikelet resistance.

5.4.4 Identification of candidate genes in QTL-2DL

The presence of SSR markers, WMC245, GPW8003, GWM539 and GWM608 was used to define the interval for QTL-2DL. These markers were sequenced and subjected to BLASTN search on the IWGSC wheat genome database for physical localization of the QTL. Our study identified several RR metabolites involved in cuticle and suberin biosynthesis. Some of the important biosynthetic genes of these RR metabolites were explored in the literature and BLAST searched in Wheat URGI BLAST (https://urgi.versailles.inra.fr/blast/?dbgroup=wheat_survey&program=blastn) tool. Coincidently, some important genes involved in cuticle and suberin biosyntheses such as glyceraldehydes 3-phosphate acyltransferase (*GPAT*), eceriferum 5 *(CER5)*, an ABC transporter and the phenylalanine ammonium lyase (*PAL*) and agmatinecoumaroyl transferase (*ACT*) involved in the biosynthesis of phenylpropanoids, were located within the FHB QTL-2DL (Chapter III & IV). The wheat contigs containing *GPAT, CER5, ACT* and *PAL* were downloaded and the gene prediction was carried out. DNA sequence was converted to amino acid sequences and used for domain prediction, which revealed the presence of protein with acyltransferase domain in *GPAT* that was involved in the biosynthesis of suberin (Beisson et al., 2012; Beisson et al., 2007; Li et al., 2007; Marchler-Bauer et al., 2014). A domain search result for the *CER5* revealed that it

belonged to the ABC transporter G family (AGCG) proteins, which are mainly involved in lipid transport in all kingdoms for cuticle deposition (Chen et al., 2011; Kunst and Samuels, 2009; McFarlane et al., 2010; Vogg et al., 2004). Whereas, the genes, *ACT* (Chapter III) and *PAL* has acyltransferase and phenylalanine ammonium lyase domain, respectively (Marchler-Bauer et al., 2014). *CER5* and *GPAT* are proposed to be involved in the biosynthesis of cuticle or aliphatic domains of suberin (Beisson et al., 2012; Beisson et al., 2007; Kunst and Samuels, 2009; Li et al., 2007; Vogg et al., 2004), whereas, *ACT* and *PAL* are involved in aromatic domains of suberin (Gou et al., 2009; Soler et al., 2007; Yang et al., 1997).

5.4.5 Gene expression based on qPCR

To check connections between the identified RR metabolites and their biosynthesis pathway genes, we used a targeted qPCR approach. Predicted gene sequences were used to design the primers for qPCR. The expression analysis of genes at 72 hpi of *F. graminearum* showed that the levels of expression of *PAL, CER5,* and *GPAT* were significantly (P<0.01) higher in NIL-R compared to NIL-S, in both pathogen treated samples. The expression of *TaACT* was higher in pathogen treated samples of NIL-R than NIL-S but was not significant (Fig. 5.5). In our previous study, *ACT* was induced only after pathogen inoculation in rachis (Chapter III). This proved the tissue-specificity for high induction in rachis, after pathogen inoculation. A higher expression of candidate genes in NIL-R relative to NIL-S is correlated with a higher abundance of RR metabolites, confirming their impending role in induction of higher abundance of metabolites in NIL-R.

5.5 Discussion

Metabolic profiling of resistant and susceptible NILs, with QTL-2DL, following mock or pathogen inoculation, identified several RR metabolites. After pathogen perception, plants trigger hierarchies of downstream genes to biosynthesize RR metabolites to contain the pathogen to the initial infected area (Kushalappa et al., 2016). In this study, highly accumulated metabolites were fatty acids, glycerophospholipids and HCAAs. These metabolites have antimicrobial and cell wall reinforcing properties.

5.5.1 Toxic phytochemicals slow down the pathogen progress in plant

A good number of antimicrobial metabolites such as fatty acids, flavonoids and HCAAs were observed with significant fold-change in NIL-R compared to NIL-S (Table 5.1). This indicated a strong defense due to antimicrobial compounds, playing an important role in wheat against infection to FHB. These observations are consistent with previous reports, indicating the antimicrobial role of phenylpropanoids and flavonoid (Bollina et al., 2010; Gunnaiah et al., 2012; Yogendra et al., 2014). Linoleic acids in vitro inhibited several pathogenic fungi: *Rhizoctonia solani, Pythium ultimum, Pyrenophora avenae and Crinipellis perniciosa* (Walters et al., 2004). Deposition of feruloyl-3'-methoxytyramine, feruloyltyramine, and *p*-coumaroyltyramine have been reported in onion cells at the sites of infection, following inoculation with *Botrytis allii* (Ishihara et al., 2008). Accumulation of the coumaroylagmatine type of HCAA was reported in barley leaves infected with *Erysiphe graminis*f. sp. *hordei* (von Röpenack et al., 1998). The p-coumaroylserotonin and feruloylserotonin types of HCAAs were detected in rice leaves infected with *Bipolaris oryzae* (McLusky et al., 1999). Several HCAAs such as feruloylputrescine, *p*-coumaroyltyramine, N-feruloyltyramine, 4-coumaroyl-3-hydroxyagmatine, feruloylagmatine, coumaroylagmatine, terrestriamide, and feruloylserotonin were induced in potato leaves against *Phytophthora infestans* (Keller et al., 1996; Pushpa et al., 2013; Yogendra et al., 2014). The flavonoids, kaempferide 3, 7-dirhamnoside, isovitexin 2″-O-rhamnoside, retusin 7-O-neohesperidoside, quercetin 3-(6-sinapylglucosyl)(1→2)-galactoside, and aliarin 4′-methyl ether, patuletin 3,7-bis (3- acetylrhamnoside), kaempferide 3-rhamnoside-7-(6″- succinylglucoside) were induced in potato genotypes challenged with *P. infestans* (Bollina et al., 2010; Kumaraswamy et al., 2011a; Yogendra et al., 2014). Whereas, the kaemferol and its glucosylated forms were identified as RR metabolites for resistance to *F. graminearum* in barley (Bollina et al., 2010; Kumaraswamy et al., 2011a). The kaempferide-O-rutinoside and kaempferide 3-O-β-D-glucopyranosyl significantly inhibited the growth of *F. oxysporum* (Galeotti et al., 2008).

5.5.2 Cell wall fortification

Antimicrobial phytochemicals that suppress the pathogen development, giving more time for plants to get prepared to induce other types of defenses (Khajuria et al., 2013). Therefore, complementary defense mechanisms are needed to intensify the defense. Various metabolites

belonging to phenylpropanoids such as p-coumaroylagmatine, cinnamoyltyramine, and N-caffeoylputrescine known as HCAAs are significantly higher in abundance in NIL-R. These HCAAs acts as phytoalexins and also their deposition help in cell wall fortification. Fast remodeling and strengthening of cell walls could prevent the supply of nutrients to the pathogen, thus starving the pathogen to death, in addition to its progress beyond the initial infection (Khajuria et al., 2013; Yogendra et al., 2015). The gene expression analysis of resistant and susceptible NILs revealed a higher transcript expression of *PAL* and *ACT* genes following pathogen inoculation, which were associated with significantly induced levels of phenylpropanoids in NIL-R. Phenolics usually cross-link with other macromolecules such as polysaccharides and lignins of the cell wall by etheric linkage and thus leading to cell wall enforcement (Marcia, 2009).

In addition to phenylpropanoids, the abundances of fatty acids such as lignoceric acid, linoleic acid, hydroxyl acids, dicarboxylic acids, C16:0, C16:1,and C18: x (x = 1, 2 &3) (Table 5.1) were higher in NIL-R than in NIL-S (RRI), and/or induced only in NIL-R and not in NIL-S (RRIq). In our previous study based on GC/MS, monopalmitoylglycerol and p-coumaric acid were highly induced after pathogen inoculation (Hamzehzarghani et al., 2008). These are monomers and oligomers involved in cutin and suberin biosynthesis in plants, which acts as a barrier for the entry of pathogen. Cutin is a polymer of predominantly C16 and C18 hydroxy fatty acids (Kolattukudy, 2005; Kumar et al., 2016). Whereas, the suberin monomers have dominant chain-lengths of 16, 18, and 22 carbons (Kolattukudy et al., 1975). Along with fatty acids, cutin and suberin also contain variable amounts of phenolic compounds, dicarboxylic acids, and glycerol (Lara et al., 2015; Stark and Tian, 2007). The glycerophospholipids like, PI(8:0/9:0), PS(9:0/14:5), PS(9:0/14:4) and monopalmitoylglycerol were induced after pathogen inoculation are mainly intermediates of phospholipid metabolic pathway. The elevation of intermediates of phospholipid pathway indicates, membrane lipids might be mobilized for defense and they are in the process of getting converted into polymers for cell wall and cuticle thickening. Our findings are consistent with previous reports (Khajuria et al., 2013; Kosma et al., 2010; Zhu et al., 2012), indicating that the membrane lipids mobilize these monomers, which are known to be converted into polymers such as oxylipins, wax, cutin and suberin to reinforce cell wall. Correspondingly, higher levels of transcript expressions of *GPAT* and *CER5* genes in NIL-R than in NIL-S after pathogen inoculation clearly indicated their potential involvement in the production and

transportation of aliphatic metabolites towards cell wall. The acyltransferase *GPAT5* is involved in the synthesis of cuticle and suberin (Beisson et al., 2012; Beisson et al., 2007; Li et al., 2007). Similarly, *CER5* also plays an important role in cuticle enforcement in plants (Chen et al., 2011; Kunst and Samuels, 2009). Cell wall suberization is a physiologically important mechanism in host plant tissue against pathogen invasion (Franke et al., 2005; Kolattukudy, 1981; Thomas et al., 2007). The suberin is a complex polymer having fatty acid derived domains (aliphatic) and hydroxycinnamate domains (aromatic). The aliphatic domains are mainly the subunits of ω-hydroxy acids and the aromatic domain, principally composed of phenolic compounds like hydroxycinnamates (Gou et al., 2009). The hydroxycinnamic acids and derived polymers constitute the polyaromatic domain of suberin (Bernards et al., 1995). The high fold-change in phenolic compounds identified here appears to be further involved in the formation of cuticle-suberin domains along with fatty acids. These aliphatic and aromatic domains link covalently through ester bonds to make it a much stronger physical barrier to the invading pathogen through natural openings, such as crevices, openings between the lemma and palea and stomata, leading to spikelet resistance at the outset. Further, these results were supported by significantly lower fungal biomass in the spikelet samples of NIL-R as compared to NIL-S, as also was observed based on field studies using spray inoculation (McCartney et al., 2007).

5.5.3 Proposed model for role of QTL-2DL in spikelet resistance to FHB

Based on metabolomics and gene expression studies, we propose a predicted model to explain the role of genes involved in wheat QTL-2DL in spikelet resistance to FHB (Fig. 5.6). Following *F. graminearum* invasion, a group of downstream resistance genes (*GPAT, CER5, PAL* and *ACT)* were induced to produce high fold-change RR metabolites belonging to fatty acids, glycerophospholipids and phenylpropanoids. These metabolites are known to have antimicrobial property and are deposited to reinforce cell walls, by cross linking with each other to form suberin. Taken together, these results indicate potential involvement of *GPAT, CER5, ACT* and *PAL* genes in spikelet resistance to FHB, thereby reducing the infection in wheat spike. Following functional validation these genes can be used to improve FHB resistance in wheat. The identified metabolites can also be used as a biomarker for FHB resistance screening following metabolite authentication using other techniques like Nuclear Magnetic Resonance (NMR) or by spiking authentic chemical compounds.

Table 5.1: Resistance related (RR) metabolites identified in spikelets of NILs, harboring contrasting alleles of QTL-2DL, upon *F. graminearum* or mock inoculation.

RRI (resistance related induced metabolites)				
Observed mass	**AME**	**Metabolite name**	**Fold change**	**Chemical group**
310.2148	1.3	9S-hydroperoxy-10E,12Z,15Z-octadecatrienoic acid	3.9	Fatty acid
326.2460	0.9	8-methoxy-13-hydroxy-9,11-octadecadienoic acid (Hydroxy fatty acids)	3.6	Fatty acid
276.1589	1.2	p-Coumaroylagmatine	3.4	Phenylpropanoid
596.2944	-3.0	1-(9Z,12Z-octadecadienoyl)-glycero-3-phospho-(1'-myo-inositol) PI(18:2(9Z,12Z)/0:0)	3.4	Fatty acid
600.2915		PI(8:0/9:0)	3.0	Glycerophospholipid
599.2880		PS(9:0/14:5)	2.8	Glycerophospholipid
342.2409	1.0	methyl 9,12-dihydroxy-13-oxo-10-octadecenoate (Hydroxy fatty acids)	2.7	Fatty acid
368.3658	1.1	Lignoceric acid	2.5	Fatty acid
601.3037		PS(9:0/14:4)	2.4	Glycerophospholipid
250.1320	1.1	N-Caffeoylputrescine	2.4	Phenylpropanoid

432.2280	0.7	1-(6Z,9Z,12Z-octadecatrienoyl)-glycero-3-phosphate PA(18:3(6Z,9Z,12Z)/0:0)	2.3	Glycerophospholipid
280.2409	2.4	Linoleic acid	2.2	Fatty acids
330.2409	1.0	9S,10S,11R-trihydroxy-12Z-octadecenoic acid (Dicarboxylic acid)	2.2	Fatty acid
444.1270	-0.2	5-Methoxypodophyllotoxin	1.8	Phenylpropanoid
328.2253	0.8	9S,10S,11R-trihydroxy-12Z,15Z-octadecadienoic acid (Dicarboxylic acid)	1.5	Fatty acid
312.2304	1.0	9Z-Octadecenedioic acid (Dicarboxylic acid)	1.4	Fatty acid
482.2650	1.1	1-(9Z-hexadecenoyl)-glycero-3-phospho-(1'-sn-glycerol) PG(16:1(9Z)/0:0)	1.4	Glycerophospholipid
RRC (resistance related constitutive metabolites)				
445.1458	0.4	PS(0:0/13:5)	2.8	Glycerophospholipid
536.1896	0.4	5-Hydroxy-6,7,3',4',5'-pentamethoxyflavanone 5-O-rhamnoside	2.7	Flavonoids
560.4808	0.6	11R-octadecanoyloxyoctadeca-9Z,12Z,15Z-	1.8	Fatty acids

		trienoic acid (Mayolene-18 – wax monoesters)		
512.2755	-3.7	Pedilstatin	1.7	Diterpine
418.0903	3.0	Cellotriose	1.7	Sub unit of cellulose
422.2074	-4.6	1-Methoxyficifolinol	1.7	Isoflavonoides
475.2702	0.7	1-(6Z,9Z,12Z-octadecatrienoyl)-glycero-3-phosphoethanolamine PE(18:3(6Z,9Z,12Z)/0:0)	1.7	Glycerophospholipid
478.1269	-0.2	PI(0:0/10:5)	1.6	Glycerophospholipid
580.1433	0.9	Quercetin 3-xylosyl-(1->2)-rhamnoside	1.6	Flavonoids
498.2599	1.0	1,2-dioctanoyl-sn-glycero-3-phospho-(1'-sn-glycerol) PG(8:0/8:0)	1.6	Glycerophospholipid
477.2860	1.1	1-(9Z,12Z-octadecadienoyl)-glycero-3-phosphoethanolamine PE(18:2(9Z,12Z)/0:0)	1.5	Glycerophospholipid
464.2544	-4.1	(-)-Jolkinol B	1.5	Diterpine
480.2493	-4.0	(-)-Jolkinol A	1.5	Diterpine
434.1217	0.9	Naringenin 7-O-beta-D-glucoside	1.5	Flavonoids
580.1584	0.5	4,2',3',4'-Tetrahydroxychalcone 4'-O-(2"-O-p-coumaroyl)glucoside	1.4	Flavonoids
731.9619	1.6	Rhamnetin 3'-glucuronide-3,5,4'-trisulfate	1.4	Flavonoids

284.2717	0.8	octadecanoic acid	1.4	Fatty acids
626.1849	0.3	5-O-Methyleriodictyol 7-glucosyl-(1->4)-galactoside	1.3	Flavonoids
266.2251	1.7	7-heptadecynoic acid	1.3	Fatty acids
302.2243	-1.1	4,8,12,15,18-eicosapentaenoic acid (C20 compound)	1.3	Fatty acids
594.1588	0.5	kaempferol-3-glucoside-3-rhamnoside	1.2	Flavonoids
564.1283	2.6	Kaempferol 3-(2"-p-coumaryl-alpha-L-arabinopyranoside)	1.2	Flavonoids
RRIq (resistance related induced metabolite, only in NIL-R and not in NIL-S)				
676.3679	1.3	gingerglycolipid A		Lipids
276.2092	1.2	(6Z,9Z,12Z,15Z)-Octadecatetraenoic acid (C18 Compound)		Fatty acid
484.2809	-3.4	1-hexadecanoyl-sn-glycero-3-phospho-(1'-sn-glycerol) (PG(16:0/0:0))		Glycerophospholipid
386.1215	0.5	1-O-Sinapoyl-beta-D-glucose		Phenylpropanoid
506.2650	0.9	1-(6Z,9Z,12Z-octadecatrienoyl)-glycero-3-phospho-(1'-sn-glycerol) (PG(18:3(6Z,9Z,12Z)/0:0)		Glycerophospholipid
172.1104	2.7	9-hydroxy-5Z-nonenoic acid (hydroxyfatty acid)		Fatty acid
267.1268	3.21	Cinnamoyltyramine		Phenylpropanoid

AME: Accurate Mass Error= ((Observed mass-expected mass) / expected mass) X 10^6, **RRC:** Resistance related constitutive, **RRI:** Resistance related induced, **RRIq**: RRI qualitative, as it was detected only in NIL-R but not in NIL-S after pathogen inoculation.

Fold-change (FC) calculation: were based on relative intensity of metabolites, RRC= RM/SM, RRI= (RP/RM)/(SP/SM). RP: resistant NIL with pathogen inoculation, RM: resistant NIL with mock inoculation, SP: susceptible NIL with pathogen inoculation, SM: susceptible NIL with mock inoculation.

t-test significance at $P<0.05$

Table 5.2: List of primers used in the study for gene expression

Gene name	**Forward primer (5´ - 3´)**	**Reverse primer (5´ - 3´)**
PAL	AGCTCCTCTTCAGCACAACC	GACGTACTAAACCAAGTGTATGTGT
ACT	ACCACGCGATCCGCCGCGAG	CGGCGTGGCGTTCGTCGTCGTT
GPAT	GACGGCCGCC TCGCTTTCCT	GGAAGCGGACTCCAAAGAACG
CER5	ATCGGCAACTGGCACCTCCGGGGCG	GAGCCGGGGCCGCATGAGGAGCT

Figure 5.1: *F. graminearum* fungal biomass estimated based on the relative gene copy number of tri6 gene in spikelets of near-isogenic lines (NILs), at 6 dpi. Significant differences in NIL-R compared with NIL-S using student *t*-test: ***P*<0.01.

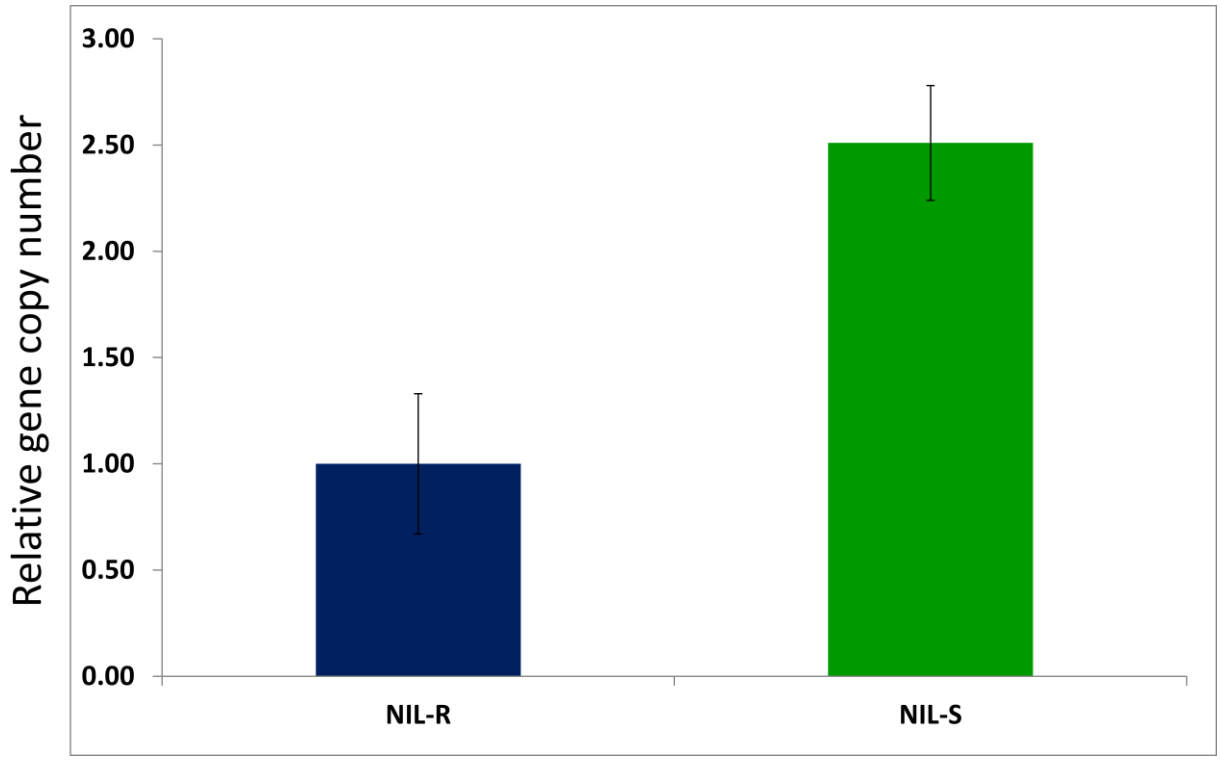

Figure 5.2: Scatter plot of canonical discriminant analysis of significant (P<0.05) metabolites from resistant and susceptible NILs following *F. graminearum* or mock inoculation. Where, RM is resistant mock treated, RP is resistant pathogen treated, SM is susceptible mock treated, and SP is susceptible pathogen treated samples. Can1 and Can2 explained 21.7% and 20.6% of variance.

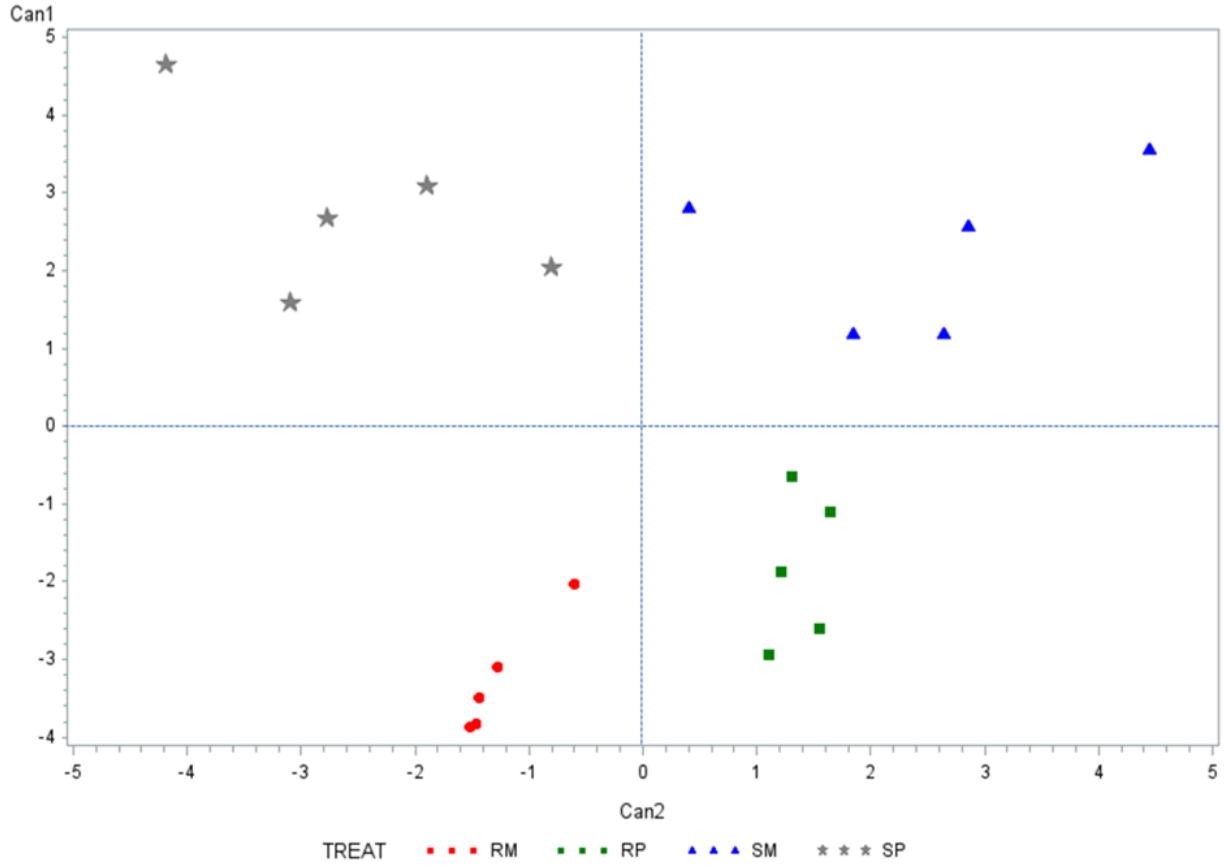

Figure 5.3: Dendrogram based on hierarchical cluster analysis (HCA) of principal components with significant (P<0.05) metabolites. The treatments are: RM, resistant mock treated; RP, resistant pathogen treated; SM, susceptible mock treated; and SP, susceptible pathogen treated samples.

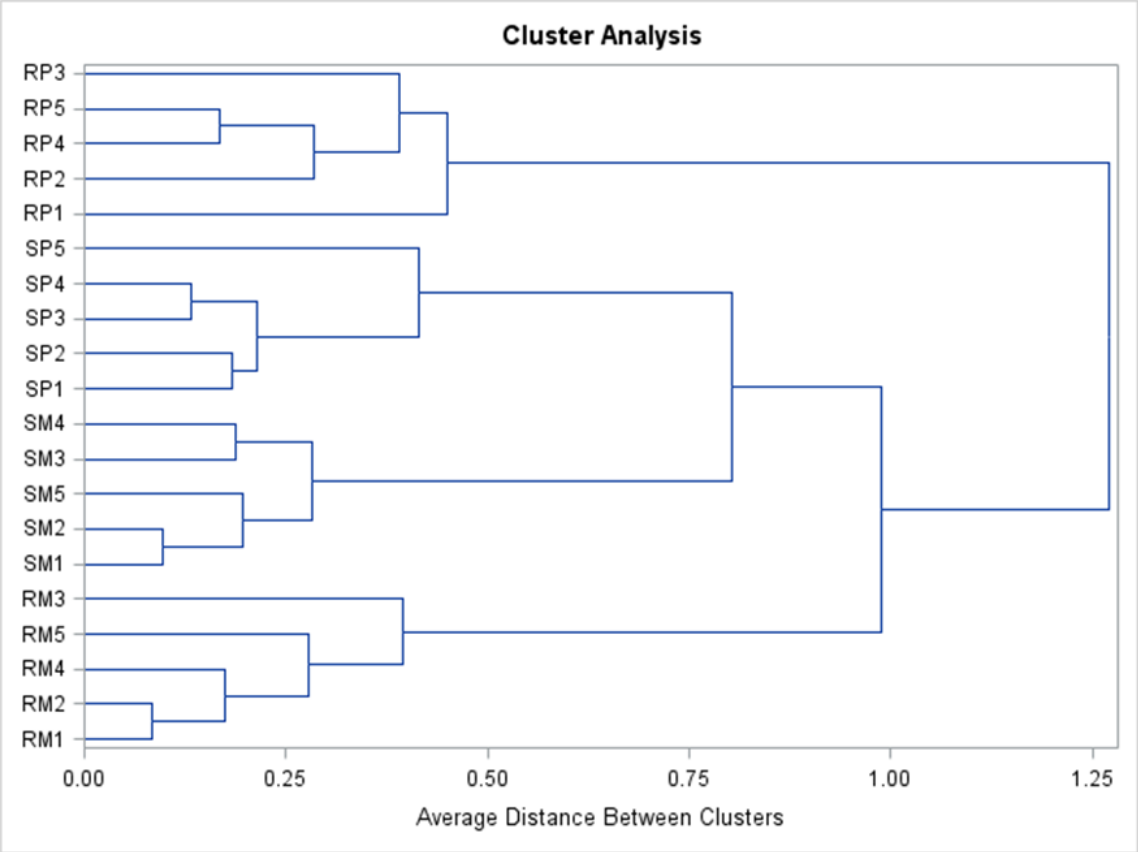

Figure 5.4: The chemical groups of resistant related (RR) metabolites detected in NILs upon pathogen inoculation. a) Total RR metabolites accumulated upon *F. graminearum* inoculations in NILs, (b) RRI metabolites accumulated in NILs upon *F. graminearum* inoculations, (c) RRC metabolites accumulated in NILs upon *F. graminearum* inoculations**.**

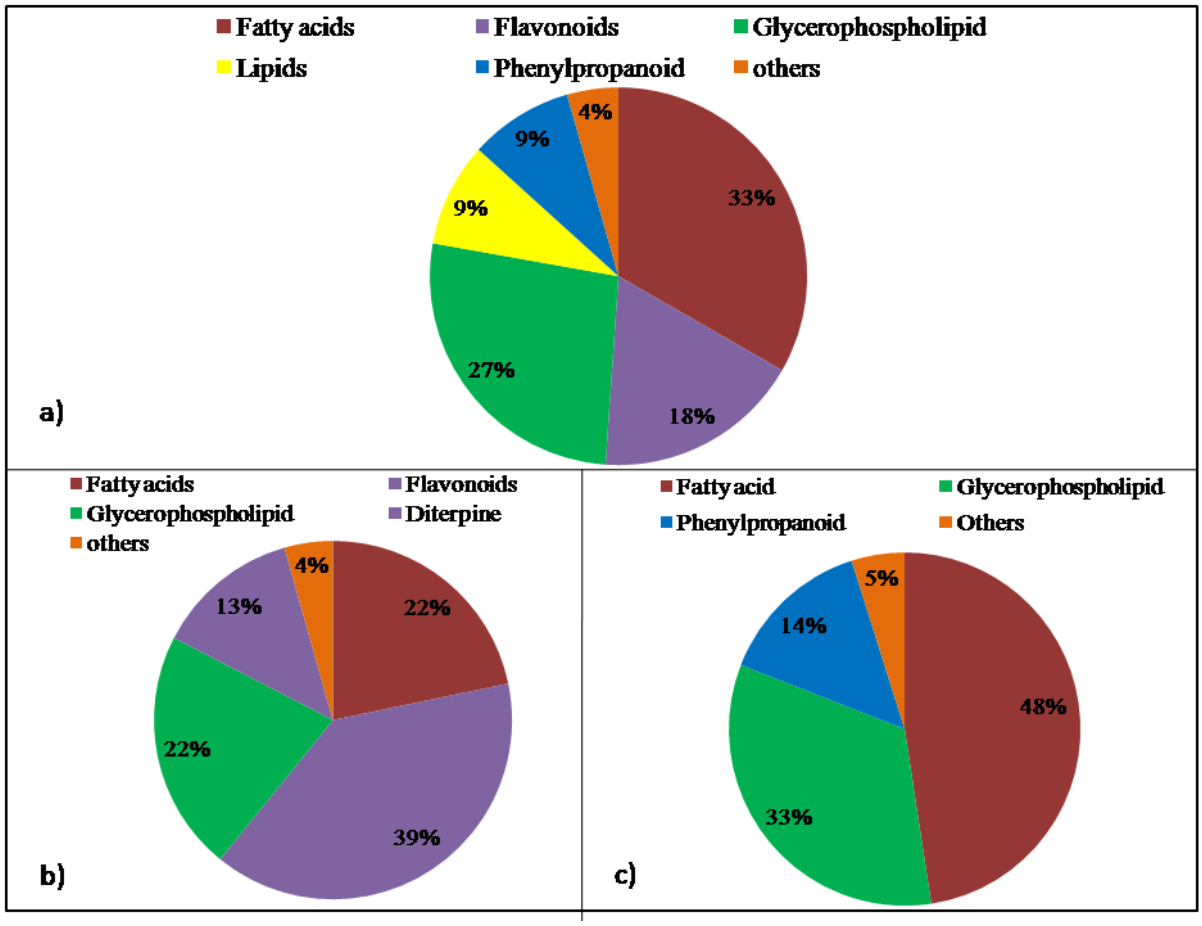

Figure 5.5: Relative transcript expression of resistance genes. The relative transcript expression was measured in the mock and pathogen treated resistant and susceptible NILs compared with mock-inoculated susceptible NIL at 72 hpi. RM is resistant mock treated, RP is resistant pathogen treated, SM is susceptible mock treated, and SP is susceptible pathogen treated samples. Significant differences in expression levels as compared in RP compared with SP using the student t - test: $^{**}P<0.01$.

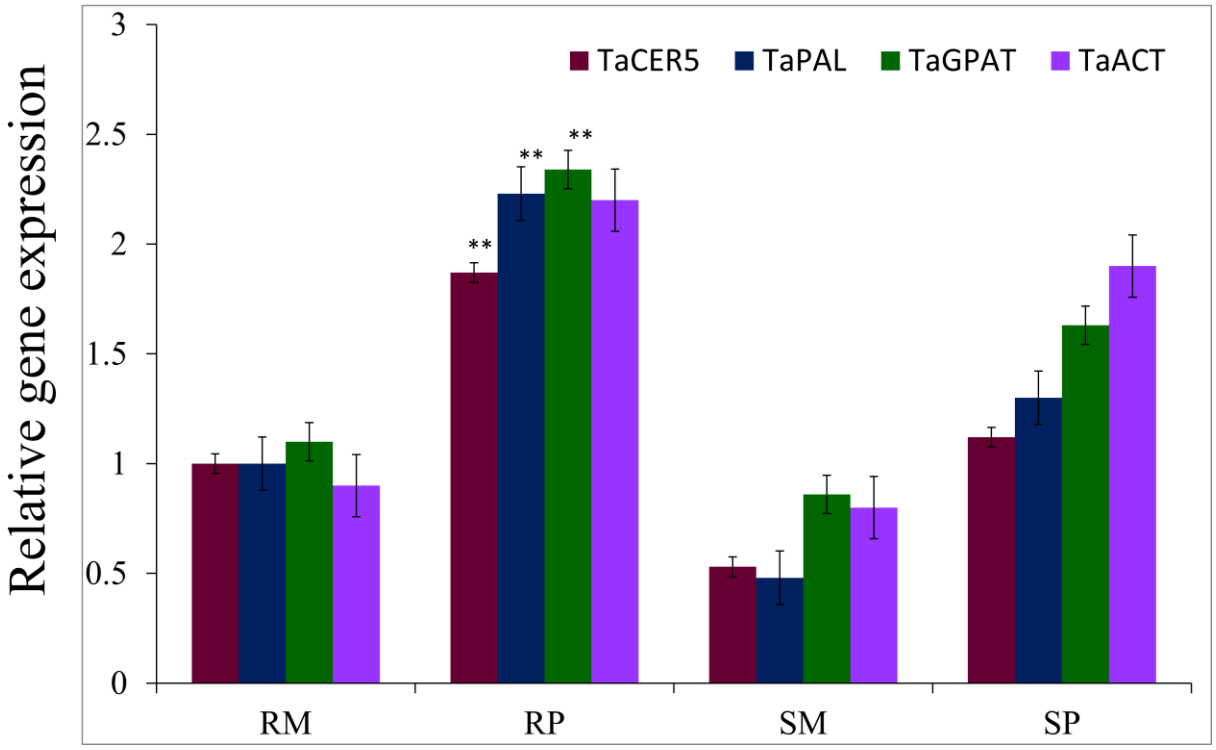

Figure 5.6: A proposed model showing the role of QTL-2DL in spikelet resistance through regulation of genes and accumulation of metabolites involved in cell wall enforcement to resist the pathogen.

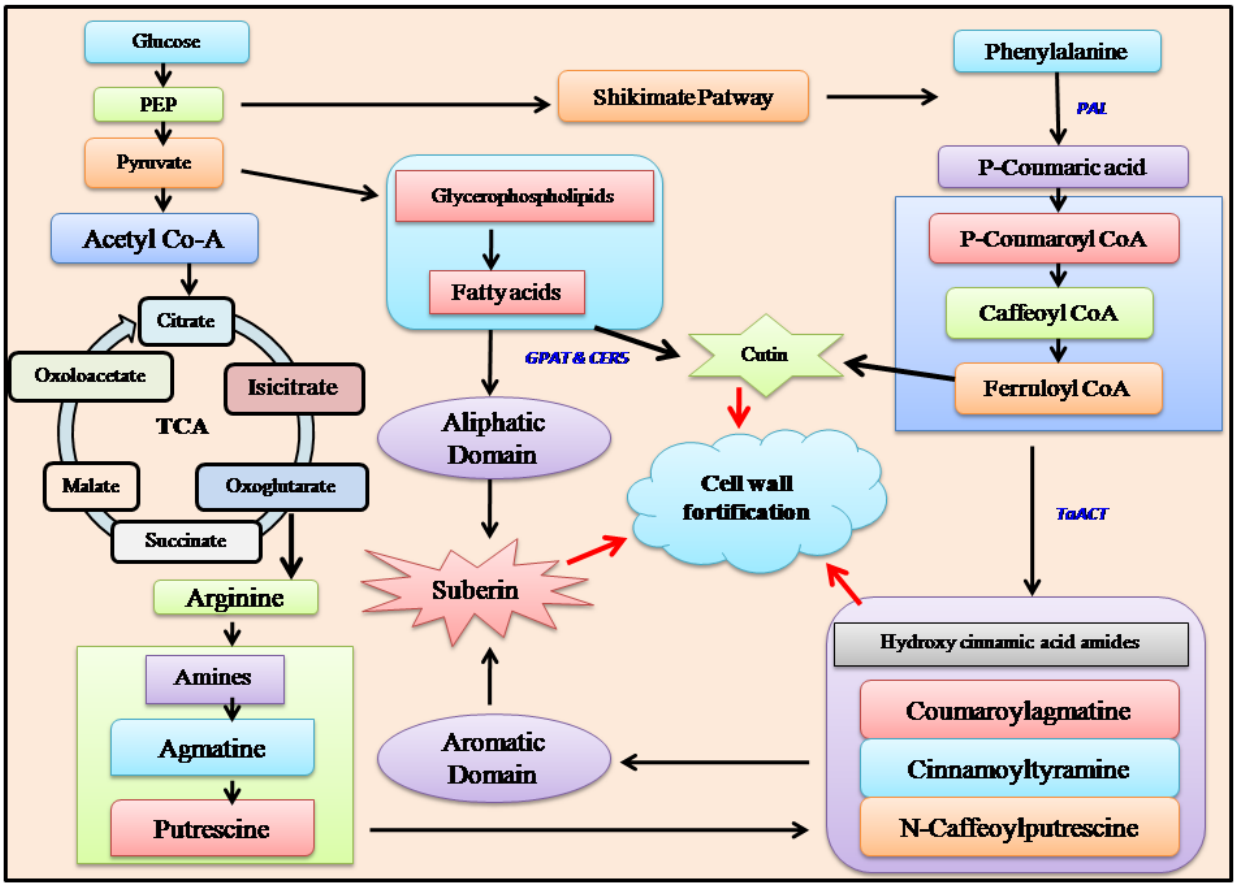

Chapter VI

General discussion and future studies

6.1 General discussion

Fusarium head blight of wheat (*Triticum aestivum* L) caused by *Fusarium graminearum* is a major disease in temperate climates around the world. In addition to a loss of grain yield, FHB causes a reduction in grain quality, by contaminating with mycotoxins, including deoxynivalenol (DON), 3-acetyl-deoxynivalenol (3-ADON) and 15-acetyl-deoxynivalenol (15-ADON) which are harmful to animal and human health. Development and cultivation of resistant cultivars is considered as the most efficient, viable and environmentally friendly approach for management of FHB (Bai and Shaner, 2004). However, genetic improvement of the resistance to FHB is impaired by its quantitative nature and low heritability (Bai and Shaner, 1994).

For the genetic dissection of FHB resistance in wheat, several studies reported a number of individual QTL located on all the chromosomes of wheat. The QTL-2DL is one of the major QTL controlling FHB resistance in wheat (Wuhan-1) (Somers et al., 2003). The mechanisms of resistance involved are very complex, with many molecular regulatory circuits, but the resistance function of none is known. Therefore, while moving toward the understanding of individual QTL contribution to FHB resistance, the present study was designed to identify some of the resistance candidate genes localized in the QTL-2DL region, using metabolo-genomics approaches. It was hypothesized that, wheat NILs with resistance and susceptible alleles at QTL-2DL, also differ in metabolic profiles, gene expression and gene sequence. The functional gene(s) in the resistant NIL biosynthesize specific metabolite(s) in significantly high abundance, while the mutated/non-functional gene(s) in the susceptible NIL are unable to synthesize these metabolite(s) or even if it can, the abundance would be significantly low. To test this hypothesis, studies in Chapter III to V were performed; this reports the contribution of QTL-2DL to FHB resistance in wheat through identification and characterization of candidate genes and deciphering the resistance mechanisms prevailing in wheat against FHB.

In chapter III, to identify RR metabolites that are highly accumulated, the NIL-R and NIL-S were inoculated with pathogen, and rachis samples were analyzed for metabolites. The RR induced metabolites with high fold-change in abundance in NIL-R, compared to NIL-S, were mapped on metabolic pathway to find their catalytic enzymes, and the corresponding genes were identified using genomic databases and available literatures.

The QTL-2DL region and genes localized in this were physically mapped, based on the flanking SSR markers reported for QTL-2DL locus. The SSR markers were amplified from genomic DNA, the PCR product was Sanger sequenced. These flanking marker sequences were BLAST (Altschul et al., 1990) searched in IWGSC (http://www.wheatgenome.org/) genomic database to physically map the QTL region. The candidate genes identified at initial step were BLAST (Altschul et al., 1990) searched in the IWGSC database to confirm their co-localization within the physically mapped QTL-2DL region. The identified contigs with best hits based on BLAST search were retrieved from the database and gene prediction was performed using SoftBery – FGENESH program (Solovyev et al., 2006) to know the gene structure.

Three candidate genes localized in the QTL-2DL region were directly associated with high fold-change RR metabolites: 1) *TaACT* (agmatine coumaroyltransferase): This is known to be involved in coumaroylagmatine and coumaroylputrescine metabolite biosynthesis; 2) *TaDGK* (Diacylglycerol kinase): This is known to be directly involved in biosynthesis of phosphatidic acid; 3) *TaGLI1* (Glycerol kinase): This is known to be indirectly involved in biosynthesis of phosphatidic acid. Further, sequencing of the candidate genes (*TaACT* and *TaDGK*) in NILs revealed the absence of sequence variation for *TaDGK* at DNA level. Thus, we speculated the involvement of regulatory genes such as transcription factors in regulating *TaDGK* for high fold-change induction of phosphatidic acid. Based on sequence variation we prioritized the *TaACT* and it was explored in detail by physical localization within the QTL region, sequencing, sequence analysis, gene expression study and histochemical localization for the metabolites biosynthesized by this gene. The *TaACT* was functionally validated using virus-induced gene silencing in wheat and by complementation study in *Arabidopsis* mutant. However, the disease increase in NIL-R, following silencing of *TaACT* was not substantial or

similar to a non-silenced NIL-S (a susceptible control). This clearly indicated, the possible involvement of other candidate genes in controlling resistance at the QTL-2DL locus.

In chapter IV, based on previous study, we searched other genes located in the QTL region by retrieving the DNA sequence from the IWGSC database and the genes were predicted. In addition, synteny mapping was also performed with rice and brachypodium. We identified 18 candidate genes, including one WRKY like transcription factor (*TaWRKY70*) within the QTL-2DL region, which may have some role in disease resistance. We confirmed the sequence variation at the *TaWRKY70* in NILs that made it to produce a truncated protein in NIL-S. The *TaWRKY70* showed differential transcript expression among NILs, with higher expression in NIL-R compared NIL-S. Further, we showed the *TaWRKY70 cis*-binding elements in the promoter regions of the *TaACT, TaDGK* and *TaGLI1* genes based on promoter analysis. We confirmed the hierarchal regulation of downstream genes by *TaWRKY70,* based on *in-silico* and *in-vivo* protein-DNA interactions. In addition, functional validation of *TaWRKY70* based on VIGS in NIL-R was done to confirm an increase in the fungal biomass, but also a decrease in the expression of downstream resistance genes: *TaACT, TaDGK* and *TaGLI1*, which were associated with reduced abundances of RR metabolites biosynthesized by them. This functional validation study proved our hypothesis, projecting a major and unique role of *TaWRKY70* as a functional regulatory gene in imparting resistance to FHB in wheat.

Chapter V was undertaken to understand the spikelet resistance mechanisms to FHB in wheat. It was proved that QTL-2DL also exhibited spikelet resistance (type I) (McCartney et al., 2007). This also confirmed the previous finding that the NIL-R with QTL-2DL not only suppressed fungal infection in inoculated spikelets but also reduced spread from the spikelets to the rachis (Long et al., 2015). This suggests the role of unknown resistance mechanisms suppressing the rise of fungal biomass at the initial point of infection in the spikelet and thus helping in cutting down the spread of fungus to rachis. Therefore, it was very crucial to understand the existing resistance mechanisms governed by QTL-2DL to suppress the fungal infection in inoculated spikelets. Thus, in the present study metabolite profiling of the spikelets of NILs containing contrasting alleles of QTL-2DL was performed. Our metabolomics and genomics studies suggested the *TaPAL, TaGPAT3* and *TaCER5* genes as potential candidate genes. These are responsible for the biosynthesis of antimicrobial and cell wall strengthening

biochemical, thus reducing the initial infection and fungal accumulation in inoculated spikelets. The functional genes validated here can be used to replace the genes in susceptible cultivars, if nonfunctional, based on genome editing tools to improve resistance in wheat against FHB.

6.2 Suggested future studies

- Sequencing of identified candidate genes across several cultivars to identify functional variations associated with the FHB.
- Development of functional genic markers based on identified functional sequence variations for potential use in marker assisted selection in FHB breeding programs.
- The susceptible alleles identified can be potentially replaced with functional DNA segment or whole gene based on genome editing tools, such as CRISPR-Cas9.
- We have also identified other genes located in the QTL-2DL based on *in-silico* gene prediction and synteny-based approach. These candidates may have a possible role in controlling FHB resistance. Functional characterization of these genes will open up new avenues in FHB resistance breeding programs.

References

Afendi, F.M., Okada, T., Yamazaki, M., Hirai-Morita, A., Nakamura, Y., Nakamura, K., Ikeda, S., Takahashi, H., Altaf-Ul-Amin, M. and Darusman, L.K. (2012) KNApSAcK family databases: integrated metabolite–plant species databases for multifaceted plant research. Plant and Cell Physiology 53: e1-e1.

Allwood, J.W. and Goodacre, R. (2010) An introduction to liquid chromatography–mass spectrometry instrumentation applied in plant metabolomic analyses. Phytochemical Analysis 21: 33-47.

Altschul, S.F., Gish, W., Miller, W., Myers, E.W. and Lipman, D.J. (1990) Basic local alignment search tool. Journal of Molecular Biology 215: 403-410.

Arisz, S.A., Testerink, C. and Munnik, T. (2009) Plant PA signaling via diacylglycerol kinase. Biochimica et Biophysica Acta (BBA)-Molecular and Cell Biology of Lipids 1791: 869-875.

Arruda, M.P., Brown, P., Brown-Guedira, G., Krill, A.M., Thurber, C., Merrill, K.R., Foresman, B.J. and Kolb, F.L. (2016) Genome-Wide Association Mapping of Fusarium Head Blight Resistance in Wheat using Genotyping-by-Sequencing. The Plant Genome 9: 1-14.

Ashikawa, I., Abe, F. and Nakamura, S. (2010) Ectopic expression of wheat and barley DOG1-like genes promotes seed dormancy in *Arabidopsis*. Plant science 179: 536-542.

Atanasov, D. (1920) Fusarium-blight (scab) of wheat and other cereals:US Government Printing Office.

Bacon, C.W. and Hinton, D.M. (2007) Potential for control of seedling blight of wheat caused by Fusarium graminearum and related species using the bacterial endophyte Bacillus mojavensis. Biocontrol Science and Technology 17: 81-94.

Bai, G. and Shaner, G. (1994) Scab of wheat: prospects for control. Plant Disease 78: 760-766.

Bai, G. and Shaner, G. (2004) Management and resistance in wheat and barley to fusarium head blight. Annual Review of Phytopathology 42: 135-161.

Bai, G.H., Plattner, R., Desjardins, A., Kolb, F. and McIntosh, R.A. (2001) Resistance to Fusarium head blight and deoxynivalenol accumulation in wheat. Plant Breeding 120: 1-6.

Balut, A.L., Clark, A.J., Brown-Guedira, G., Souza, E. and Van Sanford, D.A. (2013) Validation of Fhb1 and QFhs.nau-2DL in Several Soft Red Winter Wheat Populations. Crop Science 53: 934-945.

Bateman, G.L., Gutteridge, R.J., Gherbawy, Y., Thomsett, M.A. and Nicholson, P. (2007) Infection of stem bases and grains of winter wheat by Fusarium culmorum and F. graminearum and effects of tillage method and maize-stalk residues. Plant Pathology 56: 604-615.

Bedair, M. and Sumner, L.W. (2008) Current and emerging mass-spectrometry technologies for metabolomics. TrAC Trends in Analytical Chemistry 27, 238-250.

Beisson, F., Li-Beisson, Y. and Pollard, M. (2012) Solving the puzzles of cutin and suberin polymer biosynthesis. Current Opinion In Plant Biology 15: 329-337.

Beisson, F., Li, Y., Bonaventure, G., Pollard, M. and Ohlrogge, J.B. (2007) The acyltransferase GPAT5 is required for the synthesis of suberin in seed coat and root of *Arabidopsis*. The Plant Cell 19: 351-368.

Bernardo, A., Bai, G., Guo, P., Xiao, K., Guenzi, A.C. and Ayoubi, P. (2007) Fusarium graminearum-induced changes in gene expression between Fusarium head blight-resistant and susceptible wheat cultivars. Functional & Integrative Genomics 7: 69-77.

Bernards, M.A., Lopez, M.L., Zajicek, J. and Lewis, N.G. (1995) Hydroxycinnamic acid-derived polymers constitute the polyaromatic domain of suberin. Journal of Biological Chemistry 270: 7382-7386.

Biais, B., Beauvoit, B., William Allwood, J., Deborde, C., Maucourt, M., Goodacre, R., Rolin, D. and Moing, A. (2010) Metabolic acclimation to hypoxia revealed by metabolite gradients in melon fruit. Journal of Plant Physiology 167: 242-245.

Bollina, V., Kumaraswamy, G.K., Kushalappa, A.C., Choo, T.M., Dion, Y., Rioux, S., Faubert, D. and Hamzehzarghani, H. (2010) Mass spectrometry-based metabolomics application to identify quantitative resistance-related metabolites in barley against Fusarium head blight. Molecular Plant Pathology 11: 769-782.

Bollina, V., Kushalappa, A.C., Choo, T.M., Dion, Y. and Rioux, S. (2011) Identification of metabolites related to mechanisms of resistance in barley against Fusarium graminearum, based on mass spectrometry. Plant Molecular Biology 77: 355-370.

Brewer, H.C., and Hammond-Kosack, K.E. (2015) Host to a Stranger: *Arabidopsis* and Fusarium Ear Blight. Trends in Plant Science 10: 651-663.

Buerstmayr, H., Ban, T. and Anderson, J.A. (2009) QTL mapping and marker-assisted selection for Fusarium head blight resistance in wheat: a review. Plant Breeding 128: 1-26.

Buerstmayr, H., Lemmens, M., Hartl, L., Doldi, L., Steiner, B., Stierschneider, M. and Ruckenbauer, P. (2002) Molecular mapping of QTLs for Fusarium head blight resistance in spring wheat. I. Resistance to fungal spread (Type II resistance). Theoretical and Applied Genetics 104: 84-91.

Buerstmayr, H., Buerstmayr, M., Schweiger, W., and Steiner, B. (2014) Breeding for resistance to head blight caused by Fusarium spp. in wheat. CAB Reviews 9:007.

Burch-Smith, T.M., Anderson, J.C., Martin, G.B. and Dinesh-Kumar, S.P. (2004) Applications and advantages of virus-induced gene silencing for gene function studies in plants. The Plant Journal 39: 734-746.

Burhenne, K., Kristensen, B.K. and Rasmussen, S.K. (2003) A New Class of N-Hydroxycinnamoyltransferases purification, cloning, and expression of a barley agmatine coumaroyltransferase (EC 2.3. 1.64). Journal of Biological Chemistry 278: 13919-13927.

Bushnell, W., Hazen, B., Pritsch, C. and Leonard, K. (2003) Histology and physiology of Fusarium head blight. Fusarium head blight of wheat and barley, 44-83.

Cai, J., Abramovici, H., Gee, S.H. and Topham, M.K. (2009) Diacylglycerol kinases as sources of phosphatidic acid. Biochimica et Biophysica Acta (BBA)-Molecular and Cell Biology of Lipids 1791: 942-948.

Cakir, C., Gillespie, M.E. and Scofield, S.R. (2010) Rapid determination of gene function by virus-induced gene silencing in wheat and barley. Crop Science 50: S-77-S-84.

Cakir, C. and Scofield, S. (2008) Evaluating the ability of the barley stripe mosaic virus-induced gene silencing system to simultaneously silence two wheat genes. Cereal Research Communications 36: 217-222.

Calestani, C., Moses, M.S., Maestri, E., Marmiroli, N. and Bray, E.A. (2015) Constitutive expression of the barley dehydrin gene aba2 enhances *Arabidopsis* germination in response to salt stress. International Journal of Plant Biology 6: 20.

Caspi, R., Altman, T., Dreher, K., Fulcher, C.A., Subhraveti, P., Keseler, I.M., Kothari, A., Krummenacker, M., Latendresse, M. and Mueller, L.A. (2012) The MetaCyc database of metabolic pathways and enzymes and the BioCyc collection of pathway/genome databases. Nucleic Acids Research 40: D742-D753.

Chamarthi, S.K., Kumar, K., Gunnaiah, R., Kushalappa, A.C., Dion, Y. and Choo, T.M. (2014) Identification of fusarium head blight resistance related metabolites specific to doubled-haploid lines in barley. European Journal of Plant Pathology 138: 67-78.

Champeil, A., Dore, T. and Fourbet, J. (2004) Fusarium head blight: epidemiological origin of the effects of cultural practices on head blight attacks and the production of mycotoxins by Fusarium in wheat grains. Plant Science 166: 1389-1415.

Chanda, B., Venugopal, S.C., Kulshrestha, S., Navarre, D.A., Downie, B., Vaillancourt, L., Kachroo, A. and Kachroo, P. (2008) Glycerol-3-phosphate levels are associated with basal resistance to the hemibiotrophic fungus Colletotrichum higginsianum in *Arabidopsis*. Plant Physiology 147: 2017-2029.

Chen, G., Komatsuda, T., Ma, J.F., Nawrath, C., Pourkheirandish, M., Tagiri, A., Hu, Y.-G., Sameri, M., Li, X. and Zhao, X. (2011) An ATP-binding cassette subfamily G full transporter is essential for the retention of leaf water in both wild barley and rice. Proceedings of the National Academy of Sciences 108: 12354-12359.

Chen, K. and Gao, C. (2014) Targeted genome modification technologies and their applications in crop improvements. Plant Cell Reports 33: 575-583.

Chen, S., Songkumarn, P., Liu, J. and Wang, G.L. (2009) A versatile zero background T-vector system for gene cloning and functional genomics. Plant Physiology 150: 1111-1121.

Chen, Y.Z., Pang, Q.Y., He, Y., Zhu, N., Branstrom, I., Yan, X.-F. and Chen, S. (2012) Proteomics and metabolomics of *Arabidopsis* responses to perturbation of glucosinolate biosynthesis. Molecular Plant 5: 1138-1150.

Cheng, W., Li, H.P., Zhang, J.B., Du, H.J., Wei, Q.Y., Huang, T., Yang, P., Kong, X.W. and Liao, Y.C. (2015) Tissue-specific and pathogen-inducible expression of a fusion protein containing a Fusarium-specific antibody and a fungal chitinase protects wheat against Fusarium pathogens and mycotoxins. Plant Biotechnology Journal 13: 664-674.

Cho, K., Cho, K.S., Sohn, H.-B., Ha, I.J., Hong, S.Y., Lee, H., Kim, Y.M. and Nam, M.H. (2016) Network analysis of the metabolome and transcriptome reveals novel regulation of potato pigmentation. Journal of Experimental Botany, 67: 1519-33.

Choulet, F., Wicker, T., Rustenholz, C., Paux, E., Salse, J., Leroy, P., Schlub, S., Le Paslier, M.C., Magdelenat, G. and Gonthier, C. (2010) Megabase level sequencing reveals contrasted organization and evolution patterns of the wheat gene and transposable element spaces. The Plant Cell 22: 1686-1701.

CIMMYT. (2015) http://wheat.org/.

Collard, B., Jahufer, M., Brouwer, J. and Pang, E. (2005) An introduction to markers, quantitative trait loci (QTL) mapping and marker-assisted selection for crop improvement: the basic concepts. Euphytica 142: 169-196.

Corpet, F. (1988) Multiple sequence alignment with hierarchical clustering. Nucleic Acids Research 16: 10881-10890.

Cuthbert, P.A., Somers, D.J., Thomas, J., Cloutier, S. and Brulé-Babel, A. (2006) Fine mapping Fhb1, a major gene controlling Fusarium head blight resistance in bread wheat (Triticum aestivum L.). Theoretical and Applied Genetics 112: 1465-1472.

De Jong, C.F., Laxalt, A.M., Bargmann, B.O., De Wit, P.J., Joosten, M.H. and Munnik, T. (2004) Phosphatidic acid accumulation is an early response in the Cf-4/Avr4 interaction. The Plant Journal 39: 1-12.

De Vos, R.C., Moco, S., Lommen, A., Keurentjes, J.J., Bino, R.J. and Hall, R.D. (2007) Untargeted large-scale plant metabolomics using liquid chromatography coupled to mass spectrometry. Nature Protocols 2: 778-791.

De Wolf, E., Madden, L. and Lipps, P. (2003) Risk assessment models for wheat Fusarium head blight epidemics based on within-season weather data. Phytopathology 93: 428-435.

Dexter, J., Clear, R. and Preston, K. (1996) Fusarium head blight: effect on the milling and baking of some Canadian wheats. Cereal Chemistry 73: 695-701.

Diallo, A., Kane, N., Agharbaoui, Z., Badawi, M. and Sarhan, F. (2010) Heterologous expression of wheat vernalization 2 (TaVRN2) gene in *Arabidopsis* delays flowering and enhances freezing tolerance. PLoS ONE 5, e8690.

Dickson, J.G. (1942) Scab of wheat and barley and its control:US Dept. of Agriculture.

Dill-Macky, R., Leonard, K. and Bushnell, W. (2003) Inoculation methods and evaluation of Fusarium head blight resistance in wheat. Fusarium head blight of wheat and barley, 184-210.

Duez, P., Kumps, A. and Mardens, Y. (1996) GC-MS profiling of urinary organic acids evaluated as a quantitative method. Clinical chemistry 42: 1609-1615.

Edreva, A., Velikova, V. and Tsonev, T. (2007) Phenylamides in plants. Russian Journal of Plant Physiology 54: 287-301.

Edwards, S.G. (2004) Influence of agricultural practices on Fusarium infection of cereals and subsequent contamination of grain by trichothecene mycotoxins. Toxicology Letters 153: 29-35.

Eulgem, T., Rushton, P.J., Schmelzer, E., Hahlbrock, K. and Somssich, I.E. (1999) Early nuclear events in plant defence signalling: rapid gene activation by WRKY transcription factors. The EMBO Journal 18: 4689-4699.

Facchini, P.J., Hagel, J. and Zulak, K.G. (2002) Hydroxycinnamic acid amide metabolism: physiology and biochemistry. Canadian Journal of Botany 80: 577-589.

FAO. (2016) World Food Situation.

Farooq, S. and Azam, F. (2002) Molecular markers in plant breeding-I: Concepts and characterization. Pakistan Journal of Biological Sciences 5: 1135-1140.

Ferrari, S., Sella, L., Janni, M., De Lorenzo, G., Favaron, F. and D'Ovidio, R. (2012) Transgenic expression of polygalacturonase-inhibiting proteins in *Arabidopsis* and wheat increases resistance to the flower pathogen Fusarium graminearum. Plant Biology 14: 31-38.

Fester, T., Maier, W. and Strack, D. (1999) Accumulation of secondary compounds in barley and wheat roots in response to inoculation with an arbuscular mycorrhizal fungus and co-inoculation with rhizosphere bacteria. Mycorrhiza 8: 241-246.

Fiehn, O., Kopka, J., Trethewey, R.N. and Willmitzer, L. (2000) Identification of uncommon plant metabolites based on calculation of elemental compositions using gas chromatography and quadrupole mass spectrometry. Analytical Chemistry 72: 3573-3580.

Francki, M.G., Hayton, S., Gummer, J., Rawlinson, C. and Trengove, R.D. (2015) Metabolomic profiling and genomic analysis of wheat aneuploid lines to identify genes controlling biochemical pathways in mature grain. Plant Biotechnology Journal. 2: 649-60.

Franke, R., Briesen, I., Wojciechowski, T., Faust, A., Yephremov, A., Nawrath, C. and Schreiber, L. (2005) Apoplastic polyesters in *Arabidopsis* surface tissues–a typical suberin and a particular cutin. Phytochemistry 66: 2643-2658.

Galeotti, F., Barile, E., Curir, P., Dolci, M. and Lanzotti, V. (2008) Flavonoids from carnation (Dianthus caryophyllus) and their antifungal activity. Phytochemistry Letters 1: 44-48.

Geng, S., Li, A., Tang, L., Yin, L., Wu, L., Lei, C., Guo, X., Zhang, X., Jiang, G. and Zhai, W. (2013) TaCPK2-A, a calcium-dependent protein kinase gene that is required for wheat powdery mildew resistance enhances bacterial blight resistance in transgenic rice. Journal of Experimental Botany 64: 3125-3136.

Gertsman, I., Gangoiti, J.A. and Barshop, B.A. (2014) Validation of a dual LC–HRMS platform for clinical metabolic diagnosis in serum, bridging quantitative analysis and untargeted metabolomics. Metabolomics 10: 312-323.

Gilbert, J. and Tekauz, A. (2000) Review: recent developments in research on Fusarium head blight of wheat in Canada. Canadian Journal of Plant Pathology 22: 1-8.

Gilsinger, J., Kong, L., Shen, X. and Ohm, H. (2005) DNA markers associated with low Fusarium head blight incidence and narrow flower opening in wheat. Theoretical and Applied Genetics 110: 1218-1225.

Golkari, S., Gilbert, J., Prashar, S. and Procunier, J.D. (2007) Microarray analysis of Fusarium graminearum-induced wheat genes: identification of organ-specific and differentially expressed genes. Plant Biotechnology Journal 5: 38-49.

Gómez-Merino, F.C., Brearley, C.A., Ornatowska, M., Abdel-Haliem, M.E., Zanor, M.-I. and Mueller-Roeber, B. (2004) AtDGK2, a novel diacylglycerol kinase from *Arabidopsis* thaliana, phosphorylates 1-stearoyl-2-arachidonoyl-sn-glycerol and 1, 2-dioleoyl-sn-glycerol and exhibits cold-inducible gene expression. Journal of Biological Chemistry 279: 8230-8241.

Gong, L., Chen, W., Gao, Y., Liu, X., Zhang, H., Xu, C., Yu, S., Zhang, Q. and Luo, J. (2013) Genetic analysis of the metabolome exemplified using a rice population. Proceedings of the National Academy of Sciences 110: 20320-20325.

Gong, X., Zhang, J., Hu, J., Wang, W., Wu, H., Zhang, Q. and LIU, J.H. (2015) FcWRKY70, a WRKY protein of Fortunella crassifolia, functions in drought tolerance and modulates putrescine synthesis by regulating arginine decarboxylase gene. Plant, Cell & Environment. 11: 2248-62.

Gopaul, S., Farrell, K. and Abbott, F. (2000) Gas chromatography/negative ion chemical ionization mass spectrometry and liquid chromatography/electrospray ionization tandem mass spectrometry quantitative profiling of N-acetylcysteine conjugates of valproic acid in urine: application in drug metabolism studies in humans. Journal of Mass Spectrometry 35: 698-704.

Goswami, R.S. and Kistler, H.C. (2004) Heading for disaster: Fusarium graminearum on cereal crops. Molecular Plant Pathology 5: 515-525.

Gou, J.Y., Yu, X.H. and Liu, C.J. (2009) A hydroxycinnamoyltransferase responsible for synthesizing suberin aromatics in *Arabidopsis*. Proceedings of the National Academy of Sciences 106: 18855-18860.

Guillaumie, S., Mzid, R., Méchin, V., Léon, C., Hichri, I., Destrac-Irvine, A., Trossat-Magnin, C., Delrot, S. and Lauvergeat, V. (2010) The grapevine transcription factor WRKY2 influences the lignin pathway and xylem development in tobacco. Plant Molecular Biology 72: 215-234.

Gunnaiah, R. and Kushalappa, A.C. (2014) Metabolomics deciphers the host resistance mechanisms in wheat cultivar Sumai-3, against trichothecene producing and non-producing isolates of Fusarium graminearum. Plant Physiology and Biochemistry 83: 40-50.

Gunnaiah, R., Kushalappa, A.C., Duggavathi, R., Fox, S. and Somers, D.J. (2012) Integrated metabolo-proteomic approach to decipher the mechanisms by which wheat QTL (Fhb1) contributes to resistance against Fusarium graminearum. PLoS ONE 7, e40695.

Hahlbrock, K., Bednarek, P., Ciolkowski, I., Hamberger, B., Heise, A., Liedgens, H., Logemann, E., Nürnberger, T., Schmelzer, E. and Somssich, I.E. (2003) Non-self recognition, transcriptional reprogramming, and secondary metabolite accumulation during plant/pathogen interactions. Proceedings of the National Academy of Sciences 100: 14569-14576.

Hamzehzarghani, H., Kushalappa, A., Dion, Y., Rioux, S., Comeau, A., Yaylayan, V., Marshall, W. and Mather, D.E. (2005) Metabolic profiling and factor analysis to discriminate quantitative resistance in wheat cultivars against fusarium head blight. Physiological and Molecular Plant Pathology 66: 119-133.

Hamzehzarghani, H., Paranidharan, V., Abu-Nada, Y., Kushalappa, A., Mamer, O. and Somers, D. (2008) Metabolic profiling to discriminate wheat near isogenic lines, with quantitative trait loci at chromosome 2DL, varying in resistance to fusarium head blight. Canadian Journal of Plant Science 88: 789-797.

Hoffmann, L., Besseau, S., Geoffroy, P., Ritzenthaler, C., Meyer, D., Lapierre, C., Pollet, B. and Legrand, M. (2004) Silencing of hydroxycinnamoyl-coenzyme A shikimate/quinate hydroxycinnamoyltransferase affects phenylpropanoid biosynthesis. The Plant Cell 16: 1446-1465.

Hu, J., Wang, D., Li, J., Jing, G., Ning, K. and Xu, J. (2014) Genome-wide identification of transcription factors and transcription-factor binding sites in oleaginous microalgae Nannochloropsis. Scientific Reports 4: 5454. DOI: 10.1038/srep05454.

Ishihara, A., Hashimoto, Y., Tanaka, C., Dubouzet, J.G., Nakao, T., Matsuda, F., Nishioka, T., Miyagawa, H. and Wakasa, K. (2008) The tryptophan pathway is involved in the defense responses of rice against pathogenic infection via serotonin production. The Plant Journal 54: 481-495.

Janni, M., Sella, L., Favaron, F., Blechl, A., De Lorenzo, G. and D'Ovidio, R. (2008) The expression of a bean polygalacturonase-inhibiting proteins in transgenic wheat confers increased resistance to the fungal pathogen Bipolaris sorokiniana. Molecular Plant-Microbe Interaction 21: 171-177.

Jia, G., Chen, P., Qin, G., Bai, G., Wang, X., Wang, S., Zhou, B., Zhang, S. and Liu, D. (2005) QTLs for Fusarium head blight response in a wheat DH population of Wangshuibai/Alondra's'. Euphytica 146: 183-191.

Jia, H., Cho, S. and Muehlbauer, G.J. (2009) Transcriptome analysis of a wheat near-isogenic line pair carrying Fusarium head blight-resistant and-susceptible alleles. Molecular plant-microbe interactions 22: 1366-1378.

Jiang, G.-L. (2013) Molecular markers and marker-assisted breeding in plants. Plant Breeding from Laboratories to Fields, 45-83. DOI: 10.5772/52583.

Jiang, G.L., Dong, Y., Shi, J. and Ward, R.W. (2007a) QTL analysis of resistance to Fusarium head blight in the novel wheat germplasm CJ 9306. II. Resistance to deoxynivalenol accumulation and grain yield loss. Theoretical and Applied Genetics 115: 1043-1052.

Jiang, G.L., Shi, J. and Ward, R.W. (2007b) QTL analysis of resistance to Fusarium head blight in the novel wheat germplasm CJ 9306. I. Resistance to fungal spread. Theoretical and Applied Genetics 116: 3-13.

Jochum, C., Osborne, L. and Yuen, G. (2006) Fusarium head blight biological control with Lysobacter enzymogenes strain C3. Biological Control 39: 336-344.

Jordan, S. and Humphries, P. (1994) Single nucleotide polymorphism in exon 2 of the BCP gene on 7q31-q35. Human Molecular Genetics 3: 1915-1915.

Kage, U., Kumar, A., Dhokane, D., Karre, S. and Kushalappa, A.C. (2015) Functional molecular markers for crop improvement. Critical Reviews in Biotechnology, 1-14. DOI: 10.3109/07388551.2015.1062743

Kalde, M., Barth, M., Somssich, I.E. and Lippok, B. (2003) Members of the *Arabidopsis* WRKY group III transcription factors are part of different plant defense signaling pathways. Molecular Plant-Microbe Interactions 16: 295-305.

Kanehisa, M. and Goto, S. (2000) KEGG: kyoto encyclopedia of genes and genomes. Nucleic acids research 28: 27-30.

Kang, Z. and Buchenauer, H. (2000) Ultrastructural and immunocytochemical investigation of pathogen development and host responses in resistant and susceptible wheat spikes infected by Fusarium culmorum. Physiological and Molecular Plant Pathology 57, 255-268.

Katajamaa, M., Miettinen, J. and Orešič, M. (2006) MZmine: toolbox for processing and visualization of mass spectrometry based molecular profile data. Bioinformatics 22: 634-636.

Keller, H., Hohlfeld, H., Wray, V., Hahlbrock, K., Scheel, D. and Strack, D. (1996) Changes in the accumulation of soluble and cell wall-bound phenolics in elicitor-treated cell suspension cultures and fungus-infected leaves of Solanum tuberosum. Phytochemistry 42: 389-396.

Kelley, L.A., Mezulis, S., Yates, C.M., Wass, M.N. and Sternberg, M.J. (2015) The Phyre2 web portal for protein modeling, prediction and analysis. Nature Protocols 10: 845-858.

Khajuria, C., Wang, H., Liu, X., Wheeler, S., Reese, J.C., El Bouhssini, M., Whitworth, R.J. and Chen, M.S. (2013) Mobilization of lipids and fortification of cell wall and cuticle are important in host defense against Hessian fly. BMC Genomics 14: 423.

Kolattukudy, P., Kronman, K. and Poulose, A. (1975) Determination of structure and composition of suberin from the roots of carrot, parsnip, rutabaga, turnip, red beet, and sweet potato by combined gas-liquid chromatography and mass spectrometry. Plant Physiology 55: 567-573.

Kolattukudy, P.E. (2005) Cutin from Plants. In: Biopolymers Online. Wiley-VCH Verlag GmbH & Co. KGaA.

Kolattukudy, P.t. (1981) Structure, biosynthesis, and biodegradation of cutin and suberin. Annual Review of Plant Physiology 32: 539-567.

Kosma, D.K., Nemacheck, J.A., Jenks, M.A. and Williams, C.E. (2010) Changes in properties of wheat leaf cuticle during interactions with Hessian fly. The Plant Journal 63: 31-43.

Krishnan, P., Kruger, N. and Ratcliffe, R. (2005) Metabolite fingerprinting and profiling in plants using NMR. Journal of Experimental Botany 56: 255-265.

Kugler, K.G., Siegwart, G., Nussbaumer, T., Ametz, C., Spannagl, M., Steiner, B., Lemmens, M., Mayer, K.F., Buerstmayr, H. and Schweiger, W. (2013) Quantitative trait loci-dependent analysis of a gene co-expression network associated with Fusarium head blight resistance in bread wheat (Triticum aestivum L.). BMC Genomics 14: 728.

Kumar, A., Karre, S., Dhokane, D., Kage, U., Hukkeri, S. and Kushalappa, A.C. (2015) Real-time quantitative PCR based method for the quantification of fungal biomass to discriminate quantitative resistance in barley and wheat genotypes to fusarium head blight. Journal of Cereal Science 64: 16-22.

Kumar, A., Yogendra, K.N., Karre, S., Kushalappa, A.C., Dion, Y. and Choo, T.M. (2016) WAX INDUCER1 (HvWIN1) transcription factor regulates free fatty acid biosynthetic genes to reinforce cuticle to resist Fusarium head blight in barley spikelets. Journal of Experimental Botany, erw187.

Kumaraswamy, G.K., Bollina, V., Kushalappa, A.C., Choo, T.M., Dion, Y., Rioux, S., Mamer, O. and Faubert, D. (2011a) Metabolomics technology to phenotype resistance in barley against Gibberella zeae. European Journal of Plant Pathology 130: 29-43.

Kumaraswamy, K.G., Kushalappa, A.C., Choo, T.M., Dion, Y. and Rioux, S. (2011b) Mass spectrometry based metabolomics to identify potential biomarkers for resistance in barley against Fusarium head blight (Fusarium graminearum). Journal of Chemical Ecology 37: 846-856.

Kunst, L. and Samuels, L. (2009) Plant cuticles shine: advances in wax biosynthesis and export. Current Opinion in Plant Biology 12: 721-727.

Kushalappa, A.C. and Gunnaiah, R. (2013) Metabolo-proteomics to discover plant biotic stress resistance genes. Trends in Plant Science 18: 522-531.

Kushalappa, A.C., Yogendra, K.N. and Karre, S. (2016) Plant Innate Immune Response: Qualitative and Quantitative Resistance. Critical Reviews in Plant Sciences 35: 38-55.

Lahlali, R., Karunakaran, C., Wang, L., Willick, I., Schmidt, M., Liu, X., Borondics, F., Forseille, L., Fobert, P.R. and Tanino, K. (2015) Synchrotron based phase contrast X-ray imaging combined with FTIR spectroscopy reveals structural and biomolecular differences in spikelets play a significant role in resistance to Fusarium in wheat. BMC Plant Biology 15: 1.

Lara, I., Belge, B. and Goulao, L.F. (2015) A focus on the biosynthesis and composition of cuticle in fruits. Journal of Agricultural and Food Chemistry 63: 4005-4019.

Lee, W.-S., Rudd, J.J. and Kanyuka, K. (2015) Virus-induced gene silencing (VIGS) for functional analysis of wheat genes involved in Zymoseptoria tritici susceptibility and resistance. Fungal Genetics and Biology 79: 84-88.

Lemmens, M., Scholz, U., Berthiller, F., Dall'Asta, C., Koutnik, A., Schuhmacher, R., Adam, G., Buerstmayr, H., Mesterházy, Á. and Krska, R. (2005) The ability to detoxify the mycotoxin deoxynivalenol colocalizes with a major quantitative trait locus for Fusarium head blight resistance in wheat. Molecular Plant-Microbe Interactions 18: 1318-1324.

Li, Y., Beisson, F., Koo, A.J., Molina, I., Pollard, M. and Ohlrogge, J. (2007) Identification of acyltransferases required for cutin biosynthesis and production of cutin with suberin-like monomers. Proceedings of the National Academy of Sciences 104: 18339-18344.

Lisec, J., Schauer, N., Kopka, J., Willmitzer, L. and Fernie, A.R. (2006) Gas chromatography mass spectrometry–based metabolite profiling in plants. Nature Protocols 1: 387-396.

Liu, S., Hall, M.D., Griffey, C.A. and McKendry, A.L. (2009) Meta-analysis of QTL associated with Fusarium head blight resistance in wheat. Crop Science 49: 1955-1968.

Liu, S., Pumphrey, M.O., Gill, B.S., Trick, H.N., Zhang, J.X., Dolezel, J., Chalhoub, B. and Anderson, J.A. (2008) Toward positional cloning of Fhb1, a major QTL for Fusarium head blight resistance in wheat. Cereal Research Communications 36: 195-201.

Liu, S., Zhang, X., Pumphrey, M.O., Stack, R.W., Gill, B.S. and Anderson, J.A. (2006) Complex microcolinearity among wheat, rice, and barley revealed by fine mapping of the genomic region harboring a major QTL for resistance to Fusarium head blight in wheat. Functional & Integrative Genomics 6: 83-89.

Livak, K.J. and Schmittgen, T.D. (2001) Analysis of relative gene expression data using real-time quantitative PCR and the $2^{-\Delta\Delta CT}$ method. Methods 25: 402-408.

Loke, J.C., Stahlberg, E.A., Strenski, D.G., Haas, B.J., Wood, P.C. and Li, Q.Q. (2005) Compilation of mRNA polyadenylation signals in *Arabidopsis* revealed a new signal element and potential secondary structures. Plant Physiology 138: 1457-1468.

Long, X., Balcerzak, M., Gulden, S., Cao, W., Fedak, G., Wei, Y.M., Zheng, Y.L., Somers, D. and Ouellet, T. (2015) Expression profiling identifies differentially expressed genes associated with the fusarium head blight resistance QTL 2DL from the wheat variety Wuhan-1. Physiological and Molecular Plant Pathology 90: 1-11.

Ma, M., Yan, Y., Huang, L., Chen, M. and Zhao, H. (2012) Virus-induced gene-silencing in wheat spikes and grains and its application in functional analysis of HMW-GS-encoding genes. BMC Plant Biology 12: 141.

Mandal, M.K., Chanda, B., Xia, Y., Yu, K., Sekine, K., Gao, Q.-m., Selote, D., Kachroo, A. and Kachroo, P. (2011) Glycerol-3-phosphate and systemic immunity. Plant Signaling & Behavior 6: 1871-1874.

Marchler-Bauer, A., Derbyshire, M.K., Gonzales, N.R., Lu, S., Chitsaz, F., Geer, L.Y., Geer, R.C., He, J., Gwadz, M. and Hurwitz, D.I. (2014) CDD: NCBI's conserved domain database. Nucleic Acids Research, gku1221.

Marcia, M.d.O. (2009) Feruloylation in grasses: current and future perspectives. Molecular Plant 2: 861-872.

Marcussen, T., Sandve, S.R., Heier, L., Spannagl, M., Pfeifer, M., Jakobsen, K.S., Wulff, B.B., Steuernagel, B., Mayer, K.F. and Olsen, O.-A. (2014) Ancient hybridizations among the ancestral genomes of bread wheat. Science 345: 1250092.

Mardi, M., Pazouki, L., Delavar, H., Kazemi, M., Ghareyazie, B., Steiner, B., Nolz, R., Lemmens, M. and Buerstmayr, H. (2006) QTL analysis of resistance to Fusarium head blight in wheat using a 'Frontana'-derived population. Plant Breeding 125: 313-317.

Martinez, M., Moschini, R., Barreto, D. and Comerio, R. (2012) Effect of environment on Fusarium head blight intensity and deoxynivalenol content in wheat grains: development of a forecasting system. Cereal Research Communications 40: 74-84.

Matny, O.N. (2015) Fusarium head blight and crown rot on wheat & barley: losses and health risks. Advances in Plants & Agriculture Research 2: 00039.

Matsuda, F., Yonekura-Sakakibara, K., Niida, R., Kuromori, T., Shinozaki, K. and Saito, K. (2009) MS/MS spectral tag-based annotation of non-targeted profile of plant secondary metabolites. The Plant Journal 57: 555-577.

McCartney, C., Somers, D., Fedak, G., DePauw, R., Thomas, J., Fox, S., Humphreys, D., Lukow, O., Savard, M. and McCallum, B. (2007) The evaluation of FHB resistance QTLs introgressed into elite Canadian spring wheat germplasm. Molecular Breeding 20: 209-221.

McCartney, C., Somers, D., Brule-Babel, A., Fedak, G., Gilbert, J., Cao, W. (2011) Mapping of the Wuhan-1 chromosome 2DL FHB QTL in a uniform genetic background. 7th Canadian Workshop on Fusarium Head Blight, Winnipeg, Manitoba, Canada, 97.

McFarlane, H.E., Shin, J.J., Bird, D.A. and Samuels, A.L. (2010) *Arabidopsis* ABCG transporters, which are required for export of diverse cuticular lipids, dimerize in different combinations. The Plant Cell 22: 3066-3075.

McLusky, S.R., Bennett, M.H., Beale, M.H., Lewis, M.J., Gaskin, P. and Mansfield, J.W. (1999) Cell wall alterations and localized accumulation of feruloyl-3′-methoxytyramine in onion epidermis at sites of attempted penetration by Botrytis allii are associated with actin polarisation, peroxidase activity and suppression of flavonoid biosynthesis. The Plant Journal 17: 523-534.

McMullen, M., Halley, S., Schatz, B., Meyer, S., Jordahl, J. and Ransom, J. (2008) Integrated strategies for Fusarium head blight management in the United States. Cereal Research Communications 36: 563-568.

McMullen, M., Jones, R. and Gallenberg, D. (1997) Scab of wheat and barley: a re-emerging disease of devastating impact. Plant Disease 81: 1340-1348.

Medina-Puche, L., Cumplido-Laso, G., Amil-Ruiz, F., Hoffmann, T., Ring, L., Rodríguez-Franco, A., Caballero, J.L., Schwab, W., Muñoz-Blanco, J. and Blanco-Portales, R. (2014) MYB10 plays a major role in the regulation of flavonoid/phenylpropanoid metabolism during ripening of Fragaria × ananassa fruits. Journal of Experimental Botany 65: 401-417.

Mesterhazy, A. (1995) Types and components of resistance to Fusarium head blight of wheat. Plant Breeding 114: 377-386.

Mesterhazy, A., Bartók, T., Kászonyi, G., Varga, M., Tóth, B. and Varga, J. (2005) Common resistance to different Fusarium spp. causing Fusarium head blight in wheat. European Journal of Plant Pathology 112: 267-281.

Miller, J., Young, J. and Sampson, D. (1985) Deoxynivalenol and Fusarium head blight resistance in spring cereals. Journal of Phytopathology 113: 359-367.

Miller, S., Watson, E., Lazebnik, J., Gulden, S., Balcerzak, M., Fedak, G. and Ouellet, T. (2011) Characterization of an alien source of resistance to Fusarium head blight transferred to Chinese Spring wheat. Botany 89: 301-311.

Miyagawa, H., Ishihara, A., Nishimoto, T., Ueno, T. and Mayama, S. (1995) Induction of avenanthramides in oat leaves inoculated with crown rust fungus, Puccinia coronata f. sp. avenae. Bioscience, Biotechnology, and Biochemistry 59: 2305-2306.

Moco, S., Bino, R.J., Vorst, O., Verhoeven, H.A., de Groot, J., van Beek, T.A., Vervoort, J. and De Vos, C.R. (2006) A liquid chromatography-mass spectrometry-based metabolome database for tomato. Plant Physiology 141: 1205-1218.

Mounet, F., Moing, A., Garcia, V., Petit, J., Maucourt, M., Deborde, C., Bernillon, S., Le Gall, G., Colquhoun, I. and Defernez, M. (2009) Gene and metabolite regulatory network analysis of early developing fruit tissues highlights new candidate genes for the control of tomato fruit composition and development. Plant Physiology 149: 1505-1528.

Munnik, T. (2001) Phosphatidic acid: an emerging plant lipid second messenger. Trends in Plant Science 6: 227-233.

Muroi, A., Ishihara, A., Tanaka, C., Ishizuka, A., Takabayashi, J., Miyoshi, H. and Nishioka, T. (2009) Accumulation of hydroxycinnamic acid amides induced by pathogen infection and identification of agmatine coumaroyltransferase in *Arabidopsis* thaliana. Planta 230: 517-527.

Muroi, A., Matsui, K., Shimoda, T., Kihara, H., Ozawa, R., Ishihara, A., Nishihara, M. and Arimura, G.I. (2012) Acquired immunity of transgenic torenia plants overexpressing agmatine coumaroyltransferase to pathogens and herbivore pests. Scientific Reports 2: 689.

Musa, T., Hecker, A., Vogelgsang, S. and Forrer, H. (2007) Forecasting of Fusarium head blight and deoxynivalenol content in winter wheat with FusaProg. EPPO bulletin 37: 283-289.

Nussbaumer, T., Warth, B., Sharma, S., Ametz, C., Bueschl, C., Parich, A., Pfeifer, M., Siegwart, G., Steiner, B. and Lemmens, M. (2015) Joint transcriptomic and metabolomic analyses reveal changes in the primary metabolism and imbalances in the subgenome orchestration in the bread wheat molecular response to Fusarium graminearum. G3: Genes| Genomes| Genetics 5: 2579-2592.

Ogura, Y., Ishihara, A. and Iwamura, H. (2001) Induction of hydroxycinnamic acid amides and tryptophan by jasmonic acid, abscisic acid and osmotic stress in barley leaves. Zeitschrift für Naturforschung C 56: 193-202.

Okazaki, Y. and Saito, K. (2014) Roles of lipids as signaling molecules and mitigators during stress response in plants. The Plant Journal 79: 584-596.

Oksman-Caldentey, K.-M. and Inzé, D. (2004) Plant cell factories in the post-genomic era: new ways to produce designer secondary metabolites. Trends in Plant Science 9: 433-440.

Parinov, S. and Sundaresan, V. (2000) Functional genomics in *Arabidopsis*: large-scale insertional mutagenesis complements the genome sequencing project. Current Opinion in Biotechnology 11: 157-161.

Parry, D., Jenkinson, P. and McLeod, L. (1995) Fusarium ear blight (scab) in small grain cereals-a review. Plant Pathology 44: 207-238.

Proctor, R.H., Hohn, T.M. and McCormick, S.P. (1995) Reduced virulence of Gibberella zeae caused by disruption of a trichthecine toxin biosynthetic gene. Molecular Plant Microbe Interactions 8: 1995-1908.

Pushpa, D., Yogendra, K.N., Gunnaiah, R., Kushalappa, A.C. and Murphy, A. (2013) Identification of Late Blight Resistance-Related Metabolites and Genes in Potato through Nontargeted Metabolomics. Plant Molecular Biology Reporter 32: 585-595.

Ramegowda, V., Mysore, K.S. and Senthil-Kumar, M. (2014) Virus-induced gene silencing is a versatile tool for unraveling the functional relevance of multiple abiotic-stress-responsive genes in crop plants. Frontiers in Plant Science 5: 323.

Rischer, H., Orešič, M., Seppänen-Laakso, T., Katajamaa, M., Lammertyn, F., Ardiles-Diaz, W., Van Montagu, M.C., Inzé, D., Oksman-Caldentey, K.M. and Goossens, A. (2006) Gene-to-metabolite networks for terpenoid indole alkaloid biosynthesis in Catharanthus roseus cells. Proceedings of the National Academy of Sciences 103: 5614-5619.

Robertson, D. (2004) VIGS vectors for gene silencing: many targets, many tools. Annual Reviews of Plant Biology 55: 495-519.

Roessner, U., Luedemann, A., Brust, D., Fiehn, O., Linke, T., Willmitzer, L. and Fernie, A.R. (2001) Metabolic profiling allows comprehensive phenotyping of genetically or environmentally modified plant systems. The Plant Cell Online 13: 11-29.

Rotter, B.A. (1996) Invited review: Toxicology of deoxynivalenol (vomitoxin). Journal of Toxicology and Environmental Health Part A 48: 1-34.

Rudd, J., Horsley, R., McKendry, A. and Elias, E. (2001) Host plant resistance genes for Fusarium head blight. Crop Science 41: 620-627.

Rushton, D.L., Tripathi, P., Rabara, R.C., Lin, J., Ringler, P., Boken, A.K., Langum, T.J., Smidt, L., Boomsma, D.D. and Emme, N.J. (2012) WRKY transcription factors: key components in abscisic acid signalling. Plant Biotechnology Journal 10: 2-11.

Rushton, P.J., Somssich, I.E., Ringler, P. and Shen, Q.J. (2010) WRKY transcription factors. Trends in Plant Science 15: 247-258.

Rushton, P.J., Torres, J.T., Parniske, M., Wernert, P., Hahlbrock, K. and Somssich, I. (1996) Interaction of elicitor-induced DNA-binding proteins with elicitor response elements in the promoters of parsley PR1 genes. The EMBO Journal 15: 5690.

Sauvage, C., Segura, V., Bauchet, G., Stevens, R., Do, P.T., Nikoloski, Z., Fernie, A.R. and Causse, M. (2014) Genome-wide association in tomato reveals 44 candidate loci for fruit metabolic traits. Plant Physiology 165: 1120-1132.

Schauer, N. and Fernie, A.R. (2006) Plant metabolomics: towards biological function and mechanism. Trends in Plant Science 11: 508-516.

Schmidt, A., Scheel, D. and Strack, D. (1998) Elicitor-stimulated biosynthesis of hydroxycinnamoyltyramines in cell suspension cultures of Solanum tuberosum. Planta 205: 51-55.

Schroeder, H. and Christensen, J. (1963) Factors affecting resistance of wheat to scab caused by Gibberella zeae. Phytopathology 53: 831-838.

Schweiger, W., Steiner, B., Ametz, C., Siegwart, G., Wiesenberger, G., Berthiller, F., Lemmens, M., Jia, H., Adam, G. and Muehlbauer, G.J. (2013) Transcriptomic characterization of two major Fusarium resistance quantitative trait loci (QTLs), Fhb1 and Qfhs.ifa-5A, identifies novel candidate genes. Molecular Plant Pathology 14: 772-785.

Scofield, S.R., Huang, L., Brandt, A.S. and Gill, B.S. (2005) Development of a virus-induced gene-silencing system for hexaploid wheat and its use in functional analysis of the Lr21-mediated leaf rust resistance pathway. Plant Physiology 138: 2165-2173.

Senthil-Kumar, M., Anand, A., Uppalapati, S.R. and Mysore, K.S. (2008) Virus-induced gene silencing and its application in characterizing genes involved in water-deficit-stress tolerance 165: 1404–1421.

Shan, Q., Wang, Y., Li, J., Zhang, Y., Chen, K., Liang, Z., Zhang, K., Liu, J., Xi, J.J. and Qiu, J.L. (2013) Targeted genome modification of crop plants using a CRISPR-Cas system. Nature Biotechnology 31: 686-688.

Shin, S., Torres-Acosta, J.A., Heinen, S.J., McCormick, S., Lemmens, M., Paris, M.P.K., Berthiller, F., Adam, G. and Muehlbauer, G.J. (2012) Transgenic *Arabidopsis* thaliana expressing a barley UDP-glucosyltransferase exhibit resistance to the mycotoxin deoxynivalenol. Journal of Experimental Botany 63: 4731-4740.

Shulaev, V., Cortes, D., Miller, G. and Mittler, R. (2008) Metabolomics for plant stress response. Physiologia Plantarum 132: 199-208.

Smith, C.A., O'Maille, G., Want, E.J., Qin, C., Trauger, S.A., Brandon, T.R., Custodio, D.E., Abagyan, R. and Siuzdak, G. (2005) METLIN: a metabolite mass spectral database. Therapeutic Drug Monitoring 27: 747-751.

Smith, K., Evans, C., Dill-Macky, R., Gustus, C., Xie, W. and Dong, Y. (2004) Host genetic effect on deoxynivalenol accumulation in Fusarium head blight of barley. Phytopathology 94: 766-771.

Smoot, M.E., Ono, K., Ruscheinski, J., Wang, P.L. and Ideker, T. (2011) Cytoscape 2.8: new features for data integration and network visualization. Bioinformatics 27: 431-432.

Soler, M., Serra, O., Molinas, M., Huguet, G., Fluch, S. and Figueras, M. (2007) A genomic approach to suberin biosynthesis and cork differentiation. Plant Physiology 144: 419-431.

Solovyev, V., Kosarev, P., Seledsov, I. and Vorobyev, D. (2006) Automatic annotation of eukaryotic genes, pseudogenes and promoters. Genome Biology 7: 1-12.

Somers, D.J., Fedak, G. and Savard, M. (2003) Molecular mapping of novel genes controlling Fusarium head blight resistance and deoxynivalenol accumulation in spring wheat. Genome 46: 555-564.

Somers, D.J., Thomas, J., DePauw, R., Fox, S., Humphreys, G. and Fedak, G. (2005) Assembling complex genotypes to resist Fusarium in wheat (Triticum aestivum L.). Theoretical and Applied Genetics 111: 1623-1631.

St-Pierre, B., Laflamme, P., Alarco, A.M. and Luca, E. (1998) The terminal O-acetyltransferase involved in vindoline biosynthesis defines a new class of proteins responsible for coenzyme A-dependent acyl transfer. The Plant Journal 14: 703-713.

Stack, R.W. (2000) Return of an old problem: Fusarium head blight of small grains. APSnet Plant Health Reviews. DOI:10.1094/PHP-2000-0622-01-RV.

Stark, R.E. and Tian, S. (2007) The Cutin Biopolymer Matrix. In: Annual Plant Reviews Volume 23: Biology of the Plant Cuticle pp. 126-144. Blackwell Publishing Ltd.

Steiner, B., Lemmens, M., Griesser, M., Scholz, U., Schondelmaier, J. and Buerstmayr, H. (2004) Molecular mapping of resistance to Fusarium head blight in the spring wheat cultivar Frontana. Theoretical and Applied Genetics 109: 215-224.

Tadege, M., Ratet, P. and Mysore, K.S. (2005) Insertional mutagenesis: a Swiss Army knife for functional genomics of Medicago truncatula. Trends in Plant Science 10, 229-235.

Tanksley, S.D. (1993) Mapping polygenes. Annual Review of Genetics 27: 205-233.

Testerink, C. and Munnik, T. (2005) Phosphatidic acid: a multifunctional stress signaling lipid in plants. Trends in Plant Science 10: 368-375.

Thomas, R., Fang, X., Ranathunge, K., Anderson, T.R., Peterson, C.A. and Bernards, M.A. (2007) Soybean root suberin: anatomical distribution, chemical composition, and relationship to partial resistance to Phytophthora sojae. Plant Physiology 144: 299-311.

Tohge, T. and Fernie, A.R. (2010) Combining genetic diversity, informatics and metabolomics to facilitate annotation of plant gene function. Nature Protocols 5: 1210-1227.

Tolstikov, V.V., Lommen, A., Nakanishi, K., Tanaka, N. and Fiehn, O. (2003) Monolithic silica-based capillary reversed-phase liquid chromatography/electrospray mass spectrometry for plant metabolomics. Analytical Chemistry 75: 6737-6740.

Usadel, B., Poree, F., Nagel, A., Lohse, M., Czedik-Eysenberg, A. and Stitt, M. (2009) A guide to using MapMan to visualize and compare Omics data in plants: a case study in the crop species, Maize. Plant, Cell & Environment 32: 1211-1229.

Van Eck, L., Schultz, T., Leach, J.E., Scofield, S.R., Peairs, F.B., Botha, A.M. and Lapitan, N.L. (2010) Virus-induced gene silencing of WRKY53 and an inducible phenylalanine ammonia-lyase in wheat reduces aphid resistance. Plant Biotechnology Journal 8: 1023-1032.

Várallyay, É., Giczey, G. and Burgyán, J. (2012) Virus-induced gene silencing of MLO genes induces powdery mildew resistance in Triticum aestivum. Archives of Virology 157: 1345-1350.

Vinaixa, M., Samino, S., Saez, I., Duran, J., Guinovart, J.J. and Yanes, O. (2012) A guideline to univariate statistical analysis for LC/MS-based untargeted metabolomics-derived data. Metabolites 2: 775-795.

Vogg, G., Fischer, S., Leide, J., Emmanuel, E., Jetter, R., Levy, A.A. and Riederer, M. (2004) Tomato fruit cuticular waxes and their effects on transpiration barrier properties: functional characterization of a mutant deficient in a very-long-chain fatty acid β-ketoacyl-CoA synthase. Journal of Experimental Botany 55: 1401-1410.

von Röpenack, E., Parr, A. and Schulze-Lefert, P. (1998) Structural analyses and dynamics of soluble and cell wall-bound phenolics in a broad spectrum resistance to the powdery mildew fungus in barley. Journal of Biological Chemistry 273: 9013-9022.

Walter, S., Kahla, A., Arunachalam, C., Perochon, A., Khan, M.R., Scofield, S.R. and Doohan, F.M. (2015) A wheat ABC transporter contributes to both grain formation and mycotoxin tolerance. Journal of Experimental Botany 66: 2583-93.

Walters, D., Raynor, L., Mitchell, A., Walker, R. and Walker, K. (2004) Antifungal activities of four fatty acids against plant pathogenic fungi. Mycopathologia 157: 87-90.

Wang, X., Fan, C., Zhang, X., Zhu, J. and Fu, Y.-F. (2013) BioVector, a flexible system for gene specific-expression in plants. BMC plant biology **13**, 1.

Wang, J., Li, Q., Mao, X., Li, A., Jing, R., Wang, C., Liu, C.M., Wei, L.L., Shi, L.Y. and Pan, Z.F. (2016) Wheat Transcription Factor TaAREB3 Participates in Drought and Freezing Tolerances in *Arabidopsis*. International Journal of Biological Sciences 12: 257-269.

Wang, X., Zeng, J., Li, Y., Rong, X., Sun, J., Sun, T., Li, M., Wang, L., Feng, Y. and Chai, R. (2015) Expression of TaWRKY44, a wheat WRKY gene, in transgenic tobacco confers multiple abiotic stress tolerances. Frontiers in Plant Science 6: 615.

Warth, B., Parich, A., Bueschl, C., Schoefbeck, D., Neumann, N.K.N., Kluger, B., Schuster, K., Krska, R., Adam, G. and Lemmens, M. (2015) GC–MS based targeted metabolic profiling identifies changes in the wheat metabolome following deoxynivalenol treatment. Metabolomics 11: 722-738.

Wegulo, S.N., Bockus, W.W., Nopsa, J.F.H., Peiris, K.H. and Dowell, F.E. (2013) Integration of fungicide application and cultivar resistance to manage Fusarium head blight in wheat. Fungicides—Showcases of Integrated Plant Disease Management from Around the World. M. Nita, ed. doi 10: 3251.

Wen, W., Li, D., Li, X., Gao, Y., Li, W., Li, H., Liu, J., Liu, H., Chen, W. and Luo, J. (2014) Metabolome-based genome-wide association study of maize kernel leads to novel biochemical insights. Nature Communications 5: 3438.

Weigel, D. and Glazebrook, J. (2005) Transformation of agrobacterium using the freeze-thaw method. CSH protocols 2006: 1031-1036.

Windels, C.E. (2000) Economic and social impacts of Fusarium head blight: changing farms and rural communities in the Northern Great Plains. Phytopathology 90: 17-21.

Xia, J. and Wishart, D.S. (2011) Web-based inference of biological patterns, functions and pathways from metabolomic data using MetaboAnalyst. Nature Protocols 6, 743-760.

Xiao, J., Jin, X., Jia, X., Wang, H., Cao, A., Zhao, W., Pei, H., Xue, Z., He, L. and Chen, Q. (2013) Transcriptome-based discovery of pathways and genes related to resistance against Fusarium head blight in wheat landrace Wangshuibai. BMC Genomics 14: 197.

Xu, X. and Nicholson, P. (2009) Community ecology of fungal pathogens causing wheat head blight. Annual Review of Phytopathology 47: 83-103.

Xue, A., Chen, Y., Voldeng, H., Savard, M. and Tian, X. (2008) Biological control of fusarium head blight of wheat with Clonostachys rosea strain ACM941. Cereal Research Communications 36: 695-699.

Yang, Q., Reinhard, K., Schiltz, E. and Matern, U. (1997) Characterization and heterologous expression of hydroxycinnamoyl/benzoyl-CoA: anthranilate N-hydroxycinnamoyl/benzoyltransferase from elicited cell cultures of carnation, Dianthus caryophyllus L. Plant molecular biology 35: 777-789.

Yang, Y., Zhao, J., Liu, P., Xing, H., Li, C., Wei, G. and Kang, Z. (2013) Glycerol-3-phosphate metabolism in wheat contributes to systemic acquired resistance against Puccinia striiformis f. sp. tritici. PLoS ONE 8: e81756.

Ye, J., Coulouris, G., Zaretskaya, I., Cutcutache, I., Rozen, S. and Madden, T.L. (2012) Primer-BLAST: a tool to design target-specific primers for polymerase chain reaction. BMC Bioinformatics 13: 134.

Yli-Mattila, T., Paavanen-Huhtala, S., Jestoi, M., Parikka, P., Hietaniemi, V., Gagkaeva, T., Sarlin, T., Haikara, A., Laaksonen, S. and Rizzo, A. (2008) Real-time PCR detection and quantification of Fusarium poae, F. graminearum, F. sporotrichioides and F. langsethiae in cereal grains in Finland and Russia. Archives of Phytopathology and Plant Protection 41: 243-260.

Yogendra, K. and Kushalappa, A. (2016) Integrated Transcriptomics and Metabolomics Reveal Induction of Hierarchies of Resistance Genes in Potato against Late Blight. Functional Plant Biology. http://dx.doi.org/10.1071/FP16028

Yogendra, K.N., Kumar, A., Sarkar, K., Li, Y., Pushpa, D., Mosa, K.A., Duggavathi, R. and Kushalappa, A.C. (2015) Transcription factor StWRKY1 regulates phenylpropanoid metabolites conferring late blight resistance in potato. Journal of Experimental Botany 66: 7377-7389.

Yogendra, K.N., Pushpa, D., Mosa, K.A., Kushalappa, A.C., Murphy, A. and Mosquera, T. (2014) Quantitative resistance in potato leaves to late blight associated with induced hydroxycinnamic acid amides. Functional & Integrative Genomics 14: 285-298.

Yoo, S.D., Cho, Y.H. and Sheen, J. (2007) *Arabidopsis* mesophyll protoplasts: a versatile cell system for transient gene expression analysis. Nature Protocols 2: 1565-1572.

Young, N. (1996) QTL mapping and quantitative disease resistance in plants. Annual Review Of Phytopathology 34: 479-501.

Yu, J.B., Bai, G.H., Cai, S.B., Dong, Y.H. and Ban, T. (2008) New Fusarium head blight-resistant sources from Asian wheat germplasm. Crop Science 48: 1090-1097.

Yuen, G., Jochum, C., Halley, S., Van Ee, G., Hoffman, V. and Bleakley, B. (2007) Effects of spray application methods on biocontrol agent viability. In: 2007 National Fusarium Head Blight Forum p. 149.

Zadoks, J.C., Chang, T.T. and Konzak, C.F. (1974) A decimal code for the growth stages of cereals. Weed Research 14: 415-421.

Zhang, W., Wang, C., Qin, C., Wood, T., Olafsdottir, G., Welti, R. and Wang, X. (2003) The oleate-stimulated phospholipase D, PLDδ, and phosphatidic acid decrease H2O2-induced cell death in *Arabidopsis*. The Plant Cell 15: 2285-2295.

Zhang, Y. (2008) I-TASSER server for protein 3D structure prediction. BMC Bioinformatics 9: 40.

Zhang, Z., Chen, J., Su, Y., Liu, H., Chen, Y., Luo, P., Du, X., Wang, D. and Zhang, H. (2015) TaLHY, a 1R-MYB Transcription Factor, Plays an Important Role in Disease Resistance against Stripe Rust Fungus and Ear Heading in Wheat. PLoS ONE 10: e0127723.

Zhu, L., Liu, X., Wang, H., Khajuria, C., Reese, J.C., Whitworth, R.J., Welti, R. and Chen, M.-S. (2012) Rapid mobilization of membrane lipids in wheat leaf sheaths during incompatible interactions with hessian fly. Molecular Plant-Microbe Interactions 25: 920-930.

Zhuang, Y., Gala, A. and Yen, Y. (2013) Identification of functional genic components of major Fusarium head blight resistance quantitative trait loci in wheat cultivar Sumai 3. Molecular Plant-Microbe Interactions 26: 442-450.

Zou, X., Seemann, J.R., Neuman, D. and Shen, Q.J. (2004) A WRKY gene from creosote bush encodes an activator of the abscisic acid signaling pathway. Journal of Biological Chemistry 279: 55770-55779.

Appendix

Appendix 3.1: Resistance related (RR) metabolites (P<0.05) detected in the rachis of wheat NILs inoculated with water or spores of *F. graminearum*.

RRI									
Observed Mz	**AME**	**RT**	**Molecular formula**	**Name**	**FC**	**Observed fragmentation**	**Database fragmentation**	**Chemical group**	**Database ID**
710.4887	0.0	30.5	C40H71O8P	PA(17:0/20:4(5Z,8Z,11Z,14Z))	**54.3**	**269.25,** 309.08, 401.12, **423.25,457.24**, 492.28, 546.50, 617.05, 630.98, 677.22 , 692.24	457.24, 439.23, 423.25, 405.24, 303.23, 269.25, 259.24, 171.01, 153.00, 96.97, 78.96	Glycerophospholipids	LMGP10010003
276.1592	2.3	12.3	C14H20N4O2	p-Coumaroylagmatine	**28.7**	**119.0, 147.0, 218.1, 233.17,** 231.33**, 258.16, 260.0**	119.04, 147.0, 218.1, 233.129, 258.14, 260.0	HCAA	C00028060, In silico , (Muroi et al., 2009)
234.1373	2.2		C13H18N202	p-Coumaroylputrescine	**9.5**	**93.1, 233.11, 162.2, 204.1, 218.25,** 191.13,**119.01**	93.1, 119.04, 190.08, 204.1, 218.11, 233.12, 162.2,	HCAA	In silico , (Muroi et al., 2009)
684.4729	-0.2	30.2	C38H69O8P	PA(15:0/20:3(8Z,11Z,14Z))	**9.5**	267.26, 341.13, **377.17,** 400.99, **425.43**, **459.91**, 499.19, 520.63, 536.24, 551.10, 566.17, 585.15, 595.55, 606.45, 622.89, 650.91, 664.72	459.25, 441.24, 425.43,395.22, 377.21, 305.25, 241.22, 171.01, 153, 96.97, 78.96	Glycerophospholipids	LMGP10010151
768.5699	3.8	30.5	C44H81O8P	PA(19:0/22:2(13Z,16Z))	**2.3**	249.07, 253.32, 267.26, 281.36, 282.27, 295.41, **335.57**, 339.71, 359.21, 389.16, 407.49, 452.15, **471.25, 489.30**, 503.27, 513.14, 531.29, 532.45, 544.64, 564.77, 605.17, 669.11, 685.56, 707.13, 711.66, 747.09, 749.41, 768.85	489.30, 471.29, 451.28, 433.27, 335.30, 297.28, 171.01, 153, 96.97, 78.96	Glycerophospholipids	LMGP10010506

566.0549	-0.3	0.4	C15H24N2O17P2	UDP-glucose	**1.8**	**323.08**, 354.15, 355.19, 383.15, **384.15**, 385.15, 414.15, 426.11, 427.16, 444.14, 445.09, 474.08, 475.13, 486.10, 487.13, 504.09, 505.07, 533.14, 546.08, 547.14,	78.95,96.96, 158.92, 211.00, 241.01, 272.95, 280.02, 305.01, 320.97, 323.02, 384.98, 402.99, 467.06, 565.04	Fatty acids	C00029
765.2928	1.2	14.1	C25H44N13O13P	O-Phosphoviomycin	**1.7**	271.24, 284.88, 299.20, 314.29, 329.17, 343.35, 377.17, 505.77, 538.42, 566.98, 579.24, 609.14, 610.53, 621.13, 673.02, 685.15, 694.94, 703.35, 716.25, 728.46, 745.0, 748.57		Lipids	C02574
722.2429	1.0	13.3	C34H42O17	Amorphol	**1.5**	243.91, 271.20, 299.27, 314.07, 329.16, 343.34, 359.91, 477.25, 498.49, 525.08, 543.21, 567.24, 579.38, 639.79, 655.21, 673.11, 703.34, 712.45		Flavonoids	LMPK12060006
278.1306	2.1	9.8	C11H22N2O4S	Pantetheine	**1.5**	130.05, 146.02, 147.16, 194.94, 217.20,			C00831
256.2406	1.7	0.8	C16H32O2	Hexadecanoic acid	**1.5**	167.32, 173.2, 177.94, 195.02, 211.25, 237.12, **255.3**	255.2328	Fatty acids	C00249
528.1673	1.4	13.2	C24H32O11S	17-beta-estradiol 3-sulfate-17-(beta-D-glucuronide)	**1.5**	329.13, 330.16, 331.19		Lipids	LMST05010035
346.2361	1.6	14.4	C18H34O6	9,10-dihydroxy-Octadecanedioic acid	**1.4**	171.15, 201.18, 213.19, 229.29, 247.30, 265.28, 273.34, 283.30, 291.34, 309.33, 313.24, 317.15, 327.25		Fatty acids	LMFA01170030

760.2584	0.6	17.1	C37H44O17	Epimedoside	**1.4**	227.25, 237.13, 271.16, 299.13, 314.22, 329.18, 354.12, 369.96, 401.21, 429.20, 455.10, 477.41, 495.33, 527.29, 529.539.02, 553.24, 583.38, 587.26, 593.28, 607.13, 615.23, 619.80, 642.06, 660.18, 673.16, 686.30, 700.20, 728.16, 741.29, 743.46		Flavonoids	LMPK12112021
537.5620	4.3	5.6	C34H71N3O	79692-14-1 (Hexadecanamide)	**1.3**	281.19, 299.24, 329.24, 330.26, 373.22, 374.18, 405.32, 448.39, 449.35, 450.39, 451.42, 475.32, 491.12, 515.44, 517.49, 519.47, 520.46, 521.49, 535.49		Fatty acids	PCID315746
342.1110	2.1	16.7	C19H18O6	4',5,6,7-Tetramethoxyflavone	**1.1**	101.08, 113.03, 119.03, 130.95, 143.11, 161.02, 179.00, 291.26, 309.26, 323.25		Flavonoids	C14472
RRC									
Observed Mz	**AME**	**RT**	**Molecular formula**	**Name**	**FC**	**0bserved fragmentation**	**Database fragmentation**	Chemical group	Database ID
402.0957	1.6	22.2	C20H18O9	1-Hydroxy-2-(beta-D-glucosyloxy)-9,10-anthraquinone	**1.8**	220.17, 239.23, 269.12, 341.19, 383.23		Glycoside	C04719
354.1104	0.2	20.7	C20H18O6	Cyclokievitone	**1.7**	123.12, 271.16, 277.24, 279.13, 283.08, 295.12, 307.24, 313.12, 324.81, 325.49, 352.93, 353.65		Flavonoid	C10207
434.1582	1.0	16.1	C22H26O9	Eleganin	**1.6**	137.20, 231.25, 236.95, 249.34, 353.25, 260.12, 267.37, 271.29, 328.05, 333.41, 341.07, 373.22, 387.22, 389.22, 391.44, 415.22		Terpenoid	C09401
422.2438	1.2	27.3	C20H39O7P	PA(17:1(9Z)/0:0)	**1.5**	185.04, 253.27, 339.32		Glycerophospholipid	LMGP10050002
708.4732	-4.5	29.0	C37H73O8PS	1-tetradecanoyl-2-hexadecanoyl-sn-glycero-3-	**1.5**	291.34, 309.28, 397.18, 415.21, 643.18, 647.18, 675.16, 689.13,		Glycerophospholipid	LMGP00000052

				phosphosulfocholine					
308.2719	1.1	29.8	C20H36O2	11,14-eicosadienoic acid	**1.4**	96.94, 265.04, 269.30, 289.43, **307.40**	45.0, 52.74, 58.0, 59.01, 71.01, 86.03, 95.05, 167.10, 262.96, 274.87, **307.26**	Fatty acid	LMFA01030130
536.2278	3.7	30.4	C42H78NO9P	PS(O-18:0/18:3(6Z,9Z,12Z))	**1.4**	190.95, 192.26, 199.17, 220.97, 231.30, 235.16, 238.47, 255.31, 281.26, 299.26, 307.99, 323.38, 329.21, 338.95, 343.24, 355.14, 365.26, 373.12, 385.39, 403.04, 415.29, 427.33, 436.81, 444.29, 449.56, 457.24, 467.50, 474.40, 491.06, 499.15, 517.24, 521.57		Glycerophospholipid	LMGP03020029
462.1747	-5.0	11.6	C25H35BrO3	Ethyl 16-hydroxy-18-bromo-8E,17E19Z-tricosatrien-4,6-diynoate	**1.4**	235.25, 275.32, 293.26, 341.16		Fatty acid	LMFA01090109
234.1625	2.2	27.8	C16H30O2	(9Z)-Hexadecenoic acid	**1.3**	108.32, 189.30, 214.88, 218.27, 233.20		Fatty acid	C08362
596.4669	2.9	22.2	C35H64O7	Annonacin	**1.3**	223.13, 241.19, 242.08, 277.67, 279.38, 280.42, 298.87, 315.16, 316.36, 333.50, 354.38, 415.15, 433.21, 471.40, 493.51, 523.36, 535.24, 563.25		Fatty acid	C20213
254.2251	1.9	27.8	C30H50O3	Soyasapogenol B	**1.3**	95.27, 137.19, 171.35, 187.30, 205.19, 209.19, 224.94, 235.22, 363.22		Fatty acid	C08980
202.0333	-2.7	0.7	C5H6N4O5	5-Hydroxy-2-oxo-4-ureido-2,5-dihydro-1H-imidazole-5-carboxylate	**1.3**	59.02, 118.97, 125.12, 141.00, 157.08, 158.99, 169.37		Purine metabolism	C12248

278.2252	2.0	28.6	C18H30O2	16-methyl-6Z,9Z,12Z-heptadecatrienoic acid	**1.2**	80.07, 81.09, 83.18, 87.11, 95.19, 97.19, 101.22, 107.18, 109.23, 113.26, 121.16, 127.22, 135.11, 145.07, 149.28, 159.27, 163.16, 168.06, 177.03, 179.26, 185.39, 191.20, 195.13, 196.09, 205.28, 211.30, 219.27 229.18, 231.27, 233.28, 239.21, 241.32, 247.30, 249.20, 259.32, 261.26, 263.18, 275.28, 277.26, 278.34		Fatty acid	LMFA01020209
360.1951	4.0	25.6	C21H28O5	Cortisone	**1.2**			Steroid	
530.3096	1.0	30.7	C30H52O	24,25-Dihydrolanosterol	**1.1**	253.30, 275.35, 265.34, 393.53, 419.46, 429.15, 447.25, 469.44, 471.68, 483.40, 497.75, 510.20, 512.09, 532.15		Lipids	C05109
389.1408	-0.2	22.3	C17H18O5	Odoratol	**1.1**			Terpenes	C09807

AME: Accurate Mass Error= ((Observed mass-expected mass) / expected mass) X $10^{6,}$ **RRC:** Resistance related constitutive, **RRI:** Resistance related induced.

[@]**Fold change calculation**: were based on relative intensity of metabolites, RRC= RM/SM, RRI= (RP/RM)/(SP/SM).RP: resistant NIL with pathogen inoculation, RM: resistant NIL with mock inoculation, SP: susceptible NIL with pathogen inoculation, SM: susceptible NIL with mock inoculation.

[$]*t*-test significance at $P<0.05$.